ornl

OAK RIDGE
NATIONAL
LABORATORY

LOCKHEED MARTIN

ORNL/TM-13029

FY94 Site Characterization and Multilevel Well Installation at a West Bear Creek Valley Research Site on the Oak Ridge Reservation

G. R. Moline
M. E. Schreiber

Environmental Sciences Division

Publication No. 4427

MASTER

MANAGED AND OPERATED BY
LOCKHEED MARTIN ENERGY RESEARCH CORPORATION
FOR THE UNITED STATES
DEPARTMENT OF ENERGY

ORNL-27 (3-96)

ORNL/TM-13029

FY94 Site Characterization and Multilevel Well Installation at a West Bear Creek Valley Research Site on the Oak Ridge Reservation

G.R. Moline
Environmental Sciences Division
Oak Ridge National Laboratory

M.E. Schreiber
Department of Geology and Geophysics
University of Wisconsin - Madison

March, 1996

Prepared by
Environmental Sciences Division
Oak Ridge National Laboratory
ESD Publication 4427

Prepared for
U.S. Department of Energy
Office of Environmental Restoration and Waste Management
under budget and reporting code EW 26 45 02 00 0

OAK RIDGE NATIONAL LABORATORY
Oak Ridge, Tennessee 37831-6285
managed by
LOCKHEED MARTIN ENERGY RESEARCH CORP.
for the U.S. Department of Energy
under contract number DE-AC05-96OR22464

CONTENTS

FIGURES

TABLES

Table | Page

ACRONYMS

BLS	Below land surface
DOE	Department of Energy
EM	Electromagnetic
EPA	Environmental Protection Agency
ESD	Environmental Sciences Division
ORNL	Oak Ridge National Laboratory
ORR	Oak Ridge Reservation
ORRHAGS	Oak Ridge Reservation Hydrologic and Geologic Studies
PVC	Polyvinyl Chloride
TVA	Tennessee Valley Authority
FY	Fiscal Year (begins Oct. 1 of preceding calendar year)

EXECUTIVE SUMMARY

The goals of this project are to collect data that will assist in determining what constitutes a representative groundwater sample in fractured shale typical of much of the geology underlying the ORR waste disposal sites, and to determine how monitoring-well construction and sampling methods impact the representativeness of the sample. This report details the FY94 field activities at a research site in west Bear Creek Valley on the Oak Ridge Reservation (ORR). These activities, funded by the Energy Systems Groundwater Program Office through the Oak Ridge Reservation Hydrologic and Geologic Studies (ORRHAGS) task, focus on developing appropriate sampling protocols for the type of fractured media that underlies many of the ORR waste disposal sites. Currently accepted protocols were developed for porous media and are likely to result in nonrepresentative samples in fractured systems.

A preliminary tracer test was conducted using helium and bromide to provide information about the spatial and temporal variability in transport behavior. Results indicate that while transport is predominantly parallel to strike, transient flow both updip and downdip occurs in conjunction with storm events, indicating a highly complex flow system requiring further study in order to characterize this transient behavior. The degree of spatial and temporal variability is important to decisions regarding when and where to sample.

In June of FY94 three new boreholes were drilled to depths of 50-ft in the updip location and 70-ft in the along-strike and downdip locations. Drilling was accomplished using an acoustic drilling technology that allowed nearly continuous core recovery with minimal use of drilling fluids. Extensive borehole testing was conducted in order to locate and characterize the active flow zones within each borehole. These tests included borehole videos, electromagnetic borehole flowmeter tests, and point dilution tests. Test results and detailed core descriptions, included in this document, were used to determine the location of sampling ports. Following completion of the borehole tests, multilevel wells were installed in the boreholes, each having five sampling ports. The new multilevel wells were located adjacent to pairs of conventional screened wells to allow direct comparison between the sampling results from the different well types. The borehole tests indicated that significant flow zones were not intersected by the adjacent well pairs. The significance of these missed zones and the interconnectedness of the network of fracture zones will be tested in future activities at the site. Future activities will also include pump tests that will determine the region influenced by the removal of three well volumes from one of the screened wells. These activities will lead to recommendations for well construction and purging that will yield more representative samples and provide a more realistic assessment of contaminant flux and potential risk for a given exposure scenario.

1. INTRODUCTION

The goals of this project are to collect data that will assist in determining what constitutes a representative sample in fractured shale typical of much of the geology underlying the ORR waste disposal sites, and to determine how monitoring well construction and sampling methods impact the representativeness of the sample. The overall strategy for meeting the project goals includes the initiation of tracer injections to establish surrogate contaminant plumes; the installation of multilevel wells adjacent to standard screened well pairs to allow sampling of discrete zones and comparison of data using different monitoring well constructions; sampling from discrete zones to assess spatial and temporal variability; and field tests to quantify fracture zone characteristics, fracture connectivity, and the impact of varying purge volumes on system dynamics and analytical results. This report summarizes the results of field activities conducted during FY94.

The complexity of groundwater flow systems in fractured terrains such as those found at the Oak Ridge Reservation (ORR) raises concerns about the representativeness of groundwater samples obtained utilizing commonly prescribed sampling procedures and monitoring well construction specifications. Within these fractured shales and carbonate rocks, the majority of ground water flux within the saturated zone moves through a network of fractures that comprise only a very small percentage of the pore volume in the ORR aquitards (Solomon, et al., 1992). These fractures provide pathways for rapid transport of contaminants at velocities orders of magnitude greater than those in the low permeability matrix. Purging large volumes from low yield formations is likely to incur a large radius of influence due to the low percentage of porosity contained within high permeability fractures. This means that samples that will likely contain fracture fluids from outside of the local region, and pumping may even cause contaminants to move through the system at accelerated rates and along abnormal flow paths. In addition, monitoring wells are generally constructed using large screened intervals that may not intersect any active fracture zones or may intersect multiple fracture zones representing very different flow paths. Thus, standard well construction can mask the vertical distribution of contaminants and prevent discrimination of contributions from the matrix and from the various fracture zones.

In order to define "representativeness", one must take into account the flow system characteristics. Temporal variability in water quality may be related to seasonal and/or storm-related changes in recharge, and understanding the causes and degree of variability is a necessary prerequisite to determining an appropriate sampling schedule. The spatial variability of groundwater quality within fractured rocks is likely to be enhanced by the discrete nature of the fracture flow paths. An understanding of the heterogeneous characteristics of the formation is critical to establishing an appropriate spatial distribution of monitoring points, both vertically and laterally. In addition, representativeness will depend on the purpose of the measurement. If the goal is to establish immediate off-site risk, for example, then mass flux through active transport zones (ie, fractures or fracture zones) is the measurement target. On the other hand, if the goal is to determine the resident contaminant mass (contaminant concentration times porosity) within the rock matrix for planning cleanup measures, then the sampling method must account for the possibility that the fracture fluids may not be at equilibrium with matrix concentrations.

Recent investigations have focused on examining the potential for colloid mobilization within the groundwater system due to high purge and sampling rates (McKay, 1993). Adsorption of contaminants onto colloid surfaces may result in misleading analytical results if the colloids are immobile at in situ flow rates but are mobilized because of high purge and sampling rates. Thus, representative sampling in the presence of colloids needs to take the in situ flow rate into account as well as factors previously mentioned.

The manner in which sample representativeness is determined within fractured media has not been well defined. Purging three well volumes has been standard procedure for compliance monitoring on the ORR. This practice was designed to ensure that the sample reflects true formation water and is a reasonable practice for high yield wells where disposal of contaminated purge water is not an issue. More recently, the Environmental Protection Agency (EPA, 1992) has suggested "purging to parameters", a practice that uses stabilization of water quality parameters such as turbidity, redox, and dissolved oxygen as a measure of representativeness. However, it is not clear that stabilization of these parameters is an indication that the sample is representative of groundwater within proximity of the well. Moreover, EPA (1992) monitoring-well construction recommendations do not specifically address the special issues related to sampling from fractured rocks.

The results of this study will be used to provide input to DOE and the regulatory community on decisions regarding monitoring strategies. It is anticipated that some results could be generalized to other locations where fracture flow dominates.

2. SITE HISTORY

The field site chosen for this project is located in west Bear Creek Valley, near the intersection of Highway 95 and Bear Creek Valley Road (Figure 1). The site is underlain by the Upper Cambrian Nolichucky Shale, an assemblage of interbedded shales and limestones. Bedding in this area dips approximately 45° to the south, with respect to the ORR administrative coordinate system. Some historical information about flow characteristics within the study region was available prior to the onset of field activities. The field site is situated adjacent to a second research site where a Rhodamine WT tracer test (Lee et al., 1992) and ongoing noble gas tracer tests (Sanford et al., 1994) have been conducted. Results of these tests have demonstrated both the phenomenon of very rapid transport of tracers along discrete strike-parallel fracture flow paths, and retardation of the center of mass of the plumes resulting from diffusion of tracers into the relatively less mobile matrix porewater.

A network of wells was installed in 1987 for the purpose of conducting a pump test as part

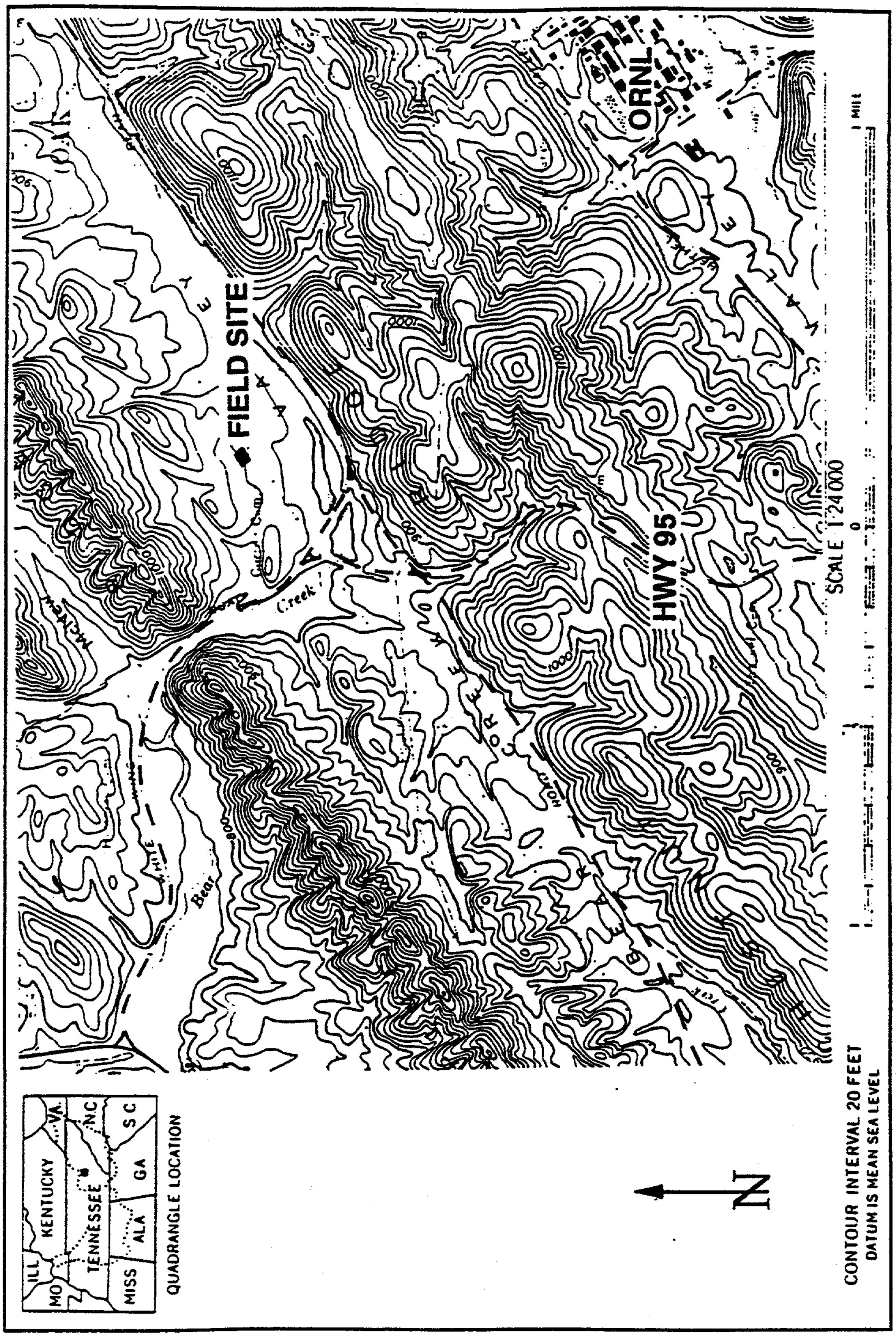

Figure 1. Field site is located in west Bear Creek Valley on the Oak Ridge Reservation.

of a valley-wide site characterization (Gierke et al., 1988). This network, shown in Figure 2, consists of an injection well, screened from depths of 20-70 ft , and three well pairs located updip, downdip, and along strike of the injection wells. For each well pair, the shallow well is screened from 15-25 ft and the deep well is screened from 60-70 ft. All depths are referenced to land surface. Results of the pump test indicated anisotropic drawdown with elongation parallel to strike (Figure 3), and an estimated anisotropy ratio of approximately 8:1. Bulk hydraulic conductivity values over the 54-ft saturated thickness of the pumping well ranged from 2.5 x 10^{-3} cm/s to 5.5 x 10^{-5} cm/s, with a geometric mean of 3.4 x 10^{-4} cm/s. Estimates of storativity ranged from 6 x 10^{-5} to 3 x 10^{-3}. Gierke et al. (1988) also noted a strong vertical anisotropy governed by strike and dip as well as indications of fracture flow in the shallow bedrock, and emphasized the "need in future tasks to more closely examine the role of discrete fractures".

3. PRELIMINARY SITE CHARACTERIZATION

Preliminary tracer experiments using the existing screened wells were conducted prior to the start of intensive field activities. In March, 1994, helium and bromide tracers were injected into GW462 to further characterize groundwater flow and transport dynamics and to establish tracer plumes that could be used to identify active transport pathways as well as to provide a surrogate "contaminant" for later sampling activities. Manual water levels were obtained 2-3 times weekly in conjunction with sampling events.

3.1. Hydraulic heads

Water level data are listed in Table A1 and summarized in Figure 4. In all cases, an upward gradient exists within each of the well pairs. The well hydrographs show both seasonal and precipitation-related variations. Large responses are observed in conjunction with storm events during both winter and summer seasons. The steep decline in water levels in April is due to evapotranspiration during rapid development of foliage. Hydraulic heads within wells GW457, GW462, and GW458 are identical over most of the time of record, reflecting the hydraulic connection seen in the pump test results as reported by Gierke et al. (1988). This hydraulic connection is consistent with the geometry of the well locations relative to the bedding dip. A bed-parallel fracture zone intersecting the shallow updip well (GW457) could pass through the injection well (GW462) and intersect the screened interval of the deep downdip well (GW458).

The horizontal component of the hydraulic gradients are oriented grid southwest in the shallow wells and grid south in the deep wells as shown by the Rose diagrams in Figure 5 (Schreiber, 1995). Gradients were calculated for each day that a set of water level measurements was obtained. Flow directions were then calculated using the 8:1 anisotropy ratio of Gierke et al. (1988).

The seasonal fluctuation in the water table, estimated from water level measurements in the shallow wells, is approximately 10 ft. The depth to water in the shallow wells ranges from

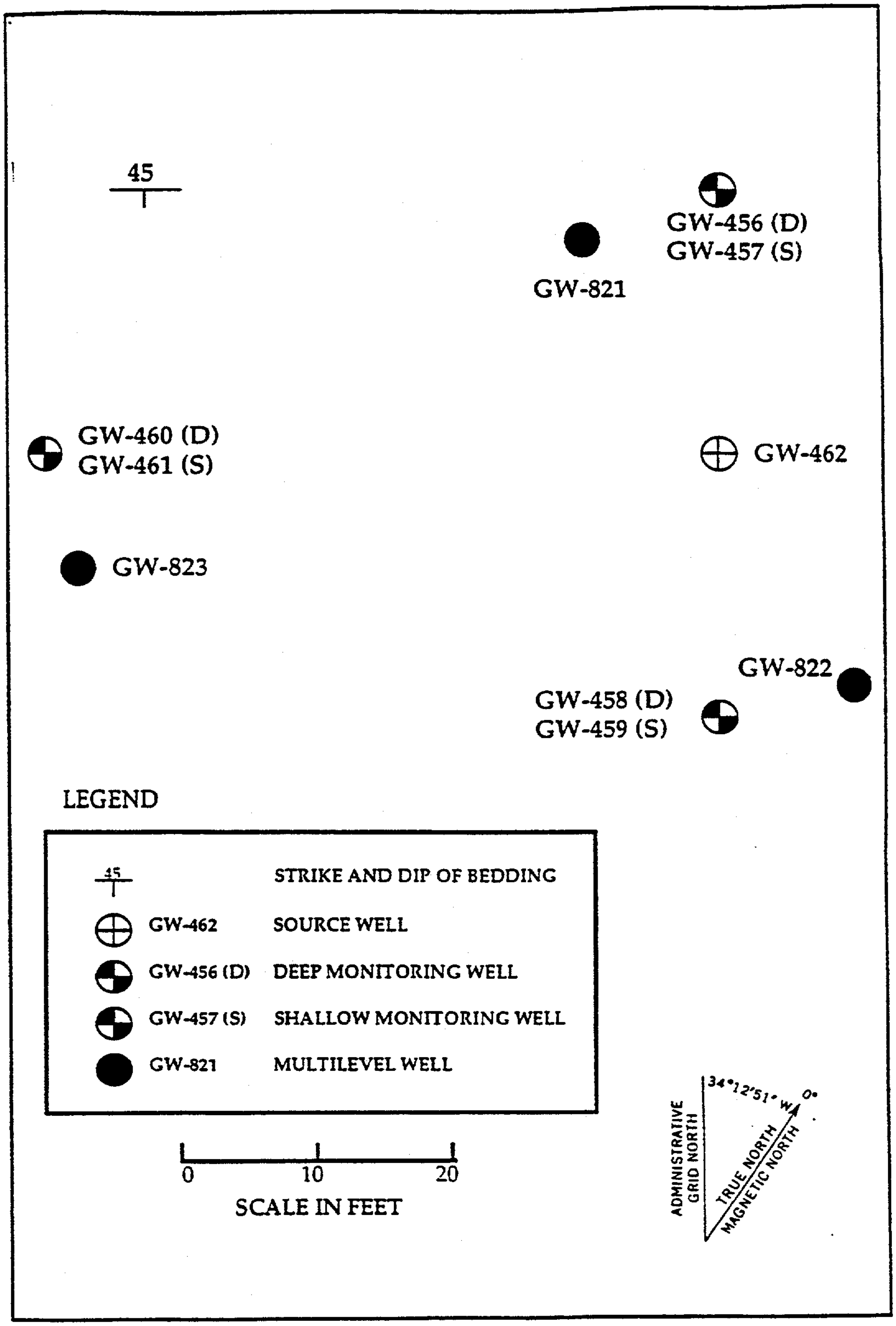

Figure 2. Location of screened and multilevel wells.

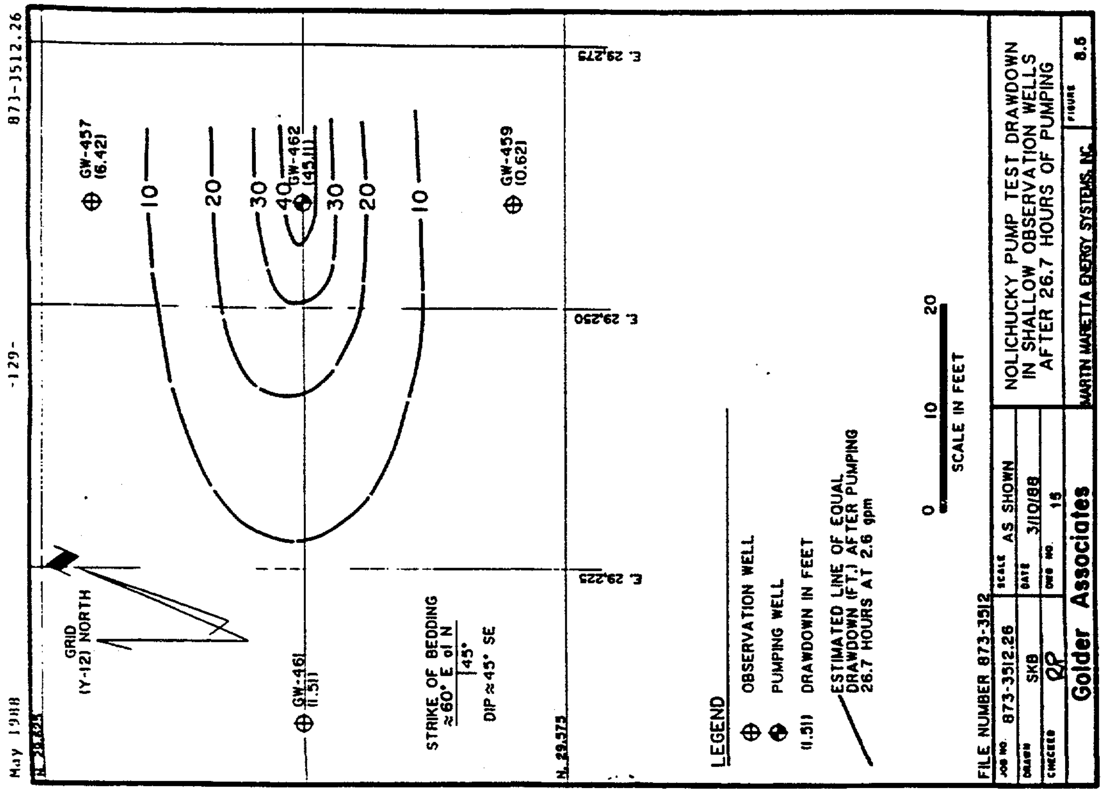

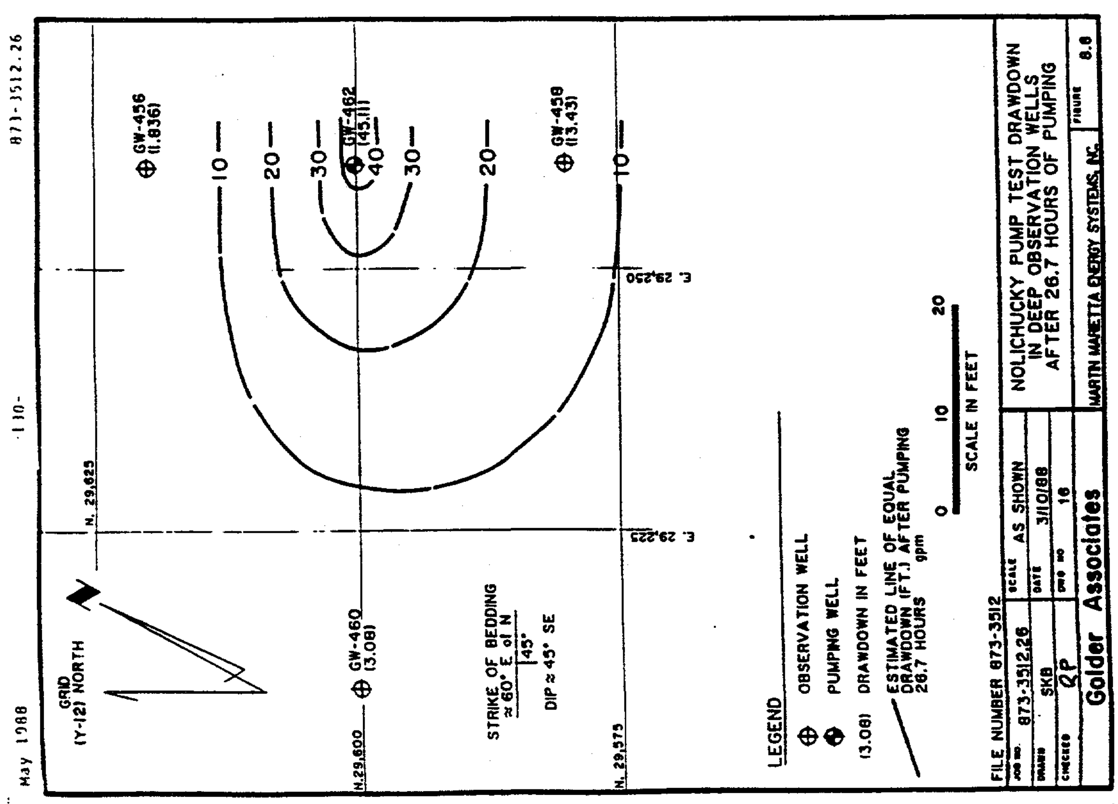

Figure 3. Results of a 1988 pump test indicating anisotropy elongated along strike (Gierke et al., 1988).

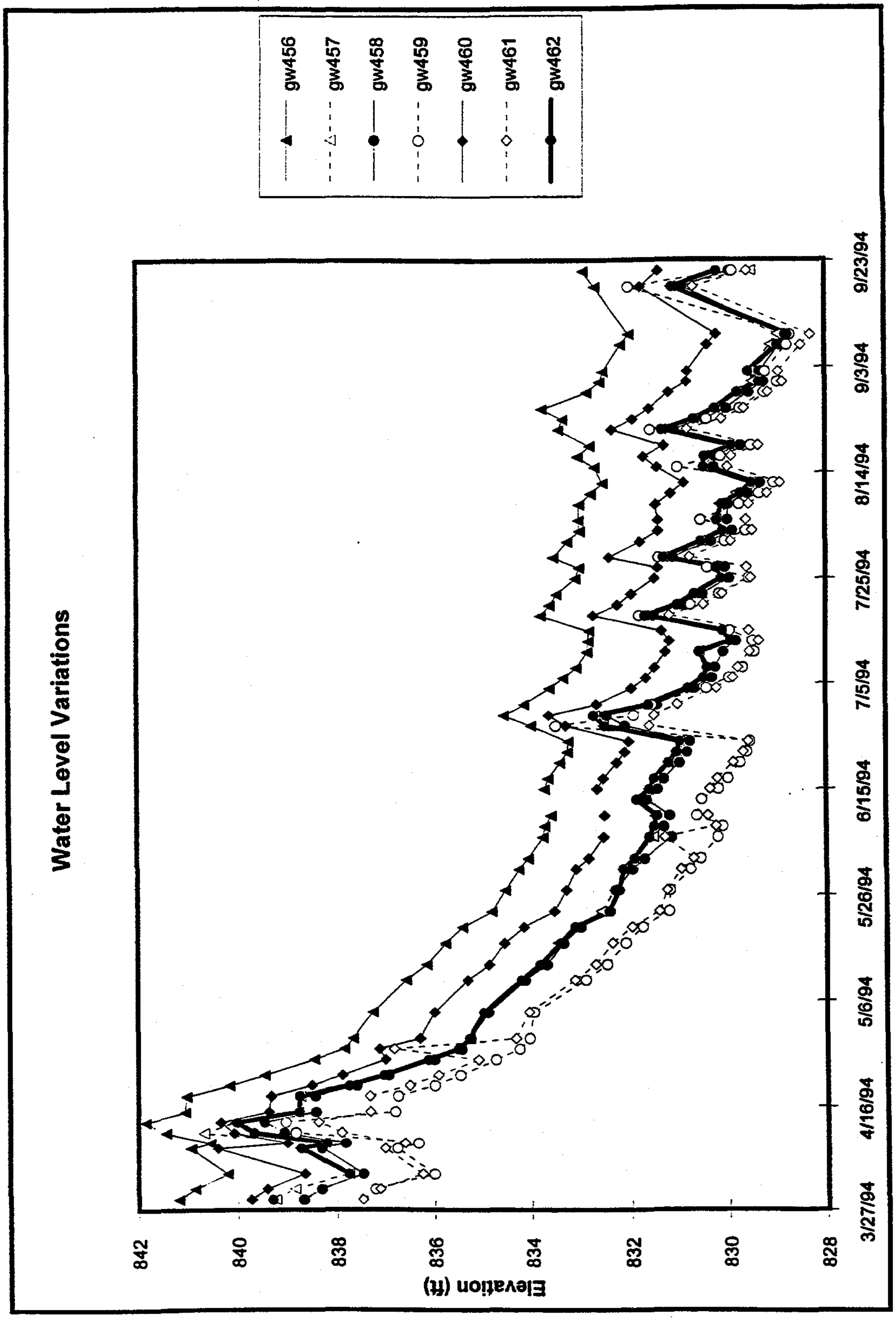

Figure 4. Water levels in screened wells showing seasonal and storm fluctuations.

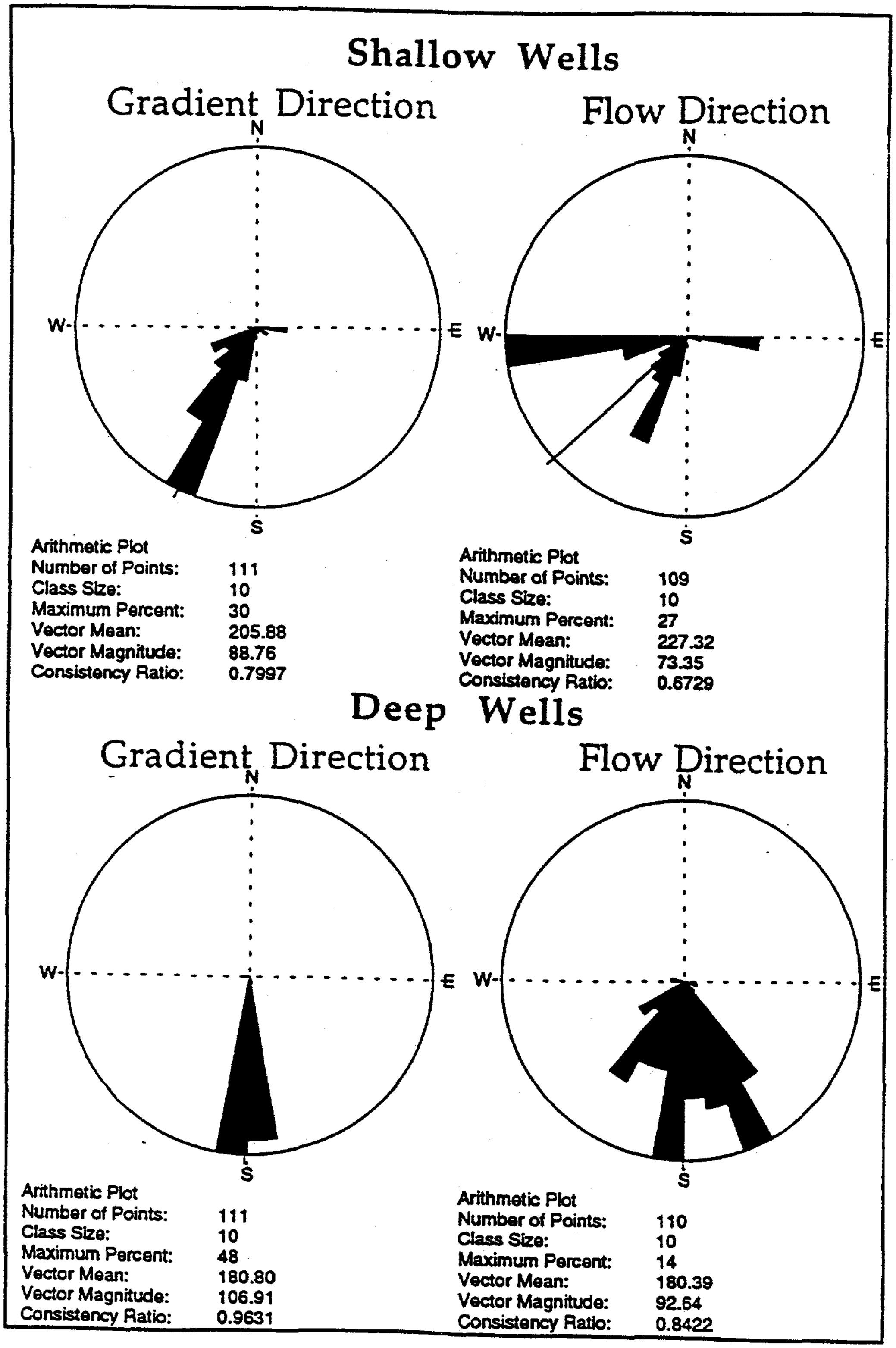

Figure 5. Rose diagrams showing hydraulic gradient and flow directions, assuming 8:1 anisotropy ratio parallel to strike (Schreiber, 1995). Directions are relative to the ORR administrative grid. Single lines represent the vector mean..

roughly 2-5 ft below land surface (BLS) in the winter to approximately 12-15 ft BLS in the summer. In the hydrologic conceptual model for the ORR (Solomon et al., 1992) this range of seasonal fluctuation is identified as the water table interval, the bottom of which roughly corresponds to the top of bedrock. Because of the strong upward gradients and the depth to water relative to the top of the well screen, it is likely that these depths slightly underestimate the depth to the actual water table.

3.2. Helium tracer test

The purpose of the helium tracer test was to provide a means for studying the natural gradient flow dynamics at the field site prior to initiation of other field activities, and to provide a means for assessing of the impact of those activities on flow and transport. Helium injection began on March 25th, 1995, and has continued up to the time of this report. The gas injection system consists of a compressed helium source connected to 400 ft of 1/16-in Teflon tubing that has been wrapped around 1-in diameter PVC screen and placed in the injection well (after that described by Sanford et al., in review). The tubing, which extends from 20-60 ft depths, provides a high surface area for diffusion of gas into the groundwater. Filter wrap was placed over the tubing-wrapped portion of the PVC to force gas bubbles up the central PVC screen and prevent them from blocking the outer well screen at the screen pack. Moderate flow of gas through the injection tubing results in diffusion to saturation levels, with saturation being governed by the temperature of the groundwater in the presence of adequate gas flow.

Helium concentration in the injection well and the six observation wells was measured three times weekly using specially designed gas samplers (Sanford et al., in review). These samplers consist of two parts: a length of copper tube that is sealed at one end and silver soldered to a tire valve stem at the other; and a length of silicon tubing filled with clean sand that is sealed at one end and contains a valve stem cap at the other that has been drilled to allow the passage of gas. When the two portions of the sampler are attached, dissolved gases diffuse through the silicon tubing and fill any void space, coming to equilibrium with groundwater concentrations within 1.5-2 days. The valve stem is held open by placing a small ball bearing in the valve cap prior to attachment. When the sampler is extracted from the well the silicon tube is disconnected, allowing the valve to close and preventing loss of the gas from the copper tube. Gas is then injected directly from the copper tube into a gas chromatograph for analysis. For this study, samplers were suspended in the middle of the screened intervals and allowed to equilibrate over a minimum of 2 days.

Helium concentrations in the source and observation wells are summarized in Table A2. Concentrations are recorded as area counts per minute rather than as absolute concentrations. However, because these area counts are linearly related to absolute concentration, C/C_0 can be calculated by dividing the area counts from an observation well sample by the area counts in a source well sample. Figure 6 shows the time-averaged concentration of helium in the source well as area counts. Averages were determined at

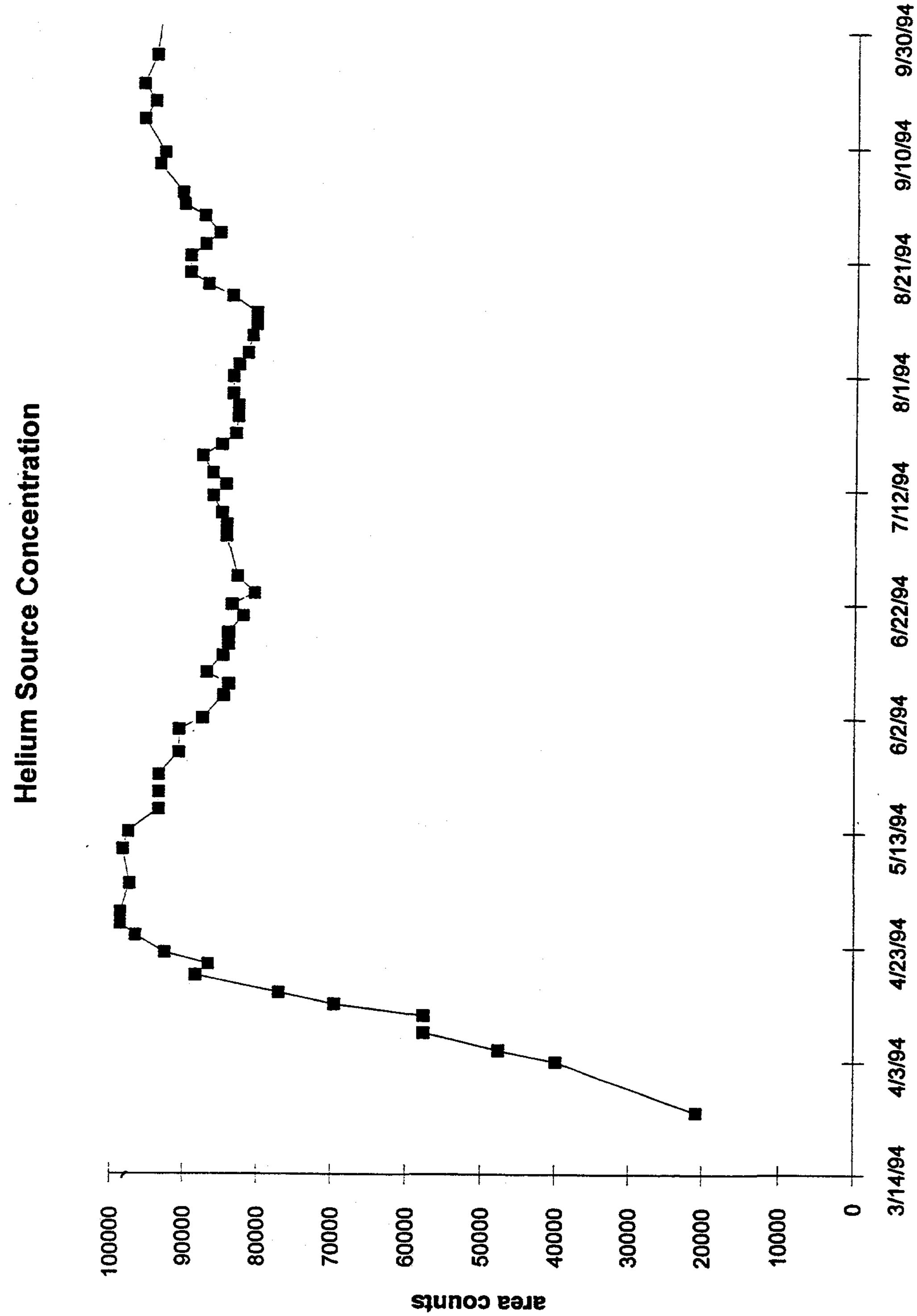

Figure 6. Time-averaged helium concentrations in the injection well, as expressed in area counts.

any given time using all previous measurements. Saturation (peak average concentration) occurred 33 days after initiation of the injection, although actual concentrations rose very quickly. A moderate decline beginning in mid-May could be due to an increase in groundwater temperature and concomitant decrease in saturation levels.

Cumulative averaging results in considerable smoothing of the concentration curve and masks the actual fluctuations in the data. The majority of these fluctuations can be attributed to measurement error caused by leakage through the valve stem (low value), leakage of water into the sampler (low value), or possible attachment of gas bubbles to the sampler tube (high value). Apparent leakage occurred on occasion even when the analyses were completed by the following day, evidenced by an impossibly low apparent concentration in the source well or by the absence of background gases such as argon that are normally present in all samples. Additional sources of fluctuation are variations in the flow rate of helium, since flow is controlled only by outlet pressure from the tank, and groundwater flux into the injection well. Flushing of the well during heavy rains will cause dilution of the source concentration. For these reasons it was felt that the cumulative averages were a better reflection of the source concentration "seen" by the observation wells than the measured concentration at any given point in time, and these were used for the calculation of C/C_0.

Helium concentrations in the observation wells are shown in Figure 7. Low but detectable concentrations of helium were observed in all six observation wells only a short time after the injection began. As seen in Figure 8, these fluctuations correlate with fluctuations in water levels in response to storm events. Helium was observed in well GW458 and GW460 during the first round of measurements on April 3rd, nine days after the start of injection. This corresponds to a minimum groundwater velocity of 0.68 and 1.7 m/day, respectively. These observations are consistent with rapid transport of small volumes of helium-saturated groundwater through discrete fracture zones. That the helium is observed in the updip wells is somewhat enigmatic, since all measurements show this to be in opposition to the hydraulic gradient. The difficulty in explaining this phenomenon is due to the low frequency of water level measurements and to the 2-day equilibration time required for the passive gas samplers. Thus, rapid transient events may not be fully recorded. Continuous water level monitoring and additional tracer tests with real-time sampling will provide a better understanding of these dynamics.

The majority of transport thus far has occurred along strike, as evidenced by the breakthrough curves shown in Figure 7. The large variations in C/C_0 are most likely due in part to the measurement error previously described. In addition, some sharp decreases may be due to dilution associated with flushing during storm events, a phenomenon observed during noble gas tracer tests elsewhere in Bear Creek Valley (Sanford et al., 1994), and due to drilling and borehole test activities conducted late June through August. Helium has persisted in both along-strike wells since May 15th, corresponding to a groundwater velocity of 0.28 m/d at the front of the tracer plume. Concentrations in the along-strike wells five months after the start of injection are still orders of magnitude lower than the

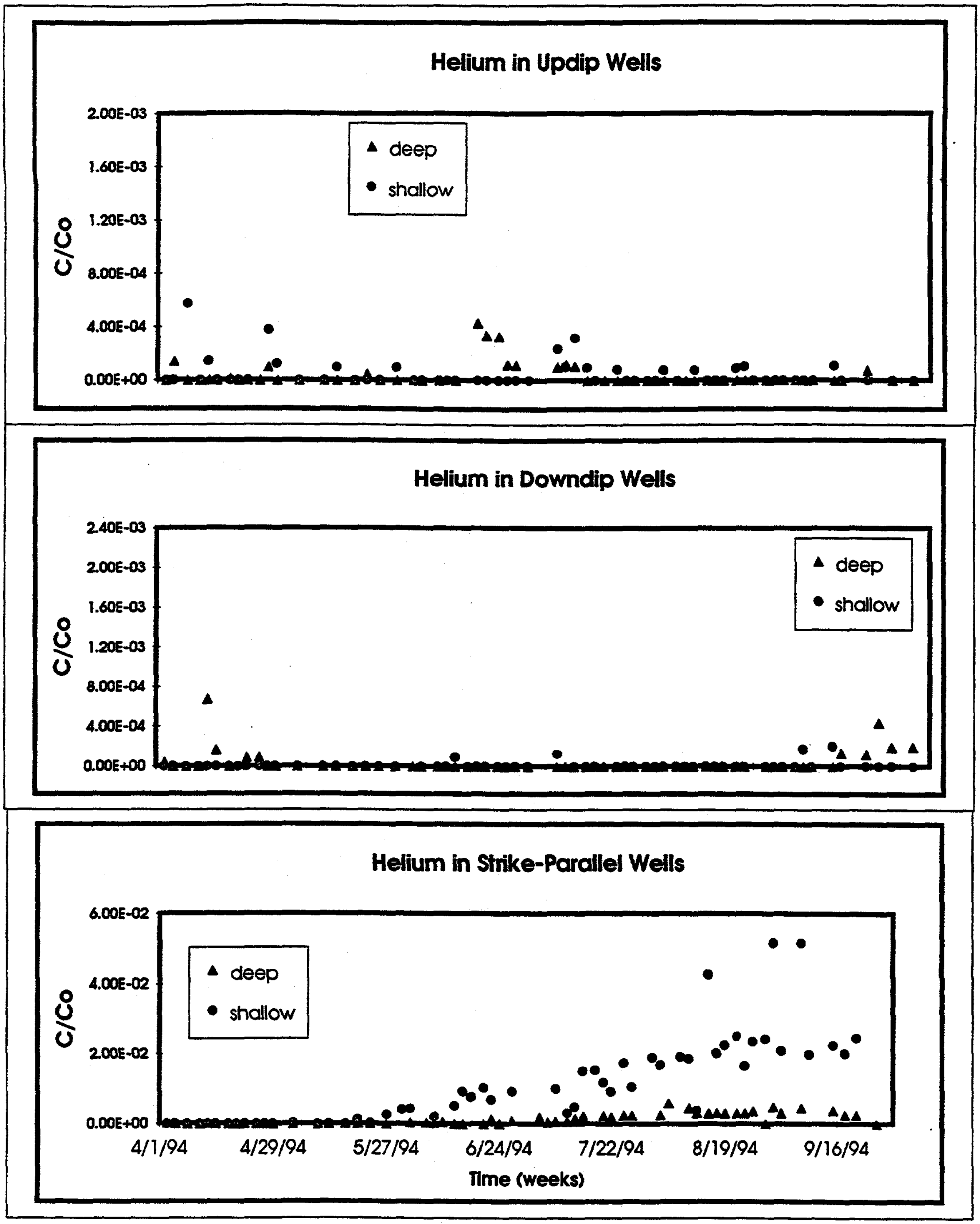

Figure 7. Helium concentrations during an eight-month period in the six observation wells showing strike-preferential transport.

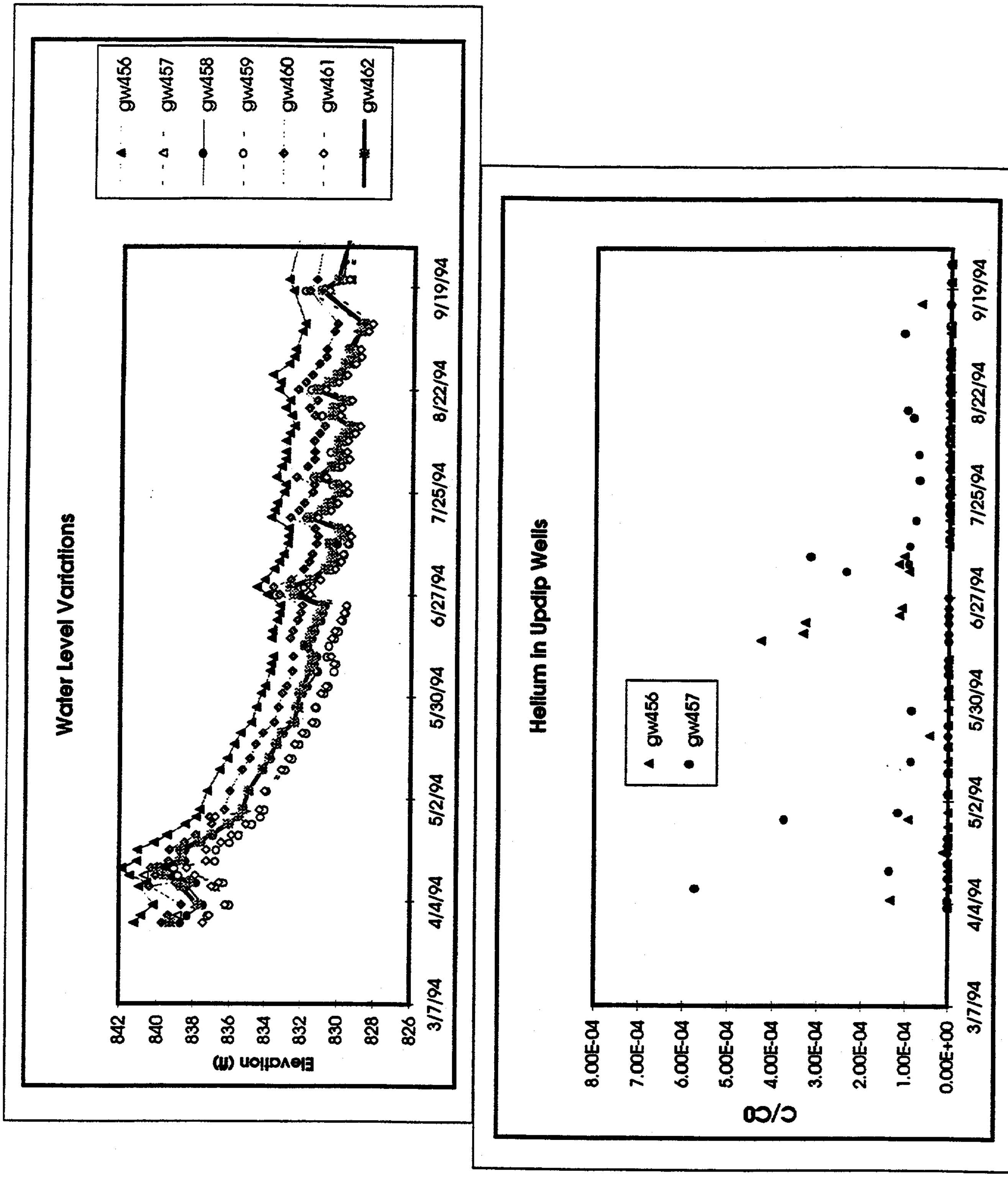

Figure 8. Sporadic low-level concentrations of helium appearing in the updip wells correlates with storm events, as evidenced by correlation with water level fluctuations.

source concentration in spite of very early breakthrough via fracture flow paths, indicating significant retardation as a result of matrix diffusion. While the majority of helium transport is parallel to strike, the occurrence of helium both up and down dip in conjunction with precipitation events suggests that flow system dynamics are very complex, perhaps varying with seasonal precipitation patterns, and most certainly resulting in increased lateral dispersion.

3.3. Bromide tracer test

The purpose of the bromide tracer was to chemically tag the active flow zones with a tracer that can be easily measured from groundwater samples and to establish a plume for testing sampling methodologies. Bromide was introduced into the source well as a single slug injection on April 11th. In order to minimize the impact of head and temperature changes, a bromide slurry was created by removing several bailers of water from the injection well, mixing with 1 kg $MgBr_2 \bullet (H_20)_6$, and reinjecting the slurry into the well. The water within the well casing was then circulated by slowly raising and lowering a bailer to ensure adequate mixing and to minimize density flow, and a grab sample was obtained for measuring the source concentration. All samples were obtained by taking a bailer grab from the screened interval. No purging was done prior to sampling, and all water left in the bailer after obtaining a small volume for sampling was reintroduced into the well in order to minimize disturbances to the flow system. Samples were analyzed using a specific ion probe with a quantitation limit of 2 ppm. For each round of analyses, the probe was calibrated using known standards, and was periodically rechecked during the analyses.

Bromide concentrations are listed in Table A3. While actual numbers for values less than 2 ppm are shown, the quantitation limit of the probe requires that these values be treated as censored data (< 2 ppm). However, these numbers do indicate a significant (albeit unquantifiable) concentration, and for this reason they are reported with the above-mentioned qualifier. In all but one of the observation wells, bromide was undetected. In the shallow along strike well (GW461), low concentrations of bromide have been observed since June 15th. Again, these numbers are below the quantitation limit of the probe and therefore cannot be taken as absolute concentrations, but can be used as indicators of the presence of bromide. This data would indicate a velocity of 0.23 m/d at the front of the bromide plume, consistent with the results obtained from the helium data for the same well. However, because of the mixing and dilution effect that is likely to occur within the well casing and the lack of any purging prior to sampling, the inability to detect bromide in most of the observation wells does not necessarily indicate that bromide is not present.

Decay of the source concentration of bromide is illustrated in Figure 9, where it is plotted as the negative log of C/C_0 versus time. The curve shows an initial rapid decay, followed by a more linear decrease, and finally a levelling off to a very small decline over time. The initial rapid decrease is most likely due to diffusion into the matrix driven by a high concentration gradient. The subsequent linear decrease is consistent with advective transport from the well, with later levelling off as elution from the secondary source in the

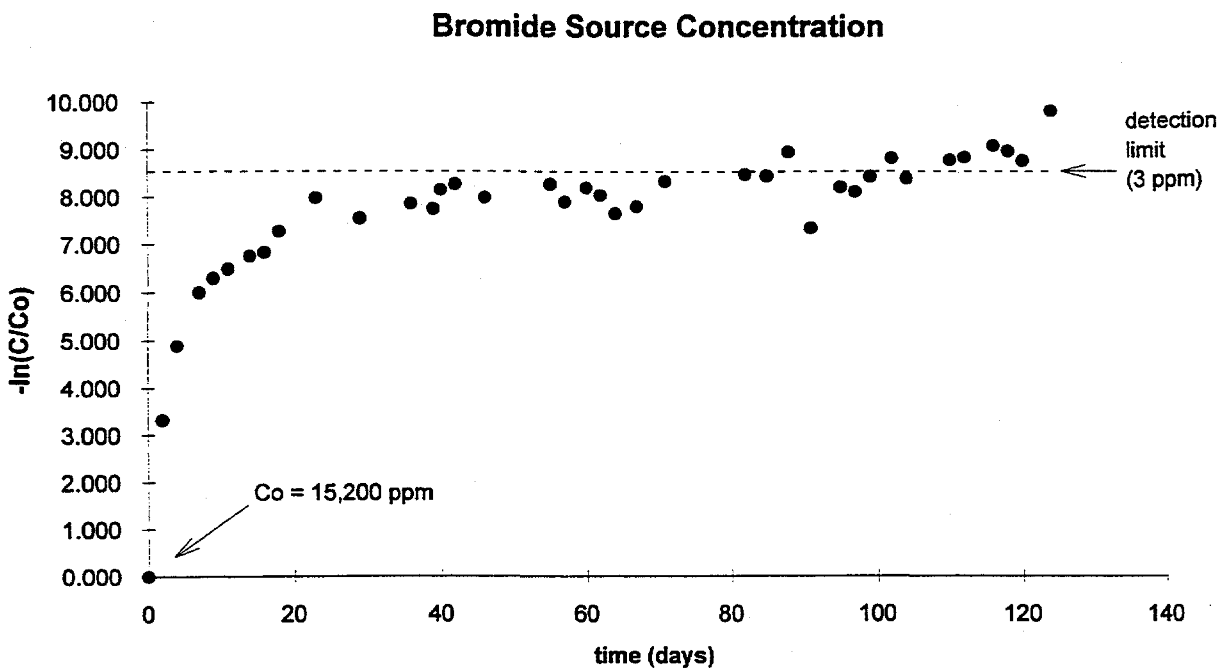

Figure 9. Bromide source concentration decayed rapidly during the first week, then leveled off after approximately one month, consistent with elution from the matrix.

matrix adjacent to the well provides a continual low-level bleeding of bromide. A specific discharge of approximately 1 cm/d through the cross-sectional area of the screened interval can be calculated from the early linear portion of the curve using the point dilution calculation described in section 5.3.

4. DRILLING AND CORING

4.1. Rotasonic™ drilling

In order to determine the vertical variability of pore water chemistry as a measure of the degree of groundwater mixing within the system and to identify the characteristics of the transition zone between the highly weathered saprolite and competent bedrock, a special type of drilling and coring was required. The transition zone has been loosely described from other drilling activities on the ORR as the zone below auger refusal but above competent bedrock where good core recovery occurs using rotary methods. Thus, it has been defined on the basis of conventional drilling methods but because of poor recovery the characteristics have not been well described. A transition zone has been described above fractured bedrock in the North Carolina Piedmont (Harned and Daniel, 1989), with higher transmissivity than either the overlying saprolite or underlying fractured crystalline rock. This is consistent with the site conceptual hydrologic model for the ORR (Solomon et al., 1992), which suggests a highly transmissive zone at the top of bedrock that accounts for nearly all of the groundwater flux within the saturated system. Harned and Daniel (1989) account for the increased transmissivity by a greater degree of fracturing than the underlying bedrock and lesser degree of weathering (and therefore reduced clay content) than the overlying saprolite. These, then, are characteristics that we would expect to observe in cores from the ORR.

On June 28-30, 1994, three boreholes (GW821, GW822, GW823) were drilled and cored at the site using Rotasonic™ drilling, an acoustic method that combines high frequency vibration with slow rotation. It has many advantages over conventional rotary drilling, including drilling speed, waste minimization, continuous core recovery, and the use of minimal drilling fluid (Godsey, 1993). The Rotasonic™ technique used cuts a 3.75-in diameter core, leaving a 4.5-in diameter borehole. This technology was chosen primarily because of the potential for obtaining nearly continuous recovery of core without the use of drilling fluids that might affect the porewater chemistry.

The Rotasonic™ drilling method proved to be only partially successful. Dry coring through the saprolite and transition zone was very successful, resulting in nearly complete recovery of undisturbed core. However, once the first competent shale was encountered the penetration decreased dramatically and the core was heavily damaged by vibration. A decision was made to drill with water below this point to preserve the quality of the core. In this report, top of bedrock is defined as beginning with the first dark grey shale encountered, and is coincident with the onset of markedly slowed penetration during dry drilling. This shale was encountered at approximately 19 ft in GW821, 31 ft in GW822, and 25-27 ft in GW823. If this marks the top of a continuous stratigraphic layer, then it represents a 30° dip, somewhat less than the 45° dip reported by Gierke et al. (1988). It is likely that these depths to top of competent bedrock differ from than those that would be determined using auger or rotary drilling, highlighting the problem posed by defining subsurface characteristics based on a particular drilling technology.

Borehole collapse occurred where very wet, highly fractured zones occurred above competent bedrock. This problem was probably exacerbated by using a vibrational drilling method. Extremely wet silty sand intervals were encountered from 18-19.5 ft in GW821, from 16-18 ft, 19-21 ft and 24-31 ft in GW822, and from 11-14 ft and at 17 ft in GW823. The borehole testing needed for the identification of multilevel sampler locations required that the boreholes remain open and uncased for two months after drilling. For this reason, temporary steel casing was installed in each of the boreholes from the ground surface through the transition zone to the top of bedrock after the holes were reamed out to a 6-inch diameter. Unfortunately, this rendered the zones above bedrock inaccessible for borehole testing. However, sampling ports were set within the transition zone as the casing was pulled during multilevel well installation.

Total depths for the three boreholes were 50 ft for GW821 and 70 ft for GW822 and GW823. Numerous problems were encountered during the drilling of GW823, primarily due to a heavily fractured zone from 46-49 ft. Core recovery through this zone was hampered by the inability to obtain a competent plug at the base of the core barrel, and significant washout and sloughing resulted in infilling of the bottom 10 ft of the borehole. The sloughed material was later cleared during well installation, but caused the borehole testing to be limited to a depth of 60 ft in this well.

An additional complication occurred because the mechanism by which the core sample was extruded from the core barrel resulted in compression of the sample. When the core barrel on the Rotasonic™ rig is brought up from the hole, the drill head is angled out for ease of core removal. A plastic sheath is then placed over the end of the barrel and the core barrel is vibrated to release the core sample into the bag. This causes any loose fragments to settle and open zones to compact within the plastic sheath, although the relative position of the rock material is retained. This was primarily a problem for zones that were wet drilled, where clays that develop due to weathering in the fracture zones are washed out in the process of drilling. For this reason, there is some uncertainty associated with depths assigned to core segments from the wet-drilled portions of the borehole.

After removal from the core barrel, the sheaths were cut open and the cores were measured, labelled, photographed, and briefly described in the field. After surveying for organic and radioactive contamination by Y-12 Plant Health Physics personnel, the cores were tightly wrapped in plastic sheeting to prevent desiccation and transported to the ORNL core barn for more detailed logging.

4.2. Core logging

Core logs describing the characteristics of the soil, saprolite, transition zone, and bedrock are presented in Appendix B. The depths of the intervals are approximate below the competent bedrock, since the cores were often compacted and/or there was not full recovery. Cores were held in the core barrel by dry drilling several inches at the bottom of each interval to obtain a tight plug. Since the depth of this core plug at the bottom of each interval was known, all compaction occurred above that point, and depths were assigned relative to the bottom of each interval without accounting for compaction. Thus the core logs overestimate the amount of incomplete recovery and assign all loss to the top of each cored interval. Open fracture zones were identified based on the presence of iron and manganese oxides on the surfaces of the core fragments.

The core lithologic sections are depicted by the diagrams in Figure 10 (Schreiber, 1995). In general, the topsoil, characterized by a dark brown color and organic matter, is approximately 6 in thick. The saprolite, or weathered bedrock, which retains the bedding characteristics of the shale bedrock, was observed from the soil zone to the bedrock. In general, the saprolite is comprised of olive to reddish-brown silty sand and clay, with shale bedding and weathered greenish-grey shale fragments. Heavy oxide staining is present on both the surface and inside of the saprolite core. The orange-red staining is assumed to be iron oxide and the darker brown/black staining is thought to be manganese oxide; however, more detailed mineralogical study will be performed to confirm this.

The bedrock underlying the site is the middle section of the Cambrian Nolichucky Formation, a dark grey to greenish-grey to reddish-grey shale containing thin carbonate interlayers and calcite (both pink and white) veins. The shale was found to be very weathered and fissile (described as "clay-rich shale" in core logs) in many parts of the core. Although these areas commonly do not contain heavy oxide staining, it is likely that some are transmissive zones based on borehole tests (described later). Other zones of more competent shale are heavily oxidized on some surfaces and are thought to be fracture zones. Oolitic limestone layers characteristic of the middle Nolichucky were encountered in each core and are more competent and less weathered than the shale. In general, red-orange staining was observed on fracture surfaces in the shale, and black staining was found on fracture surfaces in the oolite. Since competent core pieces were difficult to obtain and the core was not oriented, strike and dip of bedding planes and fracture zones could not be determined. However, bedding planes observed in a few of the intact core segments are consistent with the 45° dip reported by Gierke et al. (1988).

Several major flow zones can be inferred from the core log descriptions and are identified in the core logs (Appendix B). The saprolite, which undergoes variable saturation due to seasonal changes in the water table, is heavily iron-stained throughout much of its extent. Because of this, it was difficult to distinguish individual high flow zones on the basis of weathering alone. However, the silty-sand zones described earlier are clearly transmissive zones based on the amount of water encountered during drilling. Because of the

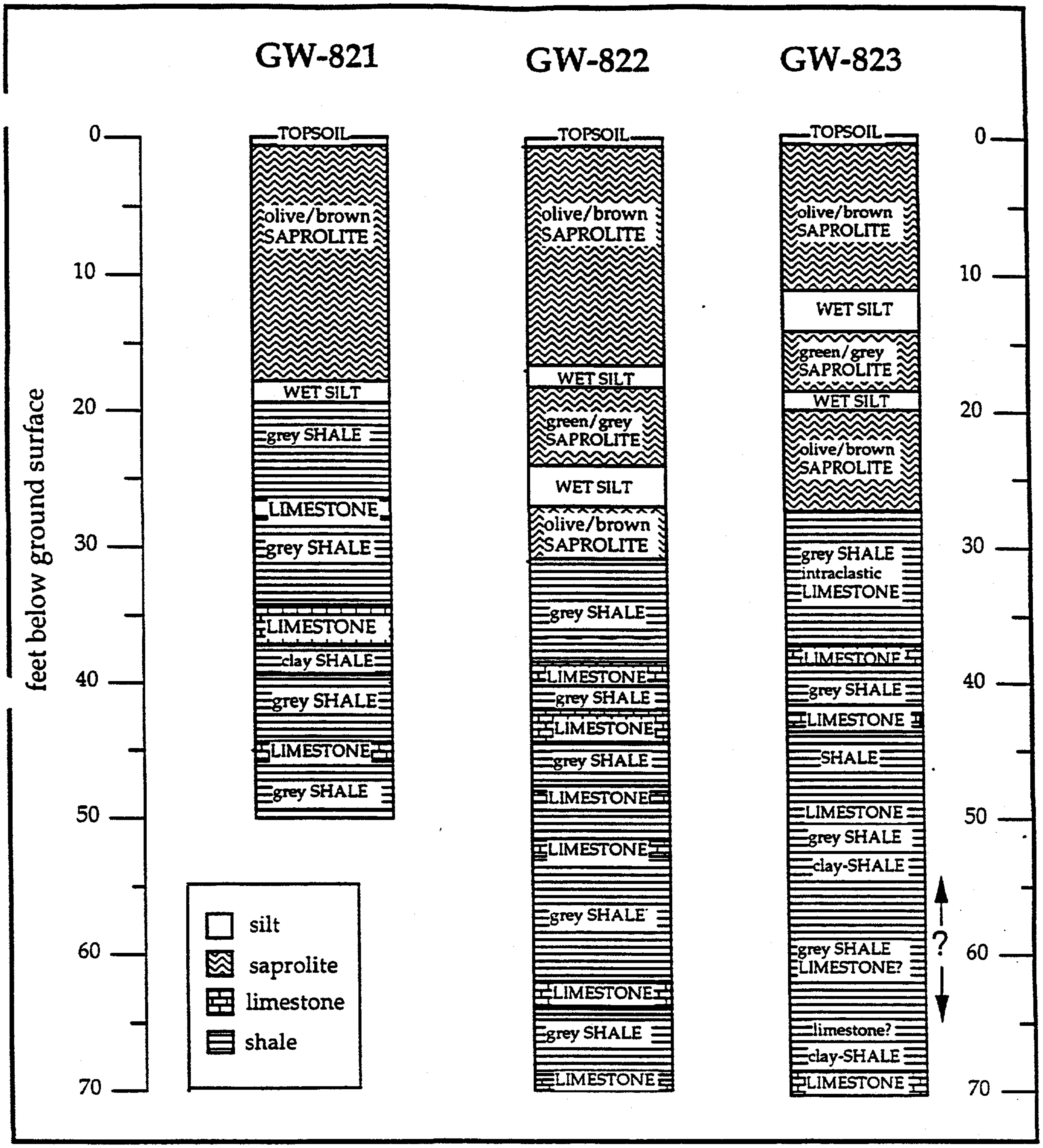

Figure 10. Core diagrams for the three new boreholes.

fragmented condition of the shale below the saprolite, it was difficult to distinguish discrete fractures from fracture zones and even more difficult to place fractured intervals at precise depths within the borehole. Due to the fissile nature of the shale in this location, however, it is likely that fracturing occurred within zones, and in most cases they can be located to within a foot of their actual depth.

5. BOREHOLE TESTS

Borehole tests were conducted in the uncased portion of the boreholes following drilling and coring. The purpose of these tests was to locate and characterize active flow zones. This information combined with that obtained from core logging was used to determine optimal positioning for multilevel sampling ports and for borehole packer sampling.

5.1. Downhole camera

A borehole video camera was used to obtain information about the condition of the borehole walls and to identify individual fractures and fracture zones, bedding, and lithologic units. Due to the size of the borehole, generally only one wall could be seen with good resolution. Thus, while single fractures could be identified, dips could not be estimated. Fracture zones were inferred based on the rugosity of the borehole and the raggedness of the surface. For all three boreholes, the apparent total depth was underestimated using the camera because of the loss of visibility due to silty deposits at the base of the hole and the extension of the camera light well beyond the lens. Major features identified on the video are consistent with core observations.

5.2. Electromagnetic borehole flowmeter tests

An electromagnetic (EM) borehole flowmeter developed by TVA was used in the open interval below the temporary casing to identify the location and relative flow rate of individual fracture zones contributing groundwater flux into or out of the boreholes. The EM flowmeter measures a voltage induced by the movement of ions carried by groundwater as it flows through a metal cylinder containing a magnetic coil that is positioned vertically within the borehole (Moore and Young, 1992). The cylinder is surrounded by a packer that prevents flow from circumventing the cylinder. As the position of the flowmeter is changed, the flow zones are identified by a change in the flow rate between adjacent intervals. Flow can be either ambient or induced by pumping or injection. For this study, both ambient and injection tests were performed.

The equilibrium water level was measured using a pressure transducer and water level meter prior to insertion of the flowmeter into the well. The pressure transducer allowed continuous monitoring of the static water level, in the case of ambient tests, and constant head, in the case of injection tests. The flowmeter equipment is powered by a 120V generator. Pressure and voltage readings are fed directly into a portable computer with a printer attachment, and a specialized software package is used to analyze and record field data in both electronic and hard copy form. At each borehole interval, the voltage was sampled at five-second intervals for a total of 60 sec. The mean and standard deviation of the voltage was calculated for each 60-sec period and recorded along with the flow in L/min (negative for downward, positive for upward) and the transducer reading. If the standard deviation was too high (> 0.005 V) the test was aborted or repeated. Occasionally, a test was accepted if the standard deviation exceeded the acceptance criteria but was small relative to the measured voltage for that test. Periodic high level noise was experienced due, most likely, to the close proximity of the field site to high voltage power lines. Often, testing had to be interrupted until the noise level dropped and the equipment stabilized.

The procedure followed for ambient tests was to first inflate the packer within the cased interval, where no flow occurs, to obtain the zero offset voltage. Tests were then conducted at two-foot intervals starting at the bottom of the borehole. The zero offset was then remeasured at the end of the test in order to adjust for instrument drift. In the case of injection tests, the zero offset was measured either immediately before injection within the cased interval or after injection at the bottom of the borehole. Identical depths were measured for both the ambient and injection tests. A peristaltic pump was used to inject tap water into the borehole to raise the water level. Ideally, a 5-10-ft change in head is desirable, but the most that was obtained for these boreholes was 0.6-0.7 ft even at the highest pump rate possible due to the high specific discharge within these boreholes. The flow rate was adjusted as needed to maintain a constant head throughout the test.

The flowmeter results are contained in Tables A4-6 and are summarized graphically in Figures 11-13. Data were reduced by first removing the zero offset and instrument drift, assuming a linear change over time from beginning and final zero measurements. Injection data were further adjusted by removing the ambient flow measurement for the same interval. In this way, the flow profile for the injection test should reflect a true partitioning of the injection flow rate over the length of the borehole without the interference of natural flow. However, the injection tests for GW823 and, to a lesser extent, GW821 were confounded by intermittent rain during testing that most likely resulted in non-steady-state conditions. Thus, the ambient tests for these boreholes were probably not reflective of ambient conditions at the time of the injection tests. However, a constant head was maintained by frequent adjustment of the flow rate during testing so that the total flow into the well was held constant over the duration of the tests.

Ideally, one would expect the flowmeter survey to produce a series of steps or ramps, increasing from zero at the bottom of the borehole to the total flow rate at the top. For injection tests, this total flow should equal the injection rate. Ramps will coincide with wider zones or dispersed fractures and steps will indicate the presence of discrete fractures or narrow zones. However, the flowmeter data obtained from these boreholes were much more complex, with ambient flow entering and exiting the borehole at different depths and tests being confounded by nonsteady hydrologic conditions. Flow characteristics varied considerably from hole to hole. GW821 (Figure 11) showed very little flow within the uncased interval in either the ambient or injection tests. Because the casing was simply set

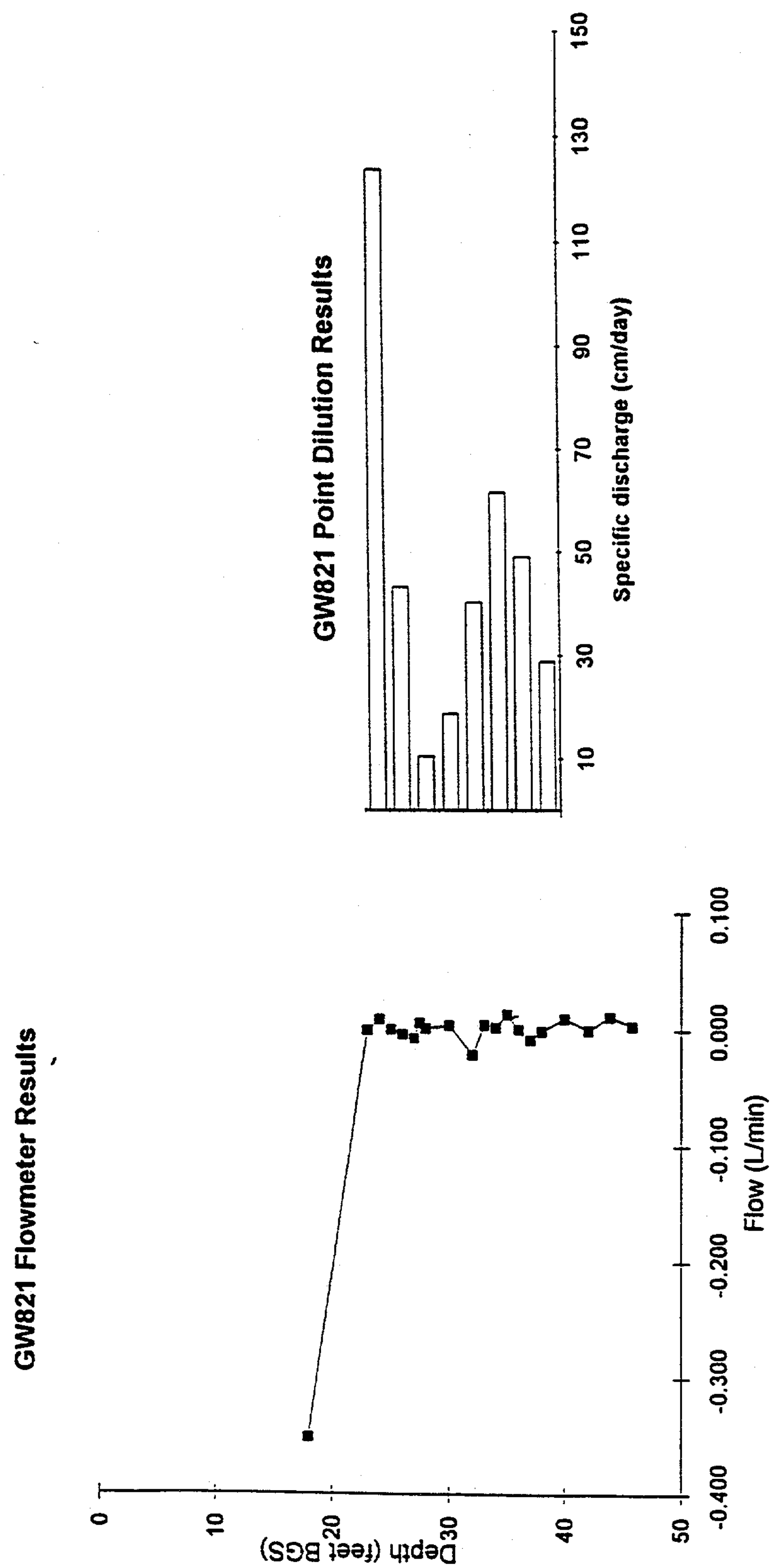

Figure 11. Borehole test results for GW821. Depths scales are aligned.

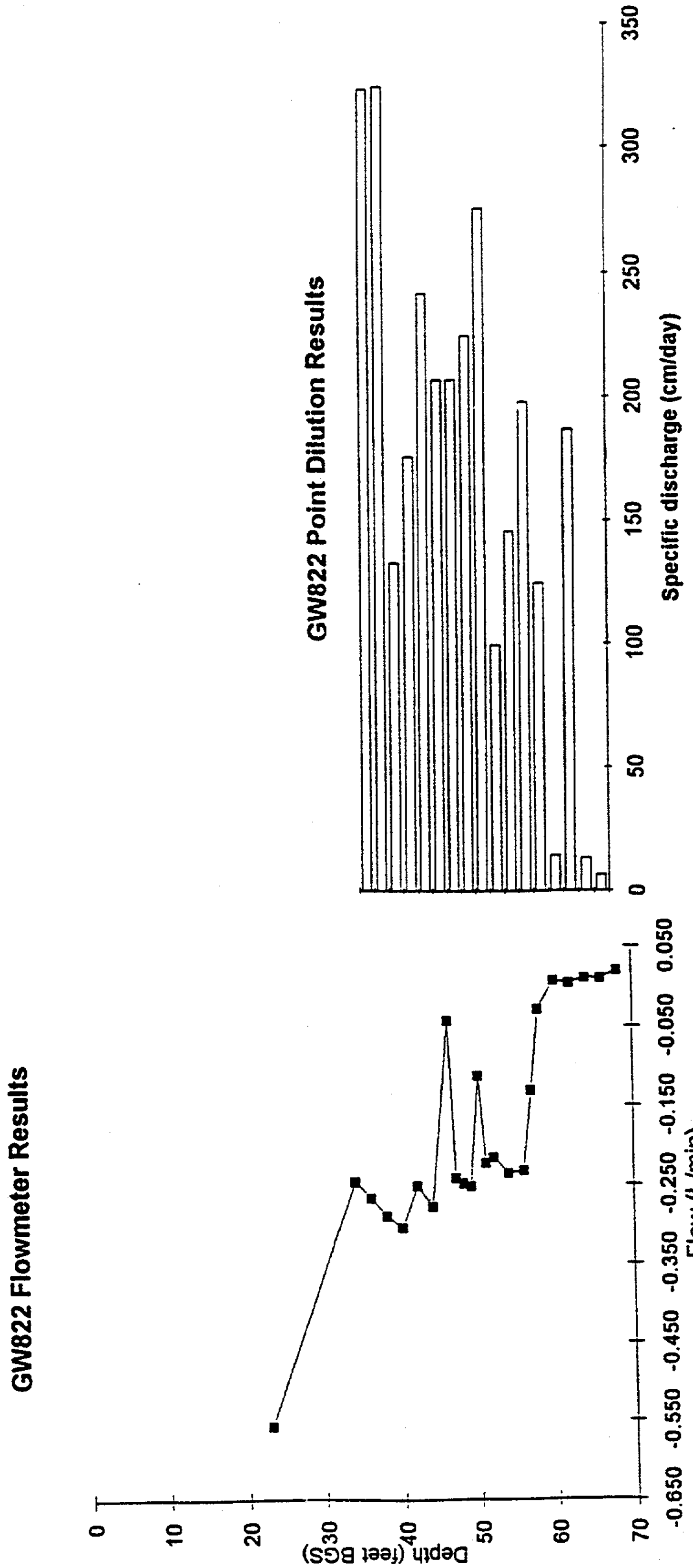

Figure 12. Borehole test results for GW822. Depth scales are aligned.

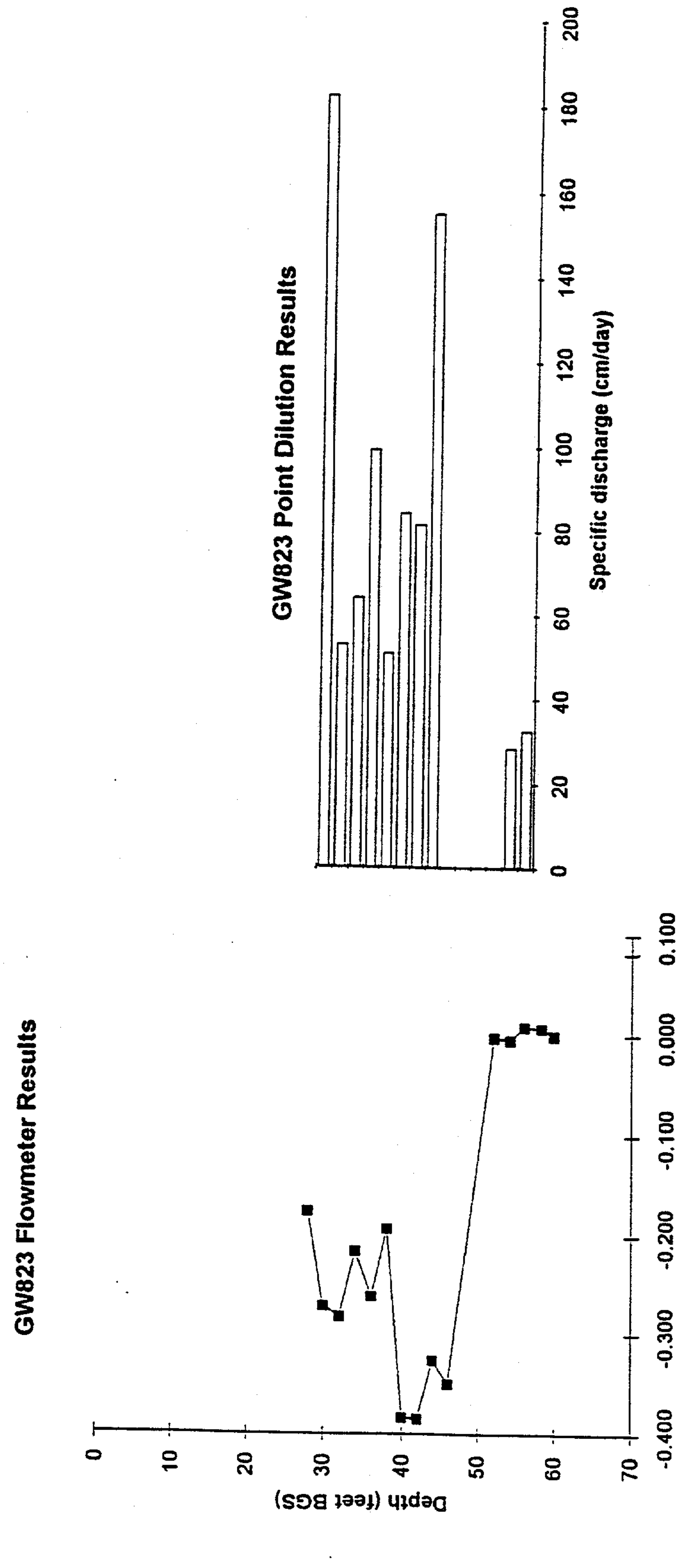

Figure 13. Borehole test results for GW823. Depth scales are aligned.

in place to prevent collapse in the transition zone, there is nothing to prevent water from flowing under the casing and into a very transmissive zone near the base. If most of the flow during the injection test was pirated at the base of the casing, then that would explain why the data nearly mirror those from the ambient test. However, both the borehole video and the core log indicate that fracturing within this borehole is minor compared to the other two boreholes.

GW822 (Figure 12) contains several stepped increases, the most notable occurring between 56 and 58 ft. As in GW821, more than half of the injected flow entered the formation at the base of the casing. Steps in the ambient flow rate coincided very well with fracture zones identified from the borehole video and by iron staining in the core. Two very sharp reversals at depths of 46 ft and 50 ft coincide with ratty, washed out zones noted in the borehole video. These reversals could be due to poor packer seating.

The flow profile for GW823 (Figure 13) was the most difficult to interpret. The tests results are confounded by the impact of rain showers during the time of the test, by having to conduct the test over multiple days (ambient + injection) due to severe background electrical interference, and because of the presence of an enormous washout zone that prevented seating of the packer within that interval. The dramatic shift between 46 ft and 52 ft indicates a large amount of flow is moving out of the borehole through the washout zone. Interestingly, this zone is completely bypassed by the adjacent monitoring well pair, which is screened well above and below the zone, underscoring the need to customize the monitoring well construction at the individual location rather than conforming to a pre-determined design.

5.3. Point dilution tests

Point dilution is a method that provides an estimate of the specific discharge of ground water through specified intervals (Drost et al., 1968; Freeze and Cherry, 1979). The basic field technique involves the injection of a tracer into borehole segments that have been isolated by packers and the subsequent measurement of the change in concentration over time. Point dilution tests have been used elsewhere on the ORR (Hicks et al., 1992; Sanford and Moore, 1994) to examine fracture characteristics.

Point dilution tests were performed in the GW821, GW822, and GW823 boreholes to further identify the major flow zones and to quantify the specific discharge from each of the zones. The results of these tests were used to identify sampling intervals for discrete borehole sampling using a packer sampler and to determine optimal locations for multilevel sampling ports. Distilled water was used as a tracer and changes in concentration were measured by monitoring the specific conductance. The basic procedure is briefly described as follows. First, the initial specific conductance of the formation groundwater within the packed interval was measured. Distilled water was then circulated through this zone until a suitable minimum conductance was achieved (for these tests, ~ 1/2 of the initial). Once this level was reached, the formation water was recirculated and the change in the specific conductance during recovery was monitored. Careful monitoring of the hydraulic head within the packed interval was done to ensure that gradients were not induced during circulation of the distilled water.

The recovery of the specific conductance over time was analyzed using the following equation (Drost et al., 1968; Freeze and Cherry, 1979):

$$dC/dt = -(AqC)/V ,$$

which, when rearranged, becomes

$$dC/C = -(Aqdt)/V,$$

and by integration and substitution

$$qAt/V = -\ln[(C_f - C_b)/(C_f - C_0)],$$

where:
q=specific discharge of interval
V=volume of interval
A=cross-sectional area of interval
t=time
C_f=specific conductance of formation water
C_b=specific conductance at time t
C_0= initial specific conductance after injection of distilled water.

By plotting the "ln term", $-\ln[(C_f - C_b)/(C_f - C_0)]$, versus recovery time, the data can be fitted with a regression line (units 1/t), the slope of which is equal to qA/V. (See Appendix C for examples.) In most of the intervals tested, these plots became linear after 10 to 15 minutes. For this reason, the tests were stopped before the recovery was complete but after a linear increase was sufficiently demonstrated. The first interval tested (66-68.5 ft in GW822) was allowed to recover for 120 minutes to ascertain the time required to reach linearity and whether or not the slope changed significantly after linearity was reached. After 120 minutes, recovery was still not complete; however, the plot became linear after approximately 20 minutes and remained consistent. All subsequent tests were run for a minimum of 30 minutes, longer if necessary until linearity was achieved.

The specific conductance of the formation water (C_f) within any given interval was highest at the beginning of the day. The C_f decreased during each series of tests because the intervals were not allowed to recover completely before deflating the packers and moving to the next interval. This allowed a gradual mixing of distilled water within the borehole. For calculating the fraction of recovery (the "ln term"), the original C_f for each series was used for all intervals within the series, since this C_f is a measure of the true formation water without the influence of the injected distilled water. This assumes that the specific conductance is invariant from one interval to the next within each series of tests. In fact, minimal variation was observed within any given borehole, where recovery time was allowed between two or more series of tests. The amount of error induced by this assumption is minimal compared to that induced by using the specific conductance value for mixed water within the borehole.

The calculations described above do not account for the effects of borehole convergence, a focusing of flow due to the presence of the borehole itself. Normally, a convergence factor generally ranging from 1-2 is applied to adjust for this effect. However because this factor, which is derived empirically, is unknown for these rocks and the primary interest is the relative discharges between intervals and the order of magnitude of the discharge, no attempt was made to include this factor.

In all cases, the specific conductance continued to drop for a few to several minutes after the start of the test due to the distilled water remaining in the intake line after switching to circulation. Several of the recovery plots are sinusoidal (e.g. 38-40.5 ft in GW822; 34-36.5 ft in GW823; 30-32.5 ft in GW821); however, they all oscillate around the best-fit line. In the case where a slope change occurred during recovery, regressions were applied to late-time data (e.g. 28-30.5 ft, 36-38.5 ft, and 40-42.5 ft in GW823).

The results of the point dilution tests are summarized in Figures 11-13, and the recovery plots are included in Appendix C. Tests were conducted at 2-ft intervals starting at the bottom of casing (22.5 ft in GW821, 32 ft in GW822, 26 ft in GW823) and extending to the bottom of borehole. Zones that were excluded from testing were the washout zone (46-51 ft) in GW823 and the extremely turbid zone (42.5-48 ft) in GW821.

The results for GW821 (Figure 11) show most specific discharge (q) values less than 50 cm/day. The highest flow measured (124 cm/day) was in the 24-26.5-ft interval; however, since the bottom of casing is at 22 ft, we could not test any zones higher than 24 ft. This is consistent with the flowmeter and core data that indicate the absence of some of the higher flow zones seen in the other boreholes. Several attempts were made to test the zones below 40 ft in GW821 but these were unsuccessful. These zones contained extremely silty water that repeatedly clogged the sample tubing. When the silty water was pumped up into the flow-through cell, the specific conductance readings would not stabilize.

The results for GW822 (Figure 12) show much higher flow than in GW821. Three zones in the interval from 60-70 ft have fluxes less than 20 cm/day, while all other zones have flow rates in excess of 100 cm/day. In five of the six zones from 40-50 ft, flow exceeds 200 cm/day, consistent with the higher flow noted in the flowmeter tests and the observations of highly fractured and weathered rock from the core and the downhole video. The zones immediately below the casing (34-38.5 ft) have the highest discharges measured (320 cm/day). While the core from these intervals did not contain heavy oxide staining, the shale was extremely clay-rich, weathered, and fissile. The flow in the cased intervals is likely to be even higher, judging from the loss of flow at the base of the casings during flowmeter tests.

The results for GW823 (Figure 13) are misleading because the flow appears to be low, with most below 100 cm/day. However, the zone of highest flow as indicated by flowmeter data is the washout interval from 46-51 ft . An attempt was made to place a 5-ft separation between the packers to test this zone. However, we were unable to obtain good packer seating. A second major zone was identified immediately below the casing (155 cm/day from 28-30.5 ft).

The results from all borehole tests were combined with observations from the core logs to identify the major flow zones within each borehole. This information was then used to determine the locations for groundwater sampling using a fracture sampler and the locations for installation of multilevel sampling ports.

6. MULTILEVEL WELL INSTALLATION

6.1. Solinst™ multilevel well installation

Solinst™ multilevel wells were installed in the boreholes following the completion of borehole tests. The Solinst™ equipment consists of a central 2"-diameter PVC riser into which sampling ports can be inserted (Figure 14). Each port contains a stainless steel tube that is attached to the inside of the riser and opens to the formation at the lower end and attaches to a ½" ID polyethylene tube at the upper end which extends to the surface. Since the tubing from all of the sampling ports must pass inside the riser, the number of ports is limited to five per well. While Solinst™ does make inflatable packers for this system, the choice was made to use sand and bentonite and a special injection system to isolate the sampling intervals. This choice was based both on the cost of the packers and the ragged condition of the boreholes in some intervals which could result in a poor packer seal.

Two types of Solinst™ equipment were used for these wells. Two of the wells were equipped with the new style of equipment that utilizes PVC casing for the sampling port and slip lock coupling that reduces the amount of rotation required during attachment of additional riser sections. The third well (GW823) was equipped with the old style threaded couplings and stainless steel sampling ports.

Numerous problems were encountered during installation, resulting in the need to pull one of the multilevel wells and reinstall it after cleaning out the borehole. These problems are detailed below in section 7.3. The beneficial result of this was that the backfill in the lowermost ten feet of GW823 was cleaned out, allowing a port to be installed in that deeper section of the borehole where active flow was indicated by the oxide staining on core fragments recovered from that interval. Because the exact location of the fracture zone within that 10-ft section could not be determined based on the core alone, and because the zone was not open to borehole testing, the entire 10-ft section was left open to the sampling

Solinst Multilevel Sampling System

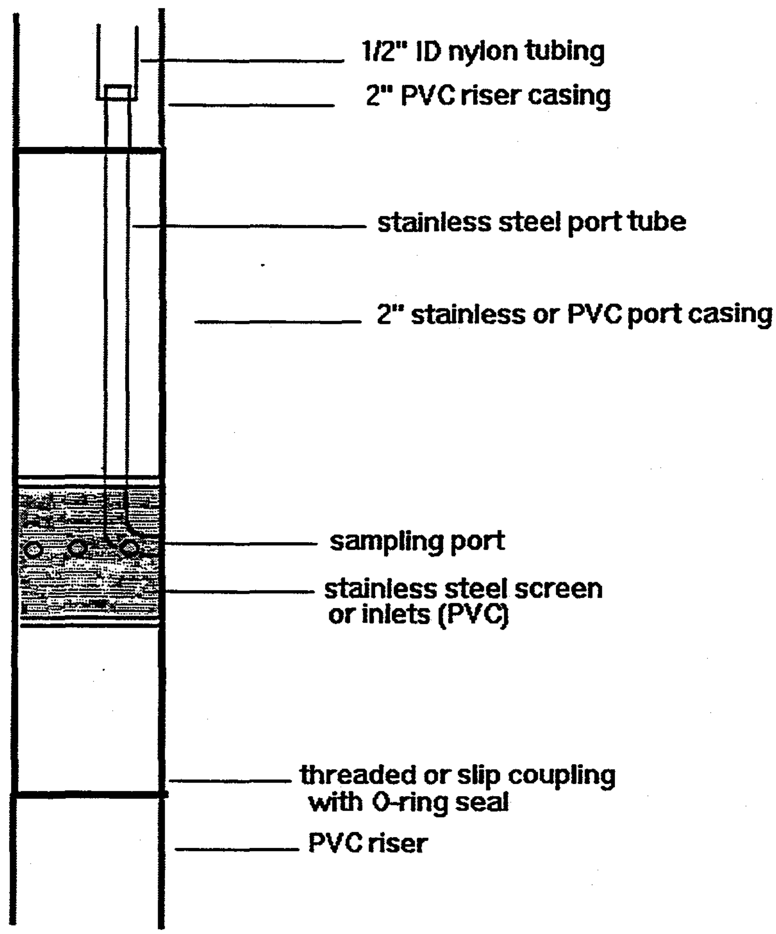

Figure 14. Schematic drawing of a Solinst™ multilevel port.

port. Thus, while the port does not isolate a narrow zone, it does allow sampling of a zone that is separated from the port above by a low-flow zone.

Following installation, the wells were developed by the removal of water using a peristalticpump until the water appeared to clear. This generally occurred after 1-2 L were removed, although a few intervals remained turbid. Because some of the ports were blocked or had sluggish yield, a compressor was used to force water in the sample tubing back through the sampling ports to clear the blockages. This was followed by again pumping 1-2 L of water which successfully cleared the ports, and subsequent sampling has been accomplished without difficulty.

6.2. Sampling port locations

The configuration of the multilevel wells was determined based on the combined results of the borehole tests and the detailed core logs. Active flow zones that appeared to be separated by less active zones were chosen for sampling port locations based on their potential for isolation from those zones immediately above and below. In most instances, these zones are separated by 10 ft or more. Wells were designed so that the depth of interest fell within the 6-in. length of the sampling port and approximately midway in the 1.5-ft length of the surrounding sandpack. The length of the sandpack was designed to extend approximately one foot on either end of the sampling port, and to coincide with the one-foot uncertainty in the location of fracture intervals from core and video information. This length is slightly less than the intervals used for the borehole tests, facilitating comparison with that data as well.

At least one sampler in each well was installed in the transition zone above the competent bedrock. This was accomplished by injecting a sandpack around the sampling port inside of the temporary surface casing and allowing the sand to collapse around the port when the casing was removed. While borehole tests could not be conducted for these zones, the presence of active flow was confirmed by oxidation surfaces and extremely wet zones.

6.3. As-built configurations

The final configurations of the multilevel wells are shown in Figure 15 and listed in Table A7. Survey markers for ground elevations were installed, and survey marks on the lip of the protective casings were marked. All elevations have been measured from the survey point on the casing. Where the interface between two materials in the borehole annulus is unknown, a question mark has been added. This occurred at one level in each of the three wells, primarily due to collapse of the borehole. Where a sampling port is not isolated from fill by a bentonite layer, the port must be assumed to be open to the entire interval that has collapsed, since the native materials do not normally provide an adequate seal. This is evident in the case of port A in GW821, which is surrounded by silt that had collected in the bottom of the borehole during the period that it was open for testing. When the well was installed, displacement by the riser casing forced the silt up around the

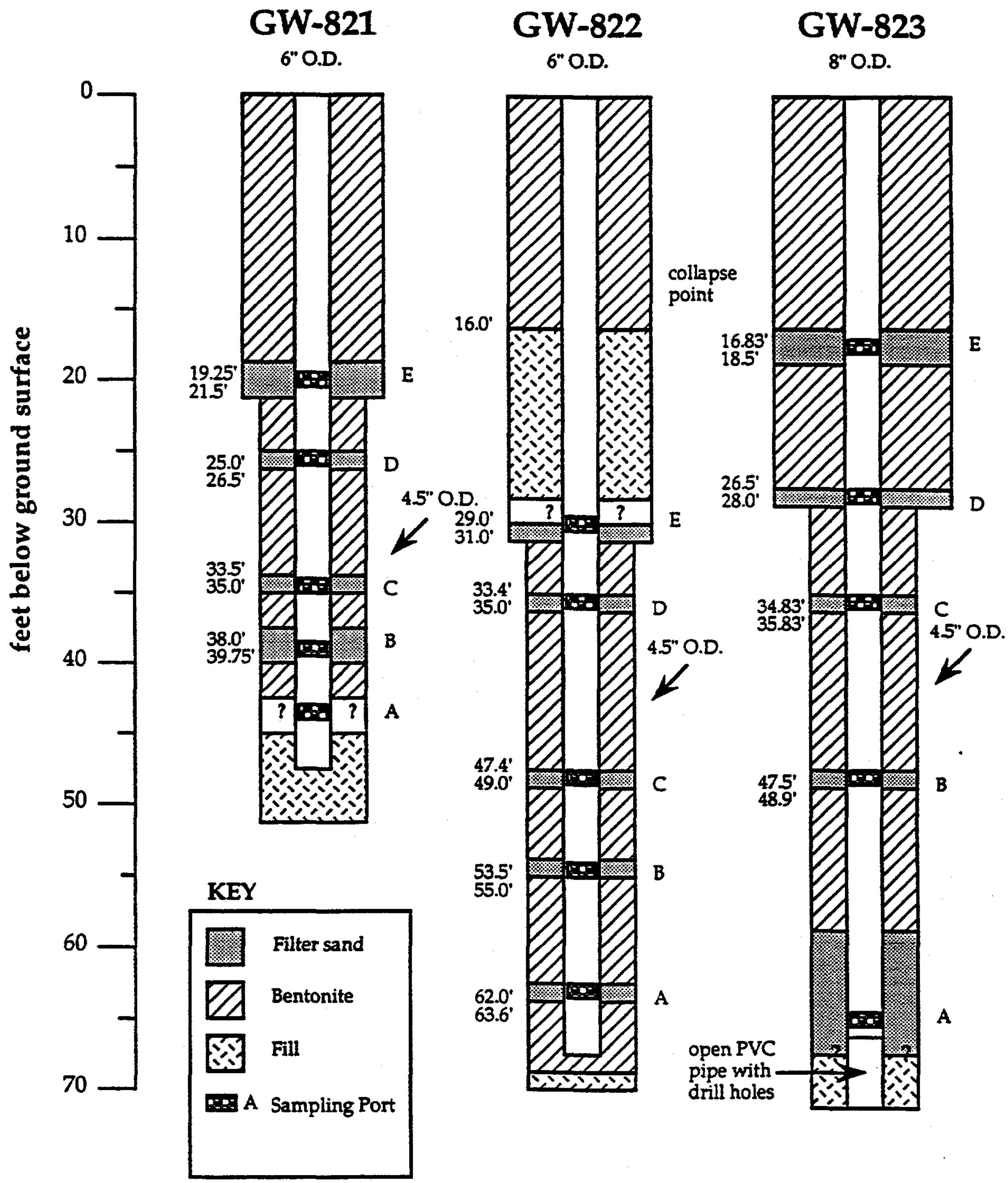

Figure 15. Final multilevel well configurations. All depths are referenced to ground surface. Survey information and sampling port elevations are contained in Table 7A.

sampling port. However, this port does yield water, although turbidity is high even at low sampling rates. The fact that it yields at all indicates that the bentonite seal is above the top of the port, although the location of the base of the seal is unknown.

In GW822, collapse occurred during the removal of the temporary casing. In addition, because the casing was a foot longer than was reported by the drillers, part of the bentonite seal below sampling port E extended into the bottom of the casing. When the casing was removed, this part of the seal came up with the casing bringing much of the sand pack surrounding port E along with it. The thickness of the remaining sand pack is unknown and could not be measured due to the blockage at a 15-ft depth which precluded passage of a weighted measuring tape down to the level of the port. It is believed that the interval below the blockage is either collapsed and filled with permeable backfill, or has remained open. In either case, port E is presumed to be open to the entire interval, which contains two active flow zones as shown in the core description. These may be correlative with two zones in the saprolite that have been isolated in GW823.

The borehole above the bedrock was widened to an 8-in diameter during the cleaning and reinstallation of the multilevel well in GW823. The borehole remained open during reinstallation, allowing the placement of two ports in the saprolite above the bedrock. This will provide a means for assessing the connectivity between flow zones in the saprolite as well as in the bedrock and between the saprolite and bedrock.

7. DISCUSSION

7.1. Lessons learned

Because many of the techniques described in the previous section are relatively new and have to be adapted to fit local site conditions, problems were encountered during nearly every field activity. The following sections summarize the nature of the problems and the solutions that were developed to address them. This chapter is intended to guide others in the use of these techniques or the decisions about their applicability at other sites in order to circumvent some of the problems encountered at this site.

7.1.1. Drilling methods

The rotasonic drilling technology presents some definite advantages and disadvantages over conventional drilling methods. The method is very fast, thus reducing costs associated with field technician and oversight personnel time. The method also reduces the volume of waste produced, particularly when dry drilling is successful. And it does have the advantage of recovery of nearly continuous core, and of minimizing worker exposure to any potential contamination brought to the surface with the core until it can be scanned by Health Physics personnel.

This technology does have some limitations, however. In very fissile materials the vibration probably exacerbates the potential for collapse of the borehole if left open for even short periods of time. We solved this problem by installing temporary surface casing above the competent bedrock, although this left the upper interval inaccessible for borehole testing. In very competent material, on the other hand, dry drilling was not very successful, and the use of water was required. We did not test whether or not we could have resumed dry drilling below the resistant shale unit due to time and monetary constraints, but that could potentially have been possible.

The vibration of the core barrel generates significant frictional heat, which has to be taken into consideration if porewater sampling for geochemistry is planned, as it was for this project. In addition to the loss of fluid volume as a result of heating the core, the geochemistry is certain to be altered if immediate extraction of the fluids is not done. On the other hand, obtaining unaltered fluids from wet zones is possible through the use of dry drilling.

The condition of the core ranged from competent core with intact structures to broken fragments with no preserved structural orientation. Dry drilling produced excellent cores due to the retention of the clay minerals that held the cores intact. Wet drilling produced good cores only where the rock was minimally fractured. The cores are extruded from the core barrel into a plastic sheath that is large enough to fit over the outer casing (4.5-in diameter); however, the core has only a 3.75-in diameter and some settling occurs when the core is highly fragmented. Thus, the relative position of the fragments is preserved but some compaction of the overall core and errors in depth assignment are incurred. However, the errors are minimized by bringing the core up in 5-ft sections, where the depth of the base of each core section is definitively known.

7.1.2. Borehole test methods

The electromagnetic borehole flowmeter measures a voltage induced by the passage of naturally-occurring ions through a magnetic coil via vertical flow in the borehole. Numerous measurements may be taken within a borehole at any desired spacing. However, background noise can interfere with the measurements by superimposing an additional signal through electric fields that are induced by high voltage power lines. A periodic noise problem was encountered at this site, requiring an interruption of the survey until the noise subsided. The tests were set up so that the voltage was read once a second and averaged over one minute. A standard deviation was also calculated, so that extremely noisy periods could be identified. Measurements were repeated until the standard deviation fell within acceptable limits (<0.005 V). Moore and Young (1992) reported being unable to conduct EM flowmeter tests in some areas due to high background noise.

Performing the tests within a single borehole over a period of more than one day, or during precipitation events can add some uncertainty to the interpretation of results. In order to properly quantify the flux through the packed interval, the ambient flow must be subtracted from the induced flow. However, if the ambient conditions change over the period of testing, then additional flow coming into the well due to a rain event, for example, will not be accounted for. Whenever possible, it is best to conduct both surveys on the same day and to avoid the time period during or immediately following a precipitation event.

Point dilution tests were significantly aided by the use of a field computer which allowed viewing of graphical results during the test to determine when to stop taking measurements and to move to the next interval. After stabilization of the water level in the well, distilled water was injected to a point where the specific conductance was reduced to about half of the initial value. During recirculation and return to equilibrium, the hydraulic head and specific conductance were monitored and the "ln term" was calculated and plotted vs time. Specific conductance changed exponentially, with the value levelling out at the initial value after an extensive time. The log of the change of conductance is linear with time, following some early time instability, so that when the linear portion of the recovery becomes sufficiently well-defined then the test can be stopped. This results in considerable time savings since the test does not have to run to full equilibrium. Because the interval is not completely flushed out, however, some mixing and reduction of overall specific conductance within the borehole occurs. The initial value of the subsequent interval may be slightly less than that of the formation as a result. This affects the denominator of the log term and the computed value of Q. If the vertical variability in the specific conductance is minimal, then the starting value for a series of tests can be used as the formation value (Q_f) for all tests in that series. When equilibration over a period of time was allowed to occur, the values were surprisingly consistent over time within a given well.

A second problem that was addressed was the unavailability of a pressure transducer that would allow measurements at 70-ft depths. The only transducers available for this project were 5- or 10-psi probes. Since the transducer must attach to the packer so that the pressure within the packed interval is monitored, a 10-psi probe would be insufficient. In an attempt to circumvent this limitation, a section of tubing filled with air was inserted between the transducer and the packer coupling. Since air is more compressible than water, much of the pressure was accommodated by compaction of the air column. While this did not allow a measurement of absolute pressure, it did permit the monitoring of changes in pressure within the packed interval to establish stability.

The point dilution method is a relatively simple and effective way to collect information about flow through discrete intervals. With the proper equipment, point dilution testing is easy to conduct and the data collected can be analyzed in the field using a portable computer with a spreadsheet program. Some uncertainty is inherent due to the inability to confirm that both packers are adequately seated, since the equipment will feel snug in the borehole with only one packer properly inflated. However, the ability to reduce the specific conductance relatively quickly during the circulation of distilled water was a good indication of proper seating.

In general, the data from all of these tests showed remarkable consistency. By far, the most definitive information was obtained from the flowmeter and point dilution tests. The borehole camera is a quick and useful tool for observing the condition of the borehole and identifying gross characteristics. The core provided detailed information and, while the presence of oxides on the fracture surfaces was relatively consistent with zones of flow, they provided no information about the relative permeability of the zones and the depths were difficult to accurately place. The borehole flowmeter is less time-consuming than the point dilution and provides good information about the relative permeability of the various flow intervals. In contaminated wells it is the method of choice because it does not require the removal of any fluids from the well if injection tests are used. However, it is subject to interference due to electrical noise and can be misleading if a single high permeability zone is able to transmit all of the injected flow at the expense of any underlying zones. Point-dilution tests provide definitive information about absolute flow rates without susceptibility to noise. They are, however, subject to uncertainty due to indeterminate packer seating and, while the flowmeter could be used to quantify the flow through the large washout zone in GW823, no information could be obtained from point-dilution. Furthermore, in contaminated wells, wastewater would require proper disposal.

7.1.3. Solinst™ multilevel equipment and installation

The installation of the multilevels proved to be challenging even though the technology is relatively simple. The greatest difficulty was due to the use of the large-diameter (0.5-in) sample tubes that attach to each sampling port. Twisting can occur at the location of the ports as additional riser sections are screwed into place, particularly above the upper port where 5 tubes are squeezed into the internal diameter of the riser. In GW823, the sample tubes became twisted at the uppermost port during installation, effectively blocking all 5 ports. This was not discovered until after the installation was complete. As a result, the entire well had to be removed and reinstalled after cleaning out the borehole. While the problem was exacerbated by the threaded couplings used in this borehole, the type of coupling also allowed the well to be pulled from the borehole. The new style of coupling uses a wire tie to hold the casing sections together, requiring fewer turns to secure the coupling and lessening the chances of crimping the sampling tubes. However, very little rotation is required to cause the wire ties to slip back out, thereby causing decoupling of the riser casing. This apparently occurred during installation of GW822, most likely when the temporary casing was being twisted during removal. While in this well the problem was probably localized above the upper port, this could pose a potential problem if multiple decoupling occurs and sampling zones are connected via the riser casing itself. A better system of coupling is still needed, although the latest version is a considerable improvement.

The sand and bentonite injection system also presented some problems. In order to keep water from backing up into the injection tubing and causing a bentonite plug to form, there had to be continuous air injection through the tube. This created significant turbulence, however, which may have resulted in greater collapse problems around the riser casing as in GW823. It also created a buoyancy that made insertion of the injection tubing down the well annulus measurement of the top of the injected layer difficult. The turbulence may have kept smaller bentonite particles in suspension, causing them to be mixed into the sand pack, thus reducing its permeability. The pressure was occasionally strong enough to blow water out of the borehole. This was improved by the replacement of a defective control valve.

We used a larger diameter tube for injection (0.5-in ID) than that which was provided with the Solinst™ injector system in order to minimize the chances of plugging. Getting tubing that is stiff enough to pass through the space between the riser and the borehole wall without kinking is difficult, particularly in the washout intervals. Ideally, one would want to inject the sand or bentonite layer, pull the tubing and wait for settling to occur, and then take a measurement before again inserting the tubing. However, getting the tubing to pass to the bottom of the borehole was such a problem for all three wells that once it was inserted it was left in and all injection took place in the presence of the turbulence created by continuous airflow. Thus, the permeability of the sandpack may have been compromised and has potential for being lower than that of the surrounding formation if the formation is densely fractured. A better method of injection is needed if this technology is going to be used effectively at a larger scale.

7.2. Summary of results

The FY94 field activities provided a preliminary characterization of flow and transport at a west Bear Creek Valley field site in the Nolichucky Shale that raises many questions about the reliability of data obtained using currently accepted groundwater sampling procedures and standard monitoring-well construction. Anisotropy induced by the fracture system has a major impact on transport, with the majority of transport occurring parallel to strike and nearly perpendicular to the hydraulic gradient. However, transport both updip and downdip occurs in conjunction with storm events, demonstrating the dynamic nature and the complexity of the hydrologic system at this site.

Three new boreholes were successfully drilled and cored and a battery of borehole tests were completed in order to identify and characterize the major flow zones within each borehole. The tests within each borehole were very consistent overall, and it was determined that the greatest amount of information could be obtained by using point dilution tests, although they are also the most time and labor intensive. The borehole tests also demonstrate a large amount of spatial variability in flow characteristics over the relatively small scale of the field site.

The installation of multilevel samplers was guided by the borehole test data. A sand and bentonite injection system was used in lieu of inflatable packers to isolate the individual sampling ports because of the much lower cost and because of the uncertainty that adequate packer sealing would occur in the presence of borehole rugosity. The multilevel system was not easy to install, although subsequent installations will benefit from what has been learned through this activity.

7.3. Future work

The primary goals for FY95 are to unravel the complexities of the storm-related transport, to use geochemical analyses to provide an indication of groundwater mixing and water sources, to compare the data obtained from multilevel and screened wells, and to determine the zone of influence during purging and the impact on tracer concentrations. In addition, the cores will be studied in greater depth to better describe the characteristics of the transition zone. To accomplish the first goal, a continuous water level monitoring system for the multilevel wells will be installed and an SF-6 tracer study will be started. The SF-6 can be analyzed from water samples, allowing acquisition of real-time data.

While groundwater samples were taken from the open boreholes using a packer sampler, interpretation of that data will be deferred until mineralogical samples and additional geochemistry can be completed in FY95. Both geochemical samples and tracer samples will be obtained from screened and multilevel wells to provide a measure of the impact of well construction on sampling results.

Finally, a pumping test to examine the region of influence, the interconnectivity of the fracture system, and the impact of pumping on tracer concentrations is scheduled for the summer of FY95. Data from these additional studies will result in recommendations for revising our sampling protocols to obtain more representative samples in fractured rocks.

ACKNOWLEDGEMENTS

The following Energy Systems personnel and subcontractors provided assistance for this project: Bill Sanford, Charles Lamb, Norman Farrow, Tom Zondlo, Larry Combs, and Melissa Brown (ORNL/ESD), Brenda Thompson and Amy Halleran (University of Tennessee, Knoxville), and Kevin Jago and Steve Jones (Y-12).

REFERENCES CITED

EPA, 1992. RCRA Ground-Water Monitoring: Draft Technical Guidance. Office of Solid Waste, U.S. Environmental Protection Agency, Washington, D.C.

Gierke, W.G., W.B. Lozier, and R. Pearson, 1988. Task 2, well logging and geohydrologic testing, site characterization and groundwater flow computer model application, Vol.1. Golder Associates, Inc., ORNL/Sub/30X-SA706C.

Godsey, K.D., 1993. The (sonic) wave of the future: Water Well Journal, May 1993.

Harned, D.A., and C.C. Daniel III, 1989. The transition zone between bedrock and regolith: conduit for contamination? *in* Ground Water in the Piedmont, C.C. Daniel III, R.K. White, and P.A. Stone (eds), Proc. of a conference on Ground Water in the Piedmont of the Eastern United States, Charlotte, NC, Oct. 16-18, 1989.

Hicks, D.S., D.K. Solomon, and N.D. Farrow, 1992. Investigation of Groundwater Flow Zones and Contaminant Transport in Solid Waste Storage Area 5 at Oak Ridge National Laboratory, Oak Ridge, Tennessee: ORNL/ER-154.

Lee, R.R., Ketelle, J.M. Bownds, and T.A. Rizk, 1992. Aquifer analysis and modeling in a fractured, heterogeneous medium: Ground Water, v.30(40), p.589-597.

McKay, L.D., 1993. Groundwater sampling in fractured clay and rock. Presentation at the EPA Workshop on Groundwater Sampling, Dallas, TX, Nov. 30, 1993.

Moore, G.K., and S.C. Young, 1992. Identification of Groundwater-Producing Fractures by Using an Electromagnetic Borehole Flowmeter in Monitoring Wells on the Oak Ridge Reservation, Oak Ridge, Tennessee. ORNL/ER-91.

Sanford, W.E., R.G. Shropshire, and D.K. Solomon, in review. Dissolved gas tracers in groundwater: simplified injection, sampling, and analysis: Water Resources Research.

Sanford, W.E., and G.K. Moore, 1994. Measurement of specific discharge with point-dilution tests in the fractured rocks of eastern Tennessee: Proceedings of Extended Abstracts, American Water Resources Association 1994 Annual Spring Symposium, Nashville, TN, pp. 449-453.

Sanford, W.E., D.K. Solomon, and R.G. Shropshire, 1994. Noble gases as groundwater tracers in fractured saprolite: EOS, American Geophysical Union 1994 Spring Meeting, v.75(16), p. 147.

Schreiber, M.E., 1995. Vertical Variability in Groundwater Chemistry in Fractured Media: Results from a Field Experiment in the Nolichucky Shale, Oak Ridge Reservation, Oak Ridge, TN. Unpublished MS thesis, University of Wisconsin - Madison, Madison, WI.

Solomon, D. K., G.K. Moore, L.E. Toran, R.B. Dreier, and W.M. McMaster, 1992. Status Report: A Hydrologic Framework for the Oak Ridge Reservation. ORNL/TM-12026.

APPENDIX A: DATA TABLES

Table A1. Water Level Data

date	GW456 depth	elevation	GW457 depth	elevation	GW458 depth	elevation	GW459 depth	elevation	GW460 depth	elevation	GW461 depth	elevation	GW462 depth	elevation
3/29/94	3.61	841.19	6.06	839.24	6.02	838.68			2.37	839.73	5.03	837.47	4.00	839.30
3/31/94	3.95	840.85	6.45	838.85	6.40	838.30	8.00	837.20	2.70	839.40	5.40	837.10		
4/3/94	4.60	840.20	7.55	837.75	7.25	837.45	9.20	836.00	3.45	838.65	6.27	836.23	5.55	837.75
4/8/94	3.86	840.94	6.55	838.75	6.40	838.30	8.45	836.75	1.70	840.40	5.50	837.00	4.58	838.72
4/9/94	4.25	840.55	7.07	838.23	6.88	837.82	8.88	836.32	3.11	838.99	5.91	836.59	5.10	838.20
4/11/94	3.36	841.44	4.62	840.68	5.64	839.06	6.37	838.83	2.03	840.07	4.60	837.90	3.63	839.67
4/13/94	2.95	841.85	5.25	840.05	5.24	839.46	6.17	839.03	1.76	840.34	4.13	838.37	3.29	840.01
4/15/94	3.74	841.06	6.51	838.79	6.28	838.42	8.41	836.79	2.73	839.37	5.20	837.30	4.53	838.77
4/18/94	3.77	841.03	6.56	838.74	6.27	838.43	8.47	836.73	2.78	839.32	5.19	837.31	4.55	838.75
4/20/94	4.64	840.16	7.56	837.74	7.12	837.58	9.21	835.99	3.60	838.50	6.01	836.49	5.56	837.74
4/22/94	5.35	839.45	8.27	837.03	7.78	836.92	9.74	835.46	4.22	837.88	6.59	835.91	6.28	837.02
4/25/94	6.35	838.45	9.20	836.10	8.71	835.99	10.47	834.73	5.11	836.99	7.41	835.09	7.19	836.11
4/27/94	6.96	837.84	9.81	835.49	9.27	835.43	10.96	834.24	4.99	837.11	5.69	836.81	7.80	835.50
4/29/94	7.14	837.66	10.04	835.26	9.45	835.25	11.17	834.03	5.82	836.28	8.18	834.32	8.03	835.27
5/4/94	7.56	837.24	10.33	834.97	9.83	834.87	11.27	833.93	6.12	835.98	8.47	834.03	8.34	834.96
5/10/94	8.25	836.55	11.12	834.18	10.59	834.11	12.31	832.89	6.80	835.30	9.39	833.11	9.11	834.19
5/13/94	8.67	836.13	11.50	833.80	11.03	833.67	12.74	832.46	7.24	834.86	9.81	832.69	9.50	833.80
5/17/94	9.05	835.75	11.85	833.45	11.36	833.34	13.11	832.09	7.56	834.54	10.15	832.35	9.90	833.40
5/20/94	9.40	835.40	12.20	833.10	11.71	832.99	13.46	831.74	7.96	834.14	10.54	831.96	10.20	833.10
5/23/94	10.00	834.80	12.72	832.58	12.30	832.40	14.00	831.20	8.58	833.52	11.10	831.40	10.88	832.42
5/27/94	10.28	834.52	13.00	832.30	12.41	832.29	14.02	831.18	8.82	833.28	11.26	831.24	11.08	832.22
5/31/94	10.56	834.24	13.16	832.14	12.75	831.95	14.45	830.75	9.02	833.08	11.55	830.95	11.17	832.13
6/2/94	10.76	834.04	13.41	831.89	13.01	831.69	14.66	830.54	9.28	832.82	11.82	830.68	11.40	831.90
6/6/94	11.06	833.74	13.78	831.52	13.56	831.14	15.00	830.20	9.58	832.52	11.22	831.28	11.70	831.60
6/8/94	11.10	833.70	13.80	831.50	13.40	831.30	15.10	830.10			12.26	830.24	11.80	831.50
6/10/94	11.22	833.58	13.82	831.48	13.52	831.18	14.58	830.62	9.60	832.50	12.10	830.40	11.86	831.44
6/13/94					13.05	831.65	14.68	830.52					11.44	831.86
6/15/94	11.09	833.71	13.69	831.61	13.27	831.43	15.01	830.19	9.45	832.65	12.14	830.36	11.70	831.60
6/17/94	11.16	833.64	13.82	831.48	13.40	831.30	15.21	829.99	9.57	832.53	12.29	830.21	11.80	831.50
6/20/94	11.40	833.40	14.08	831.22	13.72	830.98	15.46	829.74	9.84	832.26	12.62	829.88	12.09	831.21
6/22/94	11.55	833.25	14.26	831.04	13.88	830.82	15.60	829.60	10.00	832.10	12.82	829.68	12.26	831.04
6/24/94	11.58	833.22	14.32	830.98	13.94	830.76	15.66	829.54	10.08	832.02	12.92	829.58	12.32	830.98
6/27/94	10.82	833.98	12.78	832.52	12.60	832.10	11.72	833.48	8.82	833.28	10.90	831.60	10.80	832.50
6/29/94	10.26	834.54	12.60	832.70	12.24	832.46	13.28	831.92	8.48	833.62	11.00	831.50	10.58	832.72
7/1/94	10.68	834.12	13.72	831.58	13.26	831.44	13.66	831.54	9.44	832.66	11.48	831.02	11.68	831.62
7/4/94	11.20	833.60	14.50	830.80	14.04	830.66	14.78	830.42	10.14	831.96	12.28	830.22	12.50	830.80
7/6/94	11.48	833.32	14.83	830.47	14.39	830.31	15.24	829.96	10.44	831.66	12.62	829.88	12.82	830.48
7/8/94	11.74	833.06	14.93	830.37	14.45	830.25	15.52	829.68	10.62	831.48	12.72	829.78	12.90	830.40
7/11/94	11.96	832.84	14.74	830.56	14.62	830.08	15.75	829.45	10.84	831.26	12.96	829.54	12.74	830.56
7/13/94	11.98	832.82	15.39	829.91	14.88	829.82	15.72	829.48	10.92	831.18	13.14	829.36	13.36	829.94
7/15/94	12.00	832.80	15.22	830.08	14.74	829.96	15.26	829.94	10.76	831.34	12.94	829.56	13.20	830.10
7/18/94	11.02	833.78	13.60	831.70	13.20	831.50	13.40	831.80	9.38	832.72	11.32	831.18	11.62	831.68
7/20/94	11.20	833.60	14.24	831.06	13.80	830.90	14.46	830.74	9.86	832.24	12.02	830.48	12.28	831.02
7/22/94	11.34	833.46	14.63	830.67	14.20	830.50	15.04	830.16	10.14	831.96	12.40	830.10	12.64	830.66
7/25/94	11.72	833.08	15.18	830.12	14.75	829.95	15.64	829.56	10.62	831.48	12.98	829.52	13.18	830.12
7/27/94	11.80	833.00	15.08	830.22	14.66	830.04	14.80	830.40	10.68	831.42	12.90	829.60	13.08	830.22
7/29/94	11.28	833.52	14.00	831.30	13.60	831.10	13.80	831.40	9.70	832.40	11.74	830.76	12.00	831.30
8/1/94	11.56	833.24	14.78	830.52	14.38	830.32	15.16	830.04	10.32	831.78	12.58	829.92	12.78	830.52
8/3/94	11.82	832.98	15.22	830.08	14.82	829.88	15.60	829.60	10.70	831.40	13.02	829.48	13.22	830.08
8/5/94	11.80	833.00	15.09	830.21	14.72	829.98	14.68	830.52	10.70	831.40	12.90	829.60	13.10	830.20
8/8/94	11.81	832.99	15.16	830.14	14.74	829.96	15.46	829.74	10.65	831.45	12.95	829.55	13.20	830.10
8/10/94	12.04	832.76	15.50	829.80	15.13	829.57	15.86	829.34	10.96	831.14	13.32	829.18	13.58	829.72
8/12/94	12.28	832.52	15.80	829.50	15.38	829.32	16.16	829.04	11.23	830.87	13.59	828.91	13.80	829.50
8/15/94	12.12	832.68	14.84	830.46	14.44	830.26	14.20	831.00	10.68	831.42	12.52	829.98	12.84	830.46
8/17/94	11.78	833.02	14.85	830.45	14.46	830.24	15.08	830.12	10.40	831.70	12.60	829.90	12.86	830.44
8/19/94	12.02	832.78	15.37	829.93	14.99	829.71	15.70	829.50	10.82	831.28	13.14	829.36	13.39	829.91
8/22/94	11.39	833.41	13.97	831.33	13.63	831.07	13.64	831.56	9.76	832.34	11.70	830.80	11.98	831.32
8/24/94	11.48	833.32	14.64	830.66	14.27	830.43	14.80	830.40	10.18	831.92	12.40	830.10	12.64	830.66
8/26/94	11.06	833.74	15.06	830.24	14.70	830.00	15.48	829.72	10.52	831.58	12.86	829.64	13.06	830.24
8/29/94	11.96	832.84	15.52	829.78	15.16	829.54	15.96	829.24	10.92	831.18	13.34	829.16	13.52	829.78
8/31/94	12.22	832.58	15.82	829.48	15.45	829.25	16.24	828.96	11.29	830.81	13.64	828.86	13.96	829.34
9/2/94	12.30	832.50	15.78	829.52	15.39	829.31	16.00	829.20	11.32	830.78	13.57	828.93	13.75	829.55
9/7/94	12.65	832.15	16.20	829.10	15.80	828.90	16.44	828.76	11.72	830.38	14.02	828.48	14.35	828.95
9/9/94	12.82	831.98	16.34	828.96	15.92	828.78	16.50	828.70	11.90	830.20	14.22	828.28	14.55	828.75
9/18/94	12.14	832.66	14.18	831.12	13.81	830.89	13.21	831.99	10.35	831.75	11.84	830.66	12.20	831.10
9/21/94	11.90	832.90	15.80	829.50	14.77	829.93	15.33	829.87	10.71	831.39	12.92	829.58	13.10	830.20

Table A2. Helium in Source and Observation Wells
(area counts x 1000)

DATE	GW456	GW457	GW458	GW459	GW460	GW461	GW462	Ave Co
3/25/94							20900	20900
4/3/94	0	0	1.6	0	8.3	0	59052	39976
4/5/94	6.4	0	0	0	0	0	63071	47674
4/8/94	0	33	0	0	0	0	87593	57654
4/11/94	0	0	0	0	0	0		57654
4/13/94	0	9.5	46.8		6.1	5.1	117217	69567
4/15/94	0	0	12.2	0	0	4	114811	77107
4/18/94	1	0	0	0	0	0	156182	88404
4/20/94	0	0		0	0	0	74580	86676
4/22/94	0	0	7.8	0	0	0	140234	92627
4/25/94	0		8.5	0	0	0	132772	96641
4/27/94	9.4	36.9	0	0	0	0	120108	98775
4/29/94	0	11.7	0	0	0	0		98775
5/4/94	0	0	0	0	0	10.5	82740	97438
5/10/94	0	0	0	0	0	0	109407	98359
5/13/94	0	8.6	0	0	0	0	87989	97618
5/17/94	0	0	0	0	7.3	4.7	35490	93476
5/20/94	4.2	0	0	0	15.4	116		93476
5/23/94	0	0	0	0	10.8	16.3		93476
5/27/94	0	7.9	0	0	0	230	49642	90737
5/31/94	0		0			367		90737
6/2/94	0	0	0	0	35.9	371	36085	87522
6/6/94	0	0	0	0	33.3		36714	84699
6/8/94		0	0	0	22.9	169	71908	84026
6/10/94	0	0	0	7.2	41.4		143926	87021
6/13/94			0	0	0	420	40403	84801
6/15/94	36	0	0	0	0	751	69579	84109
6/17/94	28	0	0	0		634		84109
6/20/94	27	0	0	0	0	843	39041	82150
6/22/94	9.8	0	0	0	112	574	117819	83636
6/24/94	9	0	0	0	0		7980	80610
6/27/94		0	0	0	79	754	141912	82968
7/4/94	8	20	0	10	155		121444	84393
7/6/94	10	8	0		42			84393
7/8/94	9	27	0	0	66	836	102148	85027
7/11/94	0	8	0	0	70	259	120800	86260
7/13/94		0	0	0	121	415	34401	84532
7/15/94	0		0		204	1300	140253	86329
7/18/94	0	7	0	0		1348	130286	87703
7/20/94	0	0	0	0	196	978	2705	85127
7/22/94	0	0	0	0	154	749	21929	83268
7/25/94	0	0	0	0	200	1431	72014	82947
7/27/94	0	0	0	0	199	868		82947
7/29/94	0	6	0	0			107938	83641
8/1/94	0	0	0	0		1560		83641
8/3/94	0		0	0	213	1389	56576	82909
8/5/94	0	5.9	0	0	484		36503	81688
8/8/94	0	0	0	0		1540	56647	81046

Table A2. (continued)

DATE	GW456	GW457	GW458	GW459	GW460	GW461	GW462	Ave Co
8/10/94	0	0	0	0	367	1483	61007	80545
8/12/94	0	0	0	0	259	304		80545
8/15/94	0	7.1	0	0	264	3571	215228	83830
8/17/94	0	8.5	0	0	278	1750	221968	87119
8/19/94	0	0			276	2016	193146	89585
8/22/94	0	0	0	0	281	2237		89585
8/24/94	0	0	0	0	265	1447	500	87560
8/26/94	0	0	0	0	310	2006	1089	85639
8/29/94	0	0	0	0	13	2121	182061	87735
8/31/94	0	0	0	15	446	4670	214372	90429
9/2/94	0	0	0	0	282	1693	101013	90650
9/7/94	0	10	0	18	424	4846	246670	93834
9/9/94	0	0	12	0		1850	58776	93133
9/15/94	6.7	0	11.3	0	360	2159	236898	95952
9/18/94			41.1	0	249	1917	19321	94478
9/21/94	0	0	18.1	0	240	2366	178987	96072
9/26/94	0	0	18.3	0	5.2		1362	94318

Table A3. Bromide Source Concentration

date	time (day)	C (ppm)	C/C0	-ln(C/C0)
11-Apr-94	0	15200	1.000000	0.000
13-Apr-94	2	550	0.036184	3.319
15-Apr-94	4	115	0.007566	4.884
18-Apr-94	7	37.7	0.002480	5.999
20-Apr-94	9	28.1	0.001849	6.293
22-Apr-94	11	23.2	0.001526	6.485
25-Apr-94	14	17.8	0.001171	6.750
27-Apr-94	16	16.5	0.001086	6.826
29-Apr-94	18	10.6	0.000697	7.268
4-May-94	23	5.23	0.000344	7.975
10-May-94	29	8.03	0.000528	7.546
17-May-94	36	5.89	0.000388	7.856
20-May-94	39	6.59	0.000434	7.743
31-May-94	40	4.39	0.000289	8.150
2-Jun-94	42	3.9	0.000257	8.268
6-Jun-94	46	5.14	0.000338	7.992
15-Jun-94	55	3.85	0.000253	8.281
17-Jun-94	57	5.63	0.000370	7.901
20-Jun-94	60	4.18	0.000275	8.199
22-Jun-94	62	4.83	0.000322	8.041
24-Jun-94	64	7.11	0.000474	7.654
27-Jun-94	67	6.13	0.000409	7.803
1-Jul-94	71	3.61	0.000241	8.332
12-Jul-94	82	3.13	0.000209	8.475
15-Jul-94	85	3.22	0.000215	8.446
18-Jul-94	88	1.94	0.000129	8.953
21-Jul-94	91	9.68	0.000645	7.346
25-Jul-94	95	4.09	0.000273	8.207
27-Jul-94	97	4.55	0.000303	8.101
29-Jul-94	99	3.29	0.000219	8.425
1-Aug-94	102	2.23	0.000149	8.814
3-Aug-94	104	3.4	0.000227	8.392
9-Aug-94	110	2.32	0.000155	8.774
11-Aug-94	112	2.19	0.000146	8.832
15-Aug-94	116	1.7	0.000113	9.085
17-Aug-94	118	1.91	0.000127	8.969
19-Aug-94	120	2.34	0.000156	8.766
23-Aug-94	124	0.819	0.000055	9.815

Table A4. EM Flowmeter data for GW821.

GW821 Ambient Test

time	depth	volts	Q (L/min)	std dev	head	adj V	adj Q
7:52:09	18	-0.278	0.001	0.002	3.7	0.000	0.000
8:01:54	45.8	-0.279	0.001	0.004	3.71	-0.001	0.000
8:06:42	43.9	-0.276	0.002	0.003	3.73	0.002	0.001
8:13:35	42	-0.278	0.001	0.002	3.72	0.000	0.000
8:18:06	40.1	-0.271	0.004	0.001	3.71	0.007	0.003
8:24:25	38	-0.271	0.004	0.002	3.71	0.007	0.003
8:36:19	36	-0.262	0.008	0.004	3.72	0.016	0.007
8:41:00	34	-0.268	0.005	0.003	3.71	0.010	0.005
8:48:16	37	-0.259	0.009	0.006	3.72	0.019	0.009
8:53:06	35	-0.26	0.009	0.002	3.73	0.018	0.008
8:57:16	32	-0.262	0.008	0.002	3.7	0.016	0.007
9:00:26	30	-0.266	0.006	0.001	3.7	0.012	0.005
9:03:29	33	-0.264	0.007	0.003	3.71	0.014	0.006
9:06:42	30	-0.266	0.006	0.002	3.68	0.012	0.005
9:10:35	28	-0.269	0.005	0.004	3.7	0.009	0.004
9:13:46	26	-0.229	0.023	0.002	3.7	0.049	0.022
9:17:06	27	-0.227	0.024	0.004	3.71	0.051	0.023
9:21:21	27.5	-0.27	0.004	0.004	3.71	0.008	0.004
9:24:46	25	-0.233	0.021	0.002	3.7	0.045	0.020
9:29:16	24	-0.235	0.02	0.002	3.71	0.043	0.019
9:32:16	23	-0.225	0.025	0.002	3.7	0.053	0.024

GW821 Injection Test

time	depth	volts	Q (L/min)	std dev	head	adj V	adj Q
11:35:08	18	-0.292	0.003	0.003	3.74	-0.300	0.000
11:57:07	45.8	-0.285	0.007	0.004	4.38	-0.293	0.003
12:02:57	43.9	-0.265	0.016	0.002	4.38	-0.273	0.012
13:00:37	40	-0.263	0.017	0.008	4.38	-0.271	0.013
13:17:16	38	-0.287	0.006	0.002	4.37	-0.295	0.002
13:31:57	37	-0.291	0.004	0.004	4.39	-0.299	0.001
13:37:51	36	-0.274	0.012	0.003	4.38	-0.282	0.008
13:50:21	34	-0.277	0.01	0.003	4.37	-0.285	0.007
13:54:41	33	-0.268	0.014	0.006	4.38	-0.276	0.011
14:03:24	32	-0.323	-0.01	0.008	4.38	-0.331	-0.014
14:10:51	30	-0.271	0.013	0.004	4.39	-0.279	0.010
14:22:36	28	-0.28	0.009	0.007	4.39	-0.288	0.006
14:26:41	27	-0.257	0.02	0.003	4.39	-0.265	0.016
14:30:26	26	-0.252	0.021	0.005	4.38	-0.260	0.018
14:34:38	25	-0.246	0.024	0.004	4.38	-0.254	0.021
14:47:51	24	-0.23	0.031	0.007	4.36	-0.238	0.028
14:52:58	23	-0.24	0.027	0.003	4.39	-0.248	0.024
15:03:51	27.5	-0.271	0.013	0.003	4.39	-0.279	0.010
15:17:26	35	-0.244	0.025	0.005	4.38	-0.252	0.022
15:26:31	42	-0.293	0.003	0.005	4.37	-0.301	0.000
15:36:21	18	-1.074	-0.348	0.014	4.36	-1.082	-0.351
15:52:15	47	-0.28	0.009	0.002	4.37	-0.288	0.006

Table A5. EM Flowmeter data for GW822.

GW822 Ambient Test

time	depth	volts	Q (L/min)	std dev	head	adj V	adj Q
7:08:03	17.76	-0.189	-0.085	0.007	8.02	0.000	0.000
7:28:00	68	-0.251	-0.113	0.002	8.03	-0.052	-0.023
7:42:39	66	-0.255	-0.115	0.001	8.08	-0.048	-0.022
7:52:38	64	-0.26	-0.117	0.001	8.09	-0.048	-0.022
7:59:41	62	-0.202	-0.091	0.003	8.08	0.014	0.006
8:05:52	60	-0.255	-0.115	0.001	8.07	-0.036	-0.016
8:11:07	58	-0.191	-0.086	0.002	8.08	0.030	0.014
8:16:24	56	-0.074	-0.033	0.002	8.09	0.150	0.068
8:20:51	54	-0.051	-0.023	0.003	8.09	0.176	0.079
8:24:51	52	-0.07	-0.032	0.002	8.09	0.159	0.072
8:28:58	50	-0.204	-0.092	0.001	8.08	0.027	0.012
8:38:55	48	-0.043	-0.019	0.001	8.09	0.193	0.087
8:49:36	49	-0.045	-0.02	0.002	8.09	0.197	0.089
8:56:47	49.5	-0.045	-0.02	0.002	8.09	0.200	0.090
9:31:37	47	-0.062	-0.028	0.002	8	0.201	0.091
9:36:18	46	-0.177	-0.08	0.003	7.99	0.088	0.040
10:49:35	23.13	-0.308	-0.139	0.007	8.09	0.000	0.000
11:31:49	23.1	-0.303	-0.004	0.002	8.08	0.000	0.000
11:45:32	44	-0.029	0.119	0.018	8.12	0.282	0.127
11:53:00	42	-0.089	0.092	0.019	8.2	0.225	0.102
11:56:08	40	-0.059	0.106	0.002	8.17	0.257	0.116
12:02:19	38	-0.057	0.106	0.027	8.16	0.262	0.118
12:09:30	36	-0.077	0.098	0.004	8.09	0.262	0.118
12:15:10	34	-0.063	0.104	0.002	8.11	0.263	0.119
12:22:34	23.1	-0.333	-0.018	0.006	8.11	0.000	0.000

GW822 Injection test

time	depth	volts	Q (L/min)	std dev	head	adj V	adj Q
8:54:46	23	-0.241	-0.004	0.003	8.01	-0.232	0.000
9:10:23	68	-0.253	-0.01	0.002	8.5	-0.244	-0.005
9:53:08	68.1	-0.248	-0.007	0.008	8.76	-0.239	-0.003
10:05:40	66	-0.266	-0.015	0.006	8.76	-0.257	-0.011
10:13:29	64	-0.264	-0.014	0.002	8.73	-0.255	-0.010
10:19:01	62	-0.218	0.006	0.002	8.73	-0.209	0.010
10:34:06	60	-0.26	-0.013	0.002	8.75	-0.251	-0.009
10:46:03	58	-0.274	-0.019	0.004	8.76	-0.265	-0.015
11:02:20	57	-0.53	-0.134	0.03	8.75	-0.521	-0.130
11:09:11	56	-0.605	-0.168	0.002	8.76	-0.596	-0.164
11:17:57	54	-0.586	-0.159	0.005	8.76	-0.577	-0.156
11:26:18	52	-0.558	-0.147	0.005	8.75	-0.549	-0.143
11:30:59	51	-0.578	-0.156	0.003	8.75	-0.569	-0.152
11:37:53	50	-0.461	-0.103	0.005	8.75	-0.452	-0.099
11:44:05	49	-0.6	-0.166	0.003	8.75	-0.591	-0.162
11:54:16	48	-0.595	-0.163	0.005	8.76	-0.586	-0.160
12:03:22	47	-0.573	-0.153	0.002	8.74	-0.564	-0.150
12:07:39	46	-0.245	-0.006	0.001	8.75	-0.236	-0.002
12:15:23	44	-0.572	-0.153	0.003	8.75	-0.563	-0.149
12:22:23	42	-0.57	-0.152	0.004	8.74	-0.561	-0.149
13:18:02	23	-0.3	-0.032	0.002	8.24	-0.228	0.000
13:39:04	40	-0.715	-0.219	0.001	8.75	-0.643	-0.187
13:45:47	38	-0.679	-0.203	0.002	8.75	-0.607	-0.170
13:56:48	36	-0.627	-0.179	0.002	8.75	-0.555	-0.147
14:03:22	34	-0.581	-0.159	0.002	8.75	-0.509	-0.126
14:15:10	23	-1.537	-0.589	0.01	8.75	-1.465	-0.556

Table A6. EM Flowmeter data for GW823.

GW823 Ambient Test

time	depth	volts	Q (L/min)	std dev	head	adj V	adj Q
8:28:28	18	-0.273	-0.005	0.003	2.58	-0.263	0.000
8:45:35	60	-0.277	-0.007	0.003	2.6	-0.267	-0.002
8:47:55	58	-0.287	-0.011	0.004	2.57	-0.277	-0.007
8:52:32	56	-0.275	-0.006	0.002	2.58	-0.265	-0.001
8:55:49	54	-0.254	0.004	0.002	2.59	-0.244	0.008
9:02:25	52	-0.271	-0.004	0.002	2.58	-0.261	0.001
9:12:10	51	-0.279	-0.008	0.006	2.58	-0.269	-0.003
13:07:55	18	-0.293	0.003	0.003	2.55	-0.3	0.000
13:18:11	46	-0.262	0.017	0.013	2.57	-0.269	0.014
13:24:10	46.1	-0.236	0.029	0.013	2.57	-0.243	0.026
13:26:50	46.2	-0.226	0.034	0.009	2.56	-0.233	0.030
13:44:18	38	-0.261	0.018	0.006	2.58	-0.268	0.014
13:52:38	36	-0.245	0.025	0.008	2.56	-0.252	0.022
13:57:25	34	-0.243	0.026	0.007	2.57	-0.25	0.023
14:02:35	32	-0.229	0.032	0.007	2.57	-0.236	0.029
14:06:48	30	-0.222	0.035	0.005	2.57	-0.229	0.032
14:16:26	28	-0.253	0.021	0.006	2.52	-0.26	0.018
14:24:03	44	-0.231	0.031	0.005	2.58	-0.238	0.028
14:33:34	42	-0.238	0.028	0.002	2.6	-0.245	0.025
14:38:19	40	-0.232	0.031	0.003	2.59	-0.239	0.028
14:58:45	18	-0.307	-0.003	0.013	2.59	-0.314	-0.006
15:08:08	18.1	-0.293	0.003	0.008	2.6	-0.3	0.000

GW823 InjectionTest

time	depth	volts	Q (L/min)	std dev	head	adj V	adj Q
8:20:20	18	-0.268	0.002	0.003	2.65	-0.272	0.000
8:40:05	59.8	-0.273	-0.001	0.003	3.25	-0.277	-0.002
9:03:00	58	-0.272	0	0.008	3.24	-0.276	-0.002
9:19:21	56	-0.252	0.009	0.006	3.25	-0.256	0.007
9:26:15	54	-0.258	0.007	0.003	3.24	-0.262	0.005
9:28:56	54.1	-0.26	0.005	0.002	3.25	-0.264	0.004
10:03:19	52	-0.272	0	0.007	3.24	-0.276	-0.002
10:59:27	18	-0.29	-0.008	0.004	2.76	-0.294	-0.010
13:35:00	18	-0.293	0.003	0.004	2.62	-0.3	0.000
13:55:40	46	-1.002	-0.316	0.009	3.24	-1.009	-0.319
14:10:38	44	-0.956	-0.295	0.005	3.23	-0.963	-0.298
14:28:44	42	-1.094	-0.357	0.004	3.25	-1.101	-0.360
14:34:49	40	-1.084	-0.353	0.003	3.24	-1.091	-0.356
14:45:24	38	-0.69	-0.175	0.005	3.24	-0.697	-0.179
15:22:34	36	-0.826	-0.237	0.003	3.25	-0.833	-0.240
15:29:42	34	-0.723	-0.19	0.003	3.24	-0.73	-0.193
15:36:44	32	-0.856	-0.25	0.003	3.24	-0.863	-0.253
15:45:19	30	-0.825	-0.236	0.003	3.25	-0.832	-0.239
16:08:50	28	-0.645	-0.155	0.006	3.24	-0.652	-0.158
17:01:00	58.2	-0.293	0.003	0.01	2.78	-0.3	0.000

Table A7. Multilevel well as-built specifications.

well	northing	easting	ground el	casing survey	manifold meas pt	top of sand	bottom of sand	port center	bottom of borehole
GW821	29621.25	29250.08	842.40	842.80	842.59				791.90
A	"	"	"	"	"	799.40*	791.90*	799.15	"
B	"	"	"	"	"	804.40	802.65	803.65	"
C	"	"	"	"	"	808.90	807.40	808.15	"
D	"	"	"	"	"	817.40	815.90	816.65	"
E	"	"	"	"	"	823.16	820.90	822.15	"
GW822	29587.33	29270.74	842.71	843.06	843.61				772.71
A	"	"	"	"	"	780.71	779.11	779.96	"
B	"	"	"	"	"	789.21	787.71	788.46	"
C	"	"	"	"	"	795.31	793.71	793.96	"
D	"	"	"	"	"	809.31	807.71	808.46	"
E	"	"	"	"	"	826.71**	811.71	812.96	"
GW823	29591.59	29214.59	840.42	840.65	841.19				768.42
A	"	"	"	"	"	782.12	774.40+	774.67	"
B	"	"	"	"	"	792.92	791.52	792.17	"
C	"	"	"	"	"	805.62	804.62	804.67	"
D	"	"	"	"	"	813.92	812.42	813.17	"
E	"	"	"	"	"	823.59	821.92	822.67	"

Coordinates are referenced to the Y-12 grid.

All elevations referenced to mean sea level.

* Sampling port 821A is surrounded by silty fill material; top of sand is the elevation at which the bentonite seal begins.

** Borehole collapse occurred at 826.71; thus the port must be considered open up to this elevation.

+ Borehole collapse occurred below approximately 774.4 ft; thus the port must be considered open to bottom of borehole.

APPENDIX B: CORE LOGS

Core log for GW-821
Depth drilled: 50′
casing: ~ 22.5′
drilling with water begins: 25′

water at ~18′
competent bedrock: ~25′

21 mineralogy samples
4 pore water samples

Interval: 0-5′	Length: 2.6′	True interval: 2.4-5′

Top 0.3′: dark brown, organic soil, twigs.
Rest: Dark yellowish orange (10YR6/6) to moderate yellowish brown (10YR4/2), dry, crumbly, weathered silty clay/sand. Saprolite-shale structures apparent.

Min samples: 0
PW samples: 0

Interval: 5-10′ (pushed w/H20)	Length: 2.9′	True interval: 7.1-10′

Same color as above, clay-rich silty sand, some weathered pebbles, STAINED, moist.

Min samples: 0
PW samples: 0

Interval: 10-15′	Length: 3′	True interval: 12-15′

Same as above, but darker brown at bottom of interval, very rubbly. Dry and crumbly. Heavily STAINED. Lighter tan when cut.

Min samples: 0
PW samples: 0

Interval: 15-17′	Length: 1.2′	True interval: 15.8-17′

Lost top half of core.
16-17′: dusky yellow (5Y6/4) to light olive brown (5Y6/6) silty sand. Very WEATHERED but no staining apparent. Shaly bedding. Dry.

Min samples: 0
PW samples: 0

Interval: 17-18′	Length: 1′	True interval: 17-18′

Light olive brown (5Y5/6) silty sand matrix, dry and crumbly, with dark grey (N3) weathered shale fragments. Some Fe stained fragments at ~17.5′. Mn-oxide coatings observed. FE STAINED and WEATHERED observed throughout entire interval. Difficult to see because fragments covered in soil.

Min samples: 0
PW samples: 0

***********************WATER AT 18′***

Interval: 18-20.5′	Length: 2.5′	True interval: 18-20.5′

18-19.5′: Dark brown silt, WET, with fragments of heavily Fe-stained shale.
*19′: Larger pieces of rock, HEAVILY FE STAINED, one piece busted up for pore water analysis.
19.5-20.5′: Dark grey (N3), busted up shale, very dry, some indurated pieces, some weathered. No significant Fe staining.

Min samples: 2 (18.5′ and 19′: heavily stained shale)
\PW samples: 2 (18.5′ and 19′)

Interval: 20.5-22′	Length: 2.5′ (top 1′: slough)	True interval: 20.5-22′

Top 1′ (slough): brown silt-clay, moist, covering weathered shale fragments. Sampled for pore water.
20.5-22′: Dark grey (N3) fine-grained shale, dry, very powdery. Some larger pieces. No significant Fe staining, except for shale piece at 22′ which has FE STAINING and green alterations.

Min samples: 2 (20.5′: stained /weathered shale; 22′: stained/altered shale)
PW samples: 1 (20.5′)

Interval: 22-23′	Length: 13"	True interval: 22-23′

22-22.7′: Brown, clay-covered weathered shale. Soft but retains shaly structure. Calcite veins observed, some in-situ weathering, heavily FE STAINED weathering rinds on fragments. One competent piece at 22′, rest of interval is very clay-rich and soft. Clay is moist.
22.7-23′: Grey, extremely weathered shale. No competent pieces, very crumbly, dry.

Min samples: 1 (22.5′: stained/weathered shale)
PW samples: 1 (22.5′)

Interval: 23-25′	Length: 2′	True interval: 23-25′

23-24′: Dark grey (N3) fine-grained shale, very busted up, dry. Mostly small fragments, a few larger pieces.
*24′: FE STAINED shale; green alterations observed in this zone.
24-25′: Lighter grey powder on shale fragments. FE STAINING observed on many of the fragments. Most fragments less than 2" in length. A few larger pieces, one with significant FE STAINING..

Min samples: 1 (24′: heavily stained shale)
PW samples:

***************WET DRILLING BEGINS AT 25′*****************************

Interval: 25-30′	Length: ~3′	True interval: 27-30′

Top 1": FE STAINED calcite/shale. Green alteration product on shale.
27--27.5′: oolite with some BLACK STAINING. Minor Fe staining on top.
27.5-28.7′: Dark grey (N3) shale, mostly small fragments, very blocky. Minor calcite veining. No Fe staining.
28.7-30′: Clay-rich dark grey shale, no fragments. Looks like weathered in situ. Extremely soft and crumbly.

Min samples: 3 (27′: stained calcite/oolite; ? sample of reddish grey shale; 28′: grey shale with burrow.

Interval: 30-35′	Length: 2.8′	True interval: 32.2-35′

32.2-32.7′: Dark grey (N3) shale, many Fe stained fragments, some associated with calcite vein. Small to medium size fragments.
32.7-34.2′: Dark grey weathered shale with MAJOR FE STAINING, very tiny fragments of shale.
34.2-35′: oolite with calcite veins. Large (2" length) core pieces. Upper few inches are weathered.

Min samples: 2 (32′: stained calcite/shale; 33′: stained and weathered clay/shale)

Interval: 35-40′	Length: ~3.5′	True interval: 36.5-40′

36.5-37.5′: oolite, large pieces (3" long core) with cross-cutting calcite veins.
*37-37.5′: SIGNIFICANT FE STAINING ALONG SIDES OF OOLITE -VERTICAL

FRACTURE.
37.5-38': Dark grey (N3) shale, SIGNIF. FE STAINING MANY PIECES - likely part of same fracture.
38-38.5': Dark grey clay-rich shale, in-situ weathering, soft. Some larger shale pieces in clay.
38.5-40': crumbly, dark grey weathered and fissile shale. In-situ calcite vein weathering. Some small fragments.
40': 3" core of dark grey shale, FE STAINED on one face.

Min samples: 4 (~36.5', 37.5', 40': stained shale; ~37.5': stained oolite)

Interval: 40-45'	Length: 3.2'	True interval: 41.8'-45'

41.8-42.5': Brownish grey (5YR4/1) shale, some heavily STAINED Fe CALCITE vein pieces in shale. One larger (2" or so) piece, rest small fragments. Fragment of oolite but don't know placement.
42.5-42.7': Larger pieces of dark greenish grey shale, calcite growth along sides.
42.7-43.2': Clay-rich weathered, dark greenish grey shale. Very soft, some larger fragments but they break/crumble when handled.
43.2-45': Dark grey crumbly clay/shale. Calcite vein weathered in site. No larger pieces.

Min samples: 1(~42': stained calcite)

Interval: 45-48'	Length: 2.7'	True interval: 45.3-48'

45.3-46': oolite with green alteration product (glauconite??) on surface. Some thin, white, cross-cutting calcite veins. Some larger core pieces.
46-46.2': Dark greenish grey fine-grained shale, thin pieces. No Fe staining.
46.2-46.4': Dark grey clay-rich fissile shale, thin shaly bedding.
46.4-47.4': Dark greenish grey clay-rich shale, larger pieces than above interval.
47.4-50': Dark grey fissile shale, no pieces.

Min samples: 3 (45': oolite with green alteration; 46': unstained grey shale; ~47': carbonate interlayer with staining)

Interval: 48-50'	Length: 18" (rest slough)	True interval: ??

**Slough discarded
~1.5' of small to medium size fragments of mostly dark grey (N3) fine-grained shale. Some pieces of dark greenish grey (5G4/1) shale in top 6". Small pieces of calcite vein in top 6", slight Fe staining but hard to tell placement. Calcite growth along shale facies elongated. Bottom 3": thin (1/2") coarse-grained carbonate layer with some red minerals (hematite??) and black minerals (Mn oxide??).

Bottom piece: shale/carbonate interlayered, few " thick, 3" long.

Min samples: 2 (~50': coarse-grained carbonate, calcite growth on shale)

Core log for GW-822
Depth drilled: 70′
casing: ~32′
drilling with water begins: 33′

water at ~16′
competent bedrock: ~31′ (according to driller; hard to tell in cores, definitely at 32′)

26 mineralogy samples
6 pore water samples

Interval: 0-3′	Length: 3′	True interval: 0-3′

0-0.5′: Dark brown soil with organic matter, leaves, and twigs.
0.5-3′: Dark yellowish orange (10YR6/6) to light brown (5YR6/6) silty sand′, dry, crumbly, weathered saprolite, shaly bedding and clay structure preserved. Very weathered, strong reddish color.

Min samples: 0
PW samples: 0

Interval: 3-5′	Length: 2′	True interval: 3-5′

3-4′: dark organic and stained silt, some leaves, twihs, heavy staining of rock fragments.
4-5′: 4 pieces of saprolite core, heavy staining within saprolite.

Min samples: 0
PW samples: 0

Interval: 5-7′	Length: 2.25′	True interval: ~5-7′

Same as above; heavily stained silt, clay, fine sand/ saprolite.
5-6′:′ crumbly
6-7′: cohesive cores, with heavy staining on surfaces and on inside.

Min samples: 0
PW samples: 0

Interval: 7-9′	Length: 1.7′	True interval: 7.3-9′

7.3-8.6′: crumbly, heavily stained and weathered shale, all competent rock fragments are carbonate. wavy shaly bedding preserved.
8.6-9′: greenish gray shale/saprolite core, interlayed with dark brown silt/clay

Min samples: 1 (8′)

PW samples: 0

Interval: 9-11′	Length: ~34" (top 8" slough)	True interval: 9-11′

9-10′: dark yellowish orange (10YR6/6) to moderate yellowish brown (10YR5/4) silt and clay, dry and crumbly, no rock fragments, VERY HEAVY STAINING AT ~9′.
10-11′: larger cores of saprolite, same color as above.
* heavy staining throughout this interval

Min samples: 0
PW samples: 0

Interval: 11-13′	Length: 28" (top 4" slough)	True interval: 11-13′

Top 4": brown soil rubble (slough)
11-13′: same color as above, very weathered saprolite, significant Fe staining and weathering throughout. Core pieces are 3-4" in length. Hard to distinguish specific flow zones but most heavily stained at ~11.5′. Slightly moist and crumbly.

Min samples: 0
PW samples: 0

Interval: 13-14′	Length: 2′	True interval: 13?-14′

Top 1.3′: silty sand, same color oas above, moist and crumbly with blocky fragments of stained shale.
Bottom 0.7′: saprolite core, less orange tint, more olive color than above, significant Fe staining throughout.

Min samples: 1 (13-13.5′)
PW samples: 0

Interval: 14-15′	Length: 1′	True interval: 14-15′

14-14.5′: shale/saprolite moderate to dark yellowish brown with olive tint, similar to 17-19′ saprolite, slightly moist, crumbly. Heavily stained surfaces on greenish-gray shale.
14.5-15′: more competent saprolite core.

Min samples: 0
PW samples: 0

Interval: 15-16′	Length: ~2′	True interval: 15?-16′

15-15.5': grayish orange powder covering medium to large size shale pieces with HEAVY FE STAINING. Significant staining on shale surfaces throughout interval. DRY!!
15.5-16': very pale orange powder (lighter than above), appears to be same rock type as above.

Interval: 16-17'	Length: 13"	True interval: 16-17'

16-16.3': dark brown silty clay
16.3-16.4': grey silt layer, small twigs
16.4-16.8': moderate yellowish brown (10YR5/4) silty sand, some clay, moderate staining on oolite piece at 16.8', many small twigs.
16.8-17': moderate yellowish brown to light olive gray (5Y5/2), piece of heavily stained oolite at 17'.

Min samples: 1 (17', stained oolite)
PW samples: 1 (16.5', brown silty mush)

Interval: 17-19'	Length: 2'	True interval: 17-19'

WET!!!
17-18.3': very wet brown silt/clay/fine sand, very mushy, with disks of carbonate. Carbonate surfaces NOT stained.
18.3-19': very weathered/stained greenish gray shale/saprolite. moist, not as wet as above. HEAVY Fe staining along horizontal places at 18.5'
18.5-20': weathered but NO significant staining.

Min samples: 1 (18.5', stained shale)
PW samples: 1 (18.5, CHECK THIS!!!)

Interval: 19-21'	Length: 2.5'	True interval: ~19-21'

WET!!!!!!!!
19-20.5': greenish gray shale fragments, some heavily dark oxide stained, in moderate yellowish brown silty clay matrix. Most shale very soft, few more indurated pieces. MAJOR FLOW ZONE.
20.5-21': same as above but more orange staining.

Min samples: 2 (20.5-21'; ~20)
PW samples: 1 (19.4-19.8')

Interval: 21-22	Length: 1'	True interval: 21-22'

21-21.3': brown silty clay with large, dark grey piece of carbonate.
21.3-21.5': large dark grey carbonate piece.
21.5-22': moderate olive brown (5Y4/4) saprolite, same as below, moist clay,

shale fragments have heavy dark oxide staining. mostly clay, less fragments than above.

Min samples: 1 (21.5-22', stained shale/saprolite)
PW samples: 0

Interval: 22-23'	Length: 18" (4" slough)	True interval: ~22-23'

Top 4": dark brown silty clay with shale fragments (slough)
22-23': same color as below but more moist, very crumbly, weathered saprolite, staining within saprolite cores and pieces. Some greenish gray shale fragments, most HEAVILY STAINED with dark oxide.

Min samples: 1 (22.5': stained shale)
PW samples: 0

Interval: 23-24'	Length: 18" (top 6" slough)	True interval: 23-24'

DRY!!!
Top 6": brown silty clay (slough)
23-23.25': moderate to light olive brown weathered saprolite, no shale.
23.25-23.75': same as above but shale fragments present, silty clay, very crumbly , shale indurated but very fragmented. greenish grey shale. small-medium size fragments. moderate dark oxide staining on some shale fragments. can't tell if/where fracture zone occurs.
23.75-24': same as above but no shale.

Min samples: 1 (23.5')
PW samples: 0

Interval: 24-27' (dry drill)	Length: ~2'	True interval: 25-27'

EXTREMELY WET!!!!!!
25-26': moderate yellowish brown (10YR5/4) to dark yellowish brown (10YR4/2) silty sand to silty clay with small shale fragments. Shale fragments are HEAVILY STAINED with Fe and Mn oxides. Appears to be MAJOR FLOW ZONE!!!!
26-~26.5': Light olive gray (5Y5/2) silty clay with greenish gray shale fragments. WET. Shale fragments are HEAVILY STAINED with Fe and Mn oxides.
26.5-27': same as top interval.

Min samples: 3
PW samples: 2 (25', 27')

Interval: 27-31′ (dry drill)	Length: 3′	True interval: 28-31′

28-29.5′: Dark yellowish brown (10 YR 4/2) to dusky brown (5YR2/2) silty clay, WET, top few inches has few fragments of shale.
~28.5′ and 29: dark yellowish orange (10YR6/6) clay layers, very fine-grained, WET, sandwiched between thin, black, coarser-grained layers.
~29′: darker, coarser-grained layer, inches thick, some orange discoloration.
29-29.5′: dark yellowish brown (10YR4/2), same as top interval, with fragments of shale which
have significant Fe and Mn STAINING.
29.5-31′: Light olive gray (5Y5/2) saprolite disks, clay-rich weathered shale. shaly bedding. fragments of greenish gray shale within clay have dark STAINING. DRY and crumbly; minor Fe staining on surfaces of disks.

Min samples:
PW samples:

Interval: 31-32′ (dry drill)	Length: 14"	True interval: 31-32′

31-32′: Dark grey (N3) weathered shale and clay. Shale in fragments, a few larger pieces at bottom of core. Clay very crumbly, moist. Shale appears to be weathered in-situ to clay; clay retains shaly bedding characteristics. Some thin brown silty clay interlayers at ~31.2′ and ~31.4′.
* Moderate to heavy Fe staining on shale/clay at ~31′

Min samples:
PW samples:

Interval: 32-33′ (dry drill)	Length: 1′	True interval: 32-33′

Dark brown clay at top and covering sides of top portion of core.
32-33′: dark grey (N3) shale and clay. Clay is crumbly but very cohesive. Some yellow and brown alteration within clay (weathering products?) but small-scale. Three disks of shale present, very indurated, no Fe staining observed. A few smaller shale fragments. Does not appear to be significant flow zone.

Min samples:
PW samples:

Interval: 33-35′ (wet drill)	Length′: 2′	True interval: 33-35′

33-33.75': Dark to medium grey shale with reddish carbonate interlayers, some internal deformation observed. Large pink calcite vein with large crystals, elongated. Slight Fe staining at bottom of this zone. Medium size (<2" long) fragments.
33.75-34.25': clay-rich weathered shale, soft, fissile. Reddish brown interlayers. Some shale fragments in clay.
34.25': calcite vein/carbonate layer, competent.
34.25-35': clay-rich weathered shale, same as above. Solid pieces are predominantly carbonate. Carb fragments at bottom.
No significant Fe staining in this interval.

Min samples:
PW samples:

Interval: 35-40' (wet drill)	Length: 3.25'	True interval: 36.75-40'

*Slough discarded
36.75-38.25': Dark grey shale with lighter reddish grey carbonate intervals (brownish grey 5YR4/1). Large pink calcite vein, slightly Fe stained at top. Thinner white calcite cross cutting veins, many perpendicular to bedding. Nice laminations on some pieces. Some larger (few" length) pieces.
Carbonate layer (not sure about placement), with coarse-grained Mn oxide coating. Elongated crystals, intraclasts.
38.25-39.25': pulverized shale, some larger pieces retrieved, rest (slough) discarded.
39.25': oolite
39.25-40': clay-rich fissile shale and shale pieces. Very weathered, fissile, soft. Looks natural.
40': Oolite
No Fe staining observed in this interval

Min samples:
PW samples:

Interval: 40-45' (wet drill)	Length: 3.25'	True interval: 41.75-45'

41.75-43.50': Dark grey (N3) shale with brownish grey (5YR4/1) carbonate intervals. Horizontal bedding visible in shale and carb. Carb intervals up to 1" thick. oolite layer at ~52.25', coarse-grained. Thin white calcite veins, both cross-cutting and bed parallel. Some larger pieces. No Fe staining. Pieces seem to break along shale, not along carbonate.
43.5-43.75': fissile shale, mostly tiny pieces.
43.75': few inches of dusky yellowish brown (10YR2/2) shale.

43.75-44': coarse-grained brownish gray (5YR4/1) oolite, small black minerals, shale intraclasts, calcite veins. FE staining on shale (bed parallel) and on side, microfolding structures observed.
44-45': clay-rich shale, very weathered and fissile. Most incorporated in clay. Clay looks natural, clay structures observed, iron staining, in situ weathering of calcite veins. More competent pieces have carbonate layers. Moderate Fe staining, esp. in zone right below oolite. shale very fissile, clay-rich.

Min samples:
PW samples:

Interval: 45-50' (wet drill)	Length: 2.7'	True interval: 47.3-50'

47.3-48.3': predominantly medium to dark grey (N4/N3) shale, well indurated, with light carbonate intervals. One carb piece has coarse-grained infilling. Cross-cutting think white calcite veins, most perpendicular to bedding, lots of shale fragments. No Fe staining.
48.3-48.6': lighter brownish grey (5YR6/1) oolite with thin calcite veins ~ 45 deg dip to vertical axis. Oxide covering on side of larger piece. FE staining with weathered pits, parallel to calcite veins.
48.6-50': clay-covered fissile shale, very soft and weathered. Medium to dark grey (N4/N3) some in situ weathering of calcite vein, some staining in clay. Clay looks natural.

Min samples:
PW samples:

Interval: 50-55' (wet drill)	Length: 3'	True interval: 52-55'

52-54': Medium to dark grey (N4/N3) shale fragments, well indurated, most pieces 1/2" in length. Oolite with Mn oxides staining at top. some pieces of shale have structures that look like slickensides. Carb interlayers, some oolite pieces. Some larger shale pieces. No signif. Fe staining.
54-55': fissile, clay-rich, small shale fragments. Sign. Fe staining at 54'.

Min samples:
PW samples:

Interval: 55-60' (wet drill)	Length: 2.6'	True interval: 57.4-60'

57.4-58.4': dark grey (N3) fine-grained shale, well indurated, with cross-cutting

thin white calcite veins and few thicker pink veins. FE staining on several pieces but hard to tell placement. Calcite elongation.
58.4-59.1': fissile shale, mostly tiny pieces, brownish black (5YR2/1) with pieces of brownish grey (5YR4/1) to brownish black medium grained carbonate with some elongated crystals. Small black minerals. calcite veins, some with green alteration product.
59.1-60': dark greenish grey (4G4/1) to brownish grey/black (5YR4/1 to 5YR2/1) shale, tiny pieces. THIS INTERVAL DISCARDED.

Min samples:
PW samples:

Interval: 60-65' (wet drill)	Length: 2.5'	True interval: 62.5-65'

62.5-64': oolite, brownish grey (5YR4/1) to medium dark grey (N4) many thin cross-cutting white calcite veins, green shale intraclast/vein, glauconite (??) on oolite surface. stylolitic piece (sampled). large core piece (6").
64-64.25': med to dark grey (N4/N3) shale, some thin carbonate intervals. pink calcite vein, looks bed parallel. Bottom piece has small black minerals (Mn ox?)
64.25-64.75': oolite, same as top interval, heavy Fe staining on small pieces. Mn oxide.
64.75-65': HEAVILY FE STAINED shale, original core clay covered. Mostly small pieces, clay discarded.

Min samples:
PW samples:

Interval: 65-70' (wet drill)	Length: 2.25'	True interval: 67.75-70'

67.75-68': HEAVILY FE STAINED calcite veins, elongated crystal growth, in shale. some carb layers up to 1/4" thick. Shale fine-grained, shaly bedding but well indurated. medium to dark grey, carb intervals brownish grey (5YR4/1).
68-69': predom shale with carb interlayers. calcite with preferred elongation on many surfaces.
69-69.5': oolite with thin white cross cutting calcite veins, black mineral on surface. shale intraclasts, iron staining along rinds. Some Fe staining along veins.
69.5-70': Very fissile shale, clay-covered, few larger pieces.

Min samples:
PW samples:

Core log for GW-823
depth drilled: 70′
casing: ~25′
drilling with water begins: 27′

water table at ~11.5′
competent bedrock: ~25′ (?)

mineralogy samples: 34
PW samples: 4

Interval: 0-3′	Length: 3′	True interval: 0-3′

0-0.5′: dark brown organic clay soil, twigs.
0.5-1′: dark yellowish orange (10YR6/6) to moderate yellowish brown (10YR5/4) clay core.
1-3′: same color as above, dry and crumbly, clay/silt/fine sand, shaly bedding/weathering structures observed.

Min samples: 0
PW samples: 0

Interval: 3-5′ (pushed w/H2O)	Length: 2′	True interval: 3-5′

3-4′: same as above, moderate yellowish brown (10YR5/4) silty sand, crumbly, few pieces of stained shale.
4-5′: same as above, but consolidated core, laminations and weathering structures observed.

Min samples: 0
PW samples: 0

Interval: 5-7′	Length: 2′	True interval: 5-7′

Top 3" dark grey/black, organic smell, some twigs.
5-6′: moderate yellowish brown saprolite, WET (probably from above interval pushed out with water). Heavily stained, very few small shale fragments.
6-7′: dry and crumbly.

Interval: 7-9′	Length: 2′	True interval: 7-9′

7-8.4′: olive gray (5Y3/2) silty sand with dark red/black staining, dry, crumbly.
8.4-9′: same as above but more reddish staining.

Min samples: 1 (8': stained shale/saprolite)
PW samples: 0

Interval:9-11' (pushed w/H2O)	Length: 3'	True interval: 9?-11'

9-11': same as above but consolidated core (5 pieces), weathered, moist to wet, no competent pieces, heavily stained.

Min samples: 0
PW samples: 0

*****************WATER at ~11'.5**************************

Interval: 11-13'	Length: 2.5'	True interval: 11?-13'

WET!!!!!
top 6": brown clay (slough)
11-11.5': dusky yellowish brown (10YR2/2) clay and shale fragments.
11.5-13': dark brown silty MUSH; WET, some staining, many shale pieces.
12': Large (4") piece of heavily STAINED shale!!

Min samples: 2 (12.5-13': stained shale; 12': heavily stained shale)
PW samples: 0

Interval: 13-15'	Length: 1.7'	True interval: 13.3-15'

13.3-13.8': dark brown silty MUSH, WET
13.8-14.3': grayish olive (10Y4/2) weathered shale/clay, top 13.8-13.9 WET (brown clay); rest is moist in crumbly grayish olive clay. Shale fragments stained.
14.3-15': grayish olive weathered shale core, not as heavily stained as above, moist.

Min samples: 0
PW samples: 0

Interval: 15-20'	Length: 3'	True interval: 17?-20'

Top 1': dark brown WET silty mush
1-2': greenish grey shale/saprolite, fissile, moist to wet, weathered, some pieces.
2-3': MAJOR STAINING, reddish brown saprolite, very weathered and stained, DRY.

Min samples: 2 (~19-20': stained saprolite; ~18-19': stained shale/saprolite)

PW samples: 1 (top 1' ~16/17'?)

Interval: 20-21'	Length: 18" (6" slough)	True interval: 20-21'

20-21': moist to wet saprolite, same as below, crumbly, moist, no large rock pieces, very heavy dark staining.

Min samples: 0
PW samples: 1 (20-21')

Interval: 21-22.5'	Length: 3'	True interval: 21?-22.5'

21-22.5': moderate to dark yellowish brown, same as below, dry, crumbly saprolite. Heavily stained competent shale pieces.

Min samples: 1 (21-22.5': stained shale/saprolite)
PW samples: 1 (21-22.5')

Interval: 22.5-23.5'	Length: 2'	True interval: 22.5?-23.5'

Very HEAVILY STAINED AND WEATHERED!
Same as below, dark brown silty sand/clay with shale fragments.
22-22.5': Heavily stained shale, many large pieces.
22.5-23': mostly weathered, less competent.

Min samples: 1 (22-22.5': stained shale)
PW samples: 0

Interval: 23.5-24.5'	Length: 1.7' (0.5' slough)	True interval: ~23.5-24.5'

Top 6": brown clay (slough)
23.5-23.75': heavily weathered and stained shale pieces in clay, saprolite.
23.75-24.25': slightly moist, crumbly, darker than below. HEAVILY STAINED weathered shale. some small pieces of competent shale.
24.25'-25': consolidated weathered shale/saprolite, can see shaly bedding structures.

Min samples: 1 (23.75-24.25': stained/weathered shale)
PW samples: 1 (23.5-24.5')

Interval: 24.5-25'	Length: 1.3' (top 0.7' slough)	True interval: 24.5-25'

Top 0.7': brown clay with shale fragments (slough?), moist.
24.5-24.6': consolidated weathered shale/clay (saprolite), staining.
24.6-25': dark yellowish brown, dry, crumbly, silty sand with weathered shale pieces (saprolite), no competent shale, all extremely weathered.

Min samples: 0
PW samples: 0

*************TOP OF BEDROCK: 25' ??????***************

Interval: 25-26'	Length: 1.5' (top 6" slough)	True interval: 25-26'

Top 6": dark grey weathered shale covered by brown silty clay, soft, no staining.
25-26': same as below, dark yellowish brown to light olive grey, dry and crumbly, dark grey shale pieces with weathering rinds, staining on many pieces, no specific zone of staining. no competent shale, all extremely weathered.

Min samples: 0
PW samples: 0

Interval: 26-27'	Length: 1.5' (top 6" slough)	True interval: 26-27'

Top 6": brown clay with shale fragments (slough?)
26-26.5': dark yellowish brown (10YR4/2) to light olive gray (5Y5/2), dry, crumbly silty sand with pieces of heavily weathered shale. some pieces heavily stained, can't tell placement of staining.
26.5-27': same as above but lighter, more pale yellowish brown (10YR6/2)
27': competent piece of shale, moderate staining.

Min samples: 2 (26.5': heavily weathered/stained shale; 27': stained shale)
PW samples: 0

****************WET DRILLING BEGINS AT 27'****************************

Interval: 27-35'	Length: ~3'	True interval: ??

**SLOUGH DISCARDED
Top 2": weathered, Fe stained calcite vein.
0-~2': dark grey shale, some calcite veining, indurated, LARGE PIECE. carbonate intervals. HEAVY FE STAINING at 1'.
2-~2.75': oolite, small shale intraclasts, stylolite features., black minerals.
2.75-3': shale, no veining. Medium size (few " length, 1/2" thick) pieces.

Min samples: 4 (top 1": weathered calcite; 1': stained and unstained shale, 2': oolite)

Interval: 35-40'	Length: 3.25'	True interval: 36.75-40'

36.75-37.75': oolite, yellow mineralization ~37'. Mica(?) and black minerals observed, shale intraclasts. Black staining on some pieces.
37.75-38.75': shale, some large 1/2" length pieces. FE stained zone at ~38'. most pieces medium size. Burrow structures (?) . Fe staining along calcite vein. Thin white cross-cutting calcite veins.
38.75-40': clay-rich zone, much Fe staining in clay.

Min samples: 1 (~37": stained oolite)

Interval: 40-45'	Length: 3'	True interval: 42-45'

42-43': oolite, some calcite veins, one vein lined with black mineral (stylolitic), larger pieces , up to 2-3" in length.
43-44': HEAVILY STAINED SHALE, medium size pieces with carbonate interlayers.
44-45': clay-rich shale, mostly clay. some small shale pieces.

Min samples: 2 (42-43': oolite with stylolite; 43-44': heavily stained shale)

Interval: 45-49'	Length: 1' (48-49')	True interval: 48-49'

48-48.5': small pieces of stained and unstained shale, bits of oolite.
48.5-49': oolite with shale intraclasts, looks stylolitic. oolite breaks along these planes of weakness. Major FE staining along shale stylolite. FE STAINING IN THIS INTERVAL

Min samples: 2 (48-49': heavily stained shale, oolite with shale clasts.

Interval: 49-54' "top"	Length: 2'	True interval: 49-51'

49-49.25': oolite with thin white cross-cutting veins; dark staining on side. Some dark stained pieces between 49 and 49.5'; can't tell placement.
49.25-51': dark grey shale and carbonate interlayer pieces, no clay. Several stained pieces at ~50.3', but hard to tell placement. More stained pieces at 50.5'; part of same fracture?

Min samples: 3 (49-49.5': stained shale; microfault in shale; 50.3-50.5': stained shale)

Interval: 49-54' "bottom"	Length: 3'	True interval: 51-54'

51-54': small pieces of shale; rest is weathered clay-rich shale.

Min samples: 1 (top zone: small pieces of shale)

Interval: 54-65' "top"	Length: 1.5'	True interval: ??

Oolite carbonate interval, one large pink calcite vein, black minerals, one red mineral (hematite?), elongated calcite crystals. Some shale pieces at bottom.

Min samples: 3 (top zone: oolite with calcite vein; bottom zone: shale and oolite/shale)

Interval: 54-65' "bottom"	Length: 3'	True interval: ??

top 1': dark grey shale pieces, some up to 3" long, no staining observed in silt/clay.
1-1.5': dark grey fissile weathered shale in clay matrix, no staining.
1.5-2': greenish grey shale, fissile, weathered shale in clay, some larger pieces. no staining, weathered calcite vein.
2.25-2.5': dark grey, very clay-rich , small pieces of shale
2.5-2.75': dark grey and fissile
2.75-3': dark grey shale/clay with pieces.
***no staining observed, but very weathered.

Min samples: 0

Interval: 65-70' "top"	Length: 1' (~4' original)	True interval:??

Mostly broken up shale, small pieces, soft, shaly bedding. Iron stained pieces at top. Some oolite pieces; not sure about placement.
**SLOUGH DISCARDED

Min samples: 3 (top zone: stained shale; bottom zone: stained shale; ?: oolite with shale intraclasts

Interval: 65-70' "bottom"	Length: 1.5' (~4' original)	True interval: ??

**SLOUGH DISCARDED
Top 6": 2" long disk of oolite, veining and shale intraclasts/stylolite.
middle 6": dark grey shale, same as "top" interval, very soft, calcite at bottom of one piece.
next 6": clay-rich shale, mostly clay. shale structure seen when broken, very crumbly, fissile, soft.
bottom 2": oolite.

Min samples: 4 (top zone: oolite; middle zone: unstained shale; 70': oolite, ??: interesting pieces)

APPENDIX C: POINT DILUTION CURVES

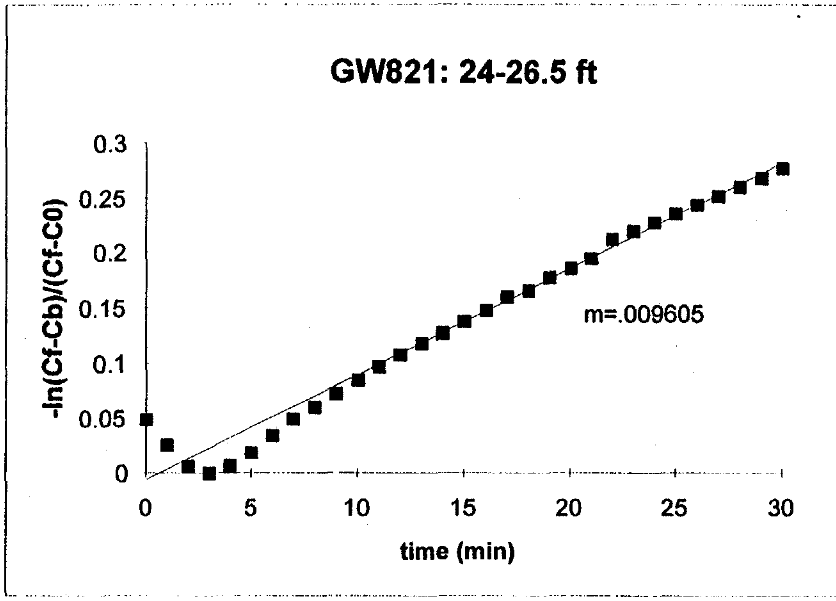
GW821: 24-26.5 ft
-ln(Cf-Cb)/(Cf-C0)
0.3
0.25
0.2
0.15
0.1
0.05
0
m=.009605
0
5
10
15
20
25
30
time (min)

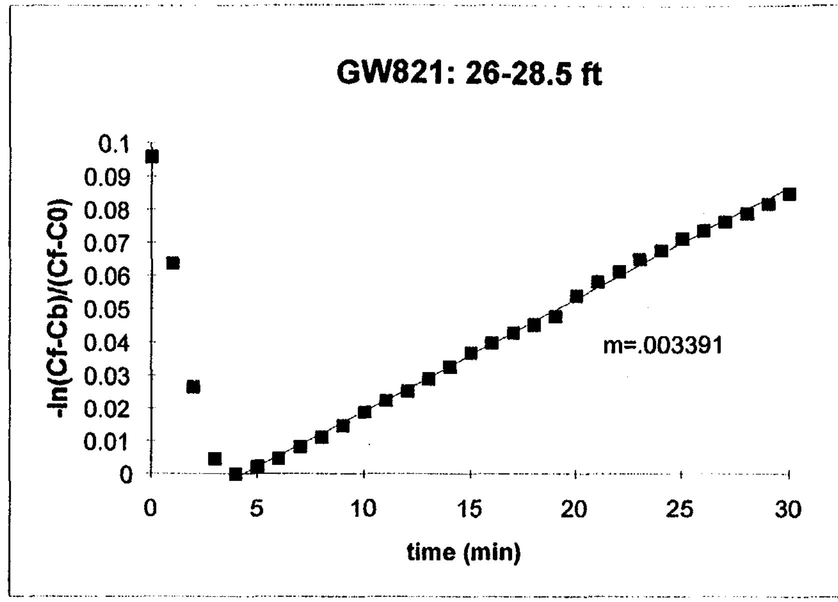
GW821: 26-28.5 ft
-ln(Cf-Cb)/(Cf-C0)
0.1
0.09
0.08
0.07
0.06
0.05
0.04
0.03
0.02
0.01
0
m=.003391
0
5
10
15
20
25
30
time (min)

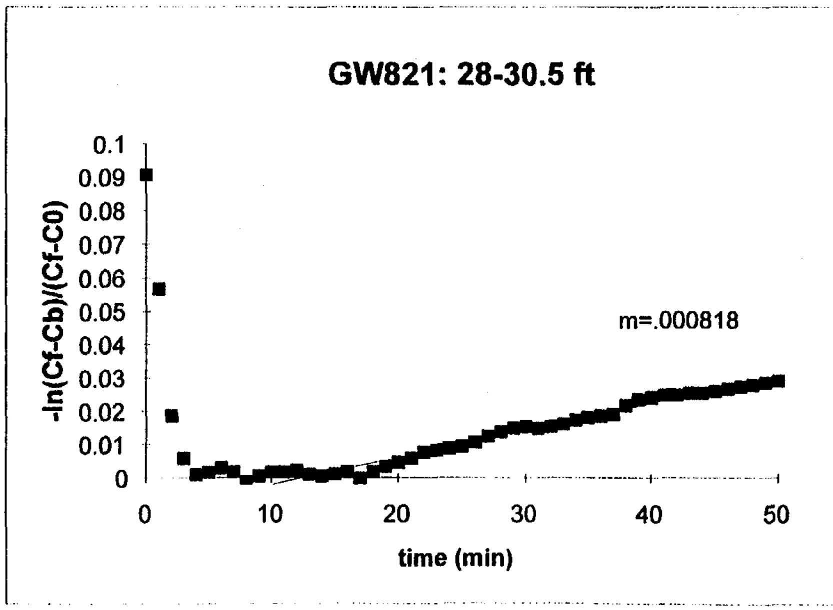
GW821: 28-30.5 ft
-ln(Cf-Cb)/(Cf-C0)
0.1
0.09
0.08
0.07
0.06
0.05
0.04
0.03
0.02
0.01
0
m=.000818
0
10
20
30
40
50
time (min)

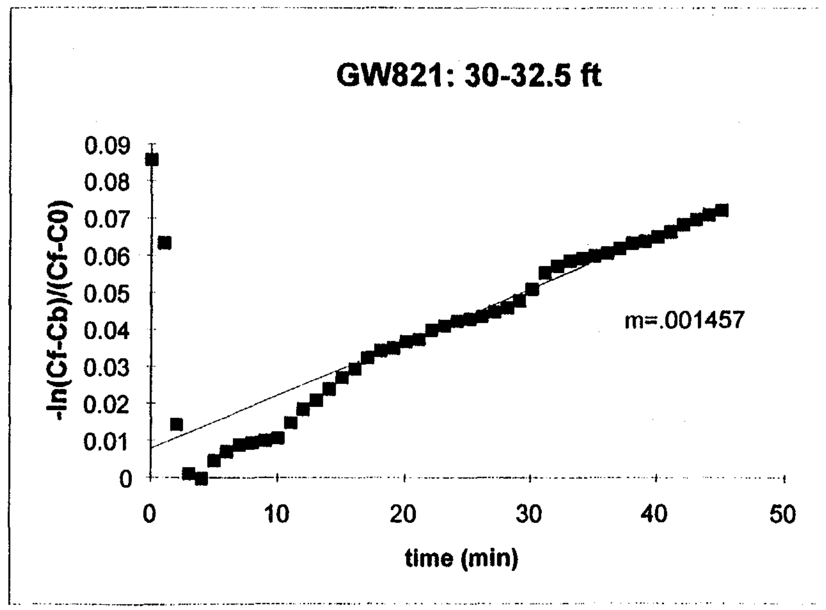
GW821: 30-32.5 ft
-ln(Cf-Cb)/(Cf-C0)
0.09
0.08
0.07
0.06
0.05
0.04
0.03
0.02
0.01
0
m=.001457
0
10
20
30
40
50
time (min)

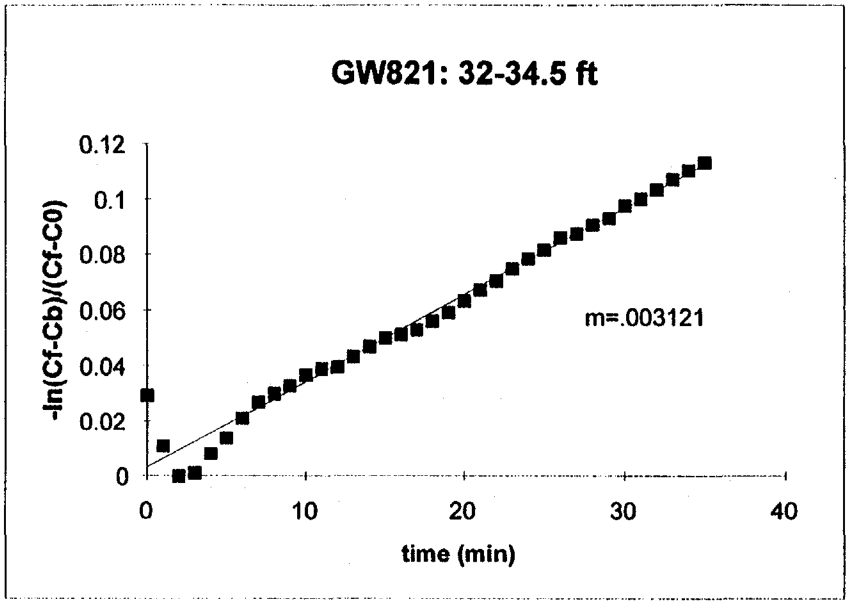
GW821: 32-34.5 ft
-ln(Cf-Cb)/(Cf-C0)
0.12
0.1
0.08
0.06
0.04
0.02
0
0
10
20
30
40
time (min)
m=.003121

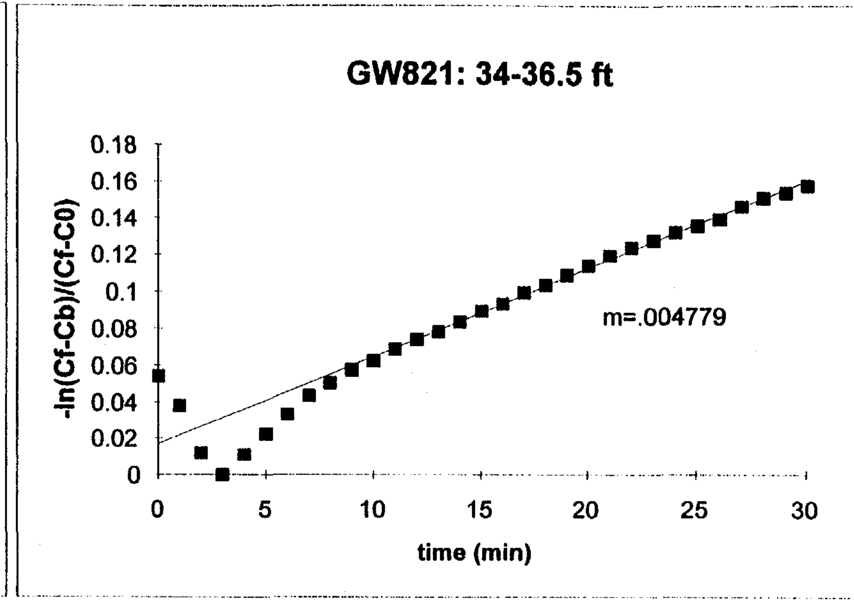
GW821: 34-36.5 ft
-ln(Cf-Cb)/(Cf-C0)
0.18
0.16
0.14
0.12
0.1
0.08
0.06
0.04
0.02
0
0
5
10
15
20
25
30
time (min)
m=.004779

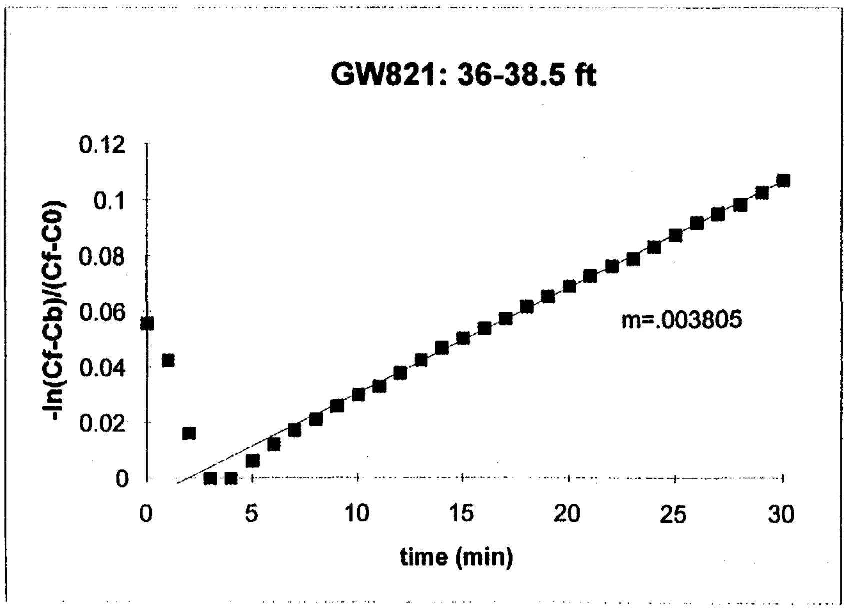
GW821: 36-38.5 ft
-ln(Cf-Cb)/(Cf-C0)
0.12
0.1
0.08
0.06
0.04
0.02
0
0
5
10
15
20
25
30
time (min)
m=.003805

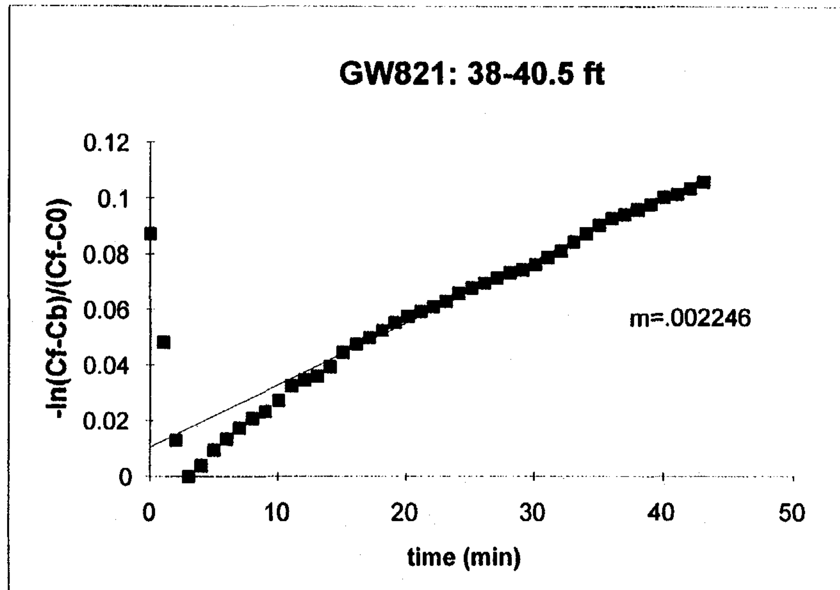
GW821: 38-40.5 ft
-ln(Cf-Cb)/(Cf-C0)
0.12
0.1
0.08
0.06
0.04
0.02
0
0
10
20
30
40
50
time (min)
m=.002246

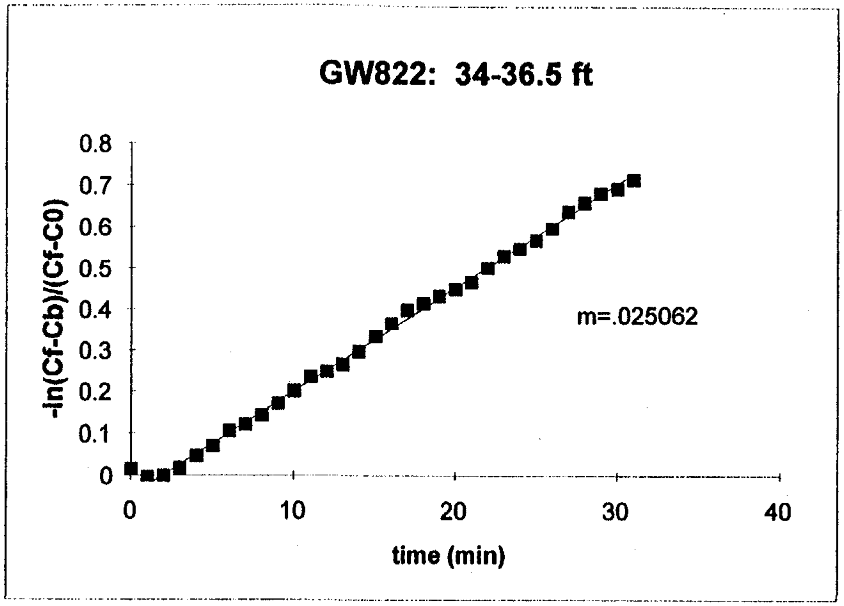
GW822: 34-36.5 ft
-ln(Cf-Cb)/(Cf-C0)
0.8
0.7
0.6
0.5
0.4
0.3
0.2
0.1
0
0
10
20
30
40
time (min)
m=.025062

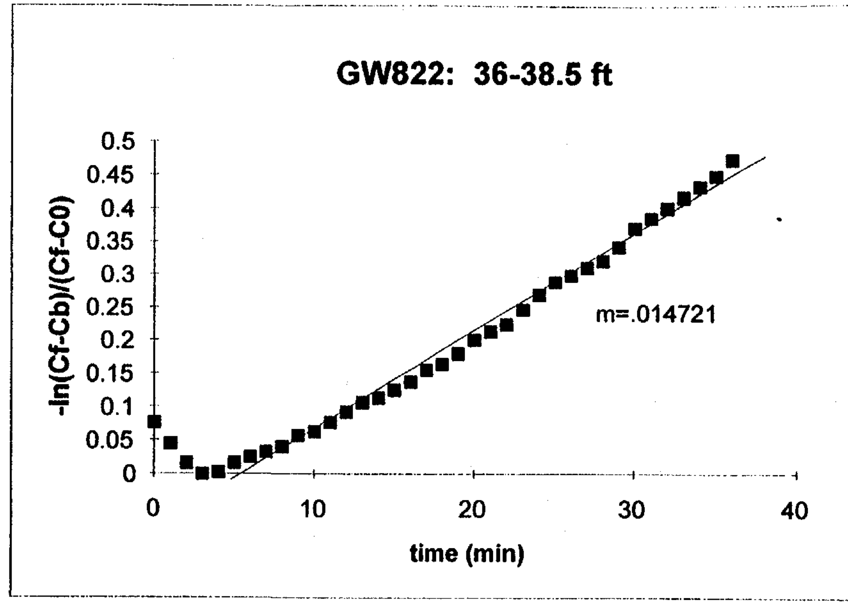
GW822: 36-38.5 ft
-ln(Cf-Cb)/(Cf-C0)
0.5
0.45
0.4
0.35
0.3
0.25
0.2
0.15
0.1
0.05
0
0
10
20
30
40
time (min)
m=.014721

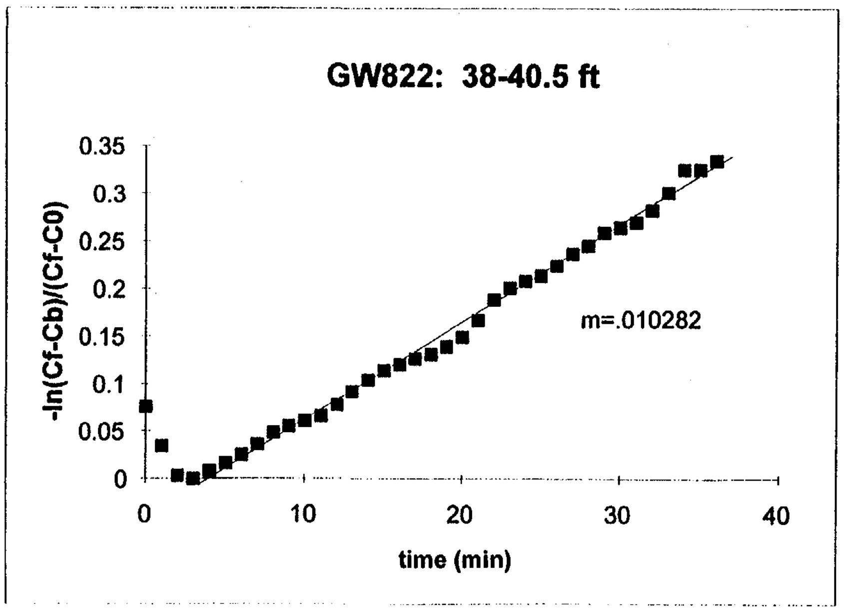
GW822: 38-40.5 ft
-ln(Cf-Cb)/(Cf-C0)
0.35
0.3
0.25
0.2
0.15
0.1
0.05
0
0
10
20
30
40
time (min)
m=.010282

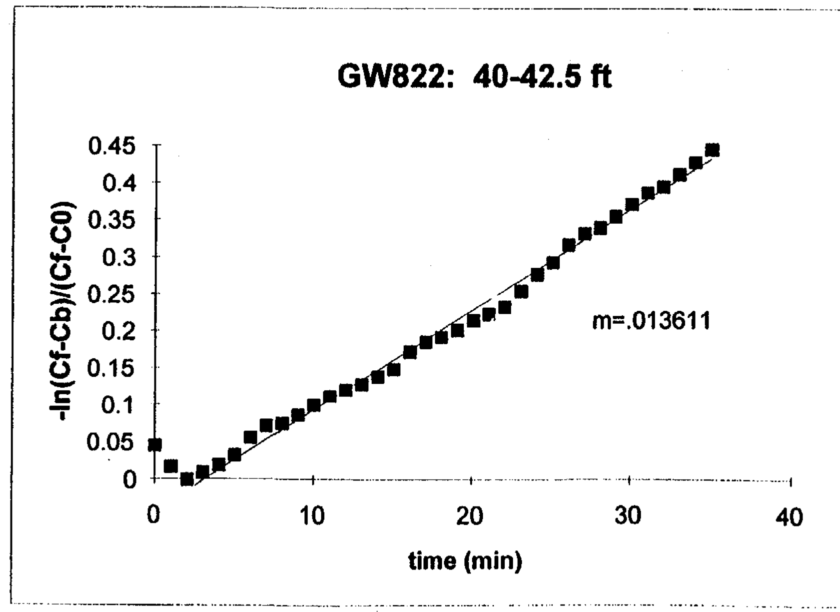
GW822: 40-42.5 ft
-ln(Cf-Cb)/(Cf-C0)
0.45
0.4
0.35
0.3
0.25
0.2
0.15
0.1
0.05
0
0
10
20
30
40
time (min)
m=.013611

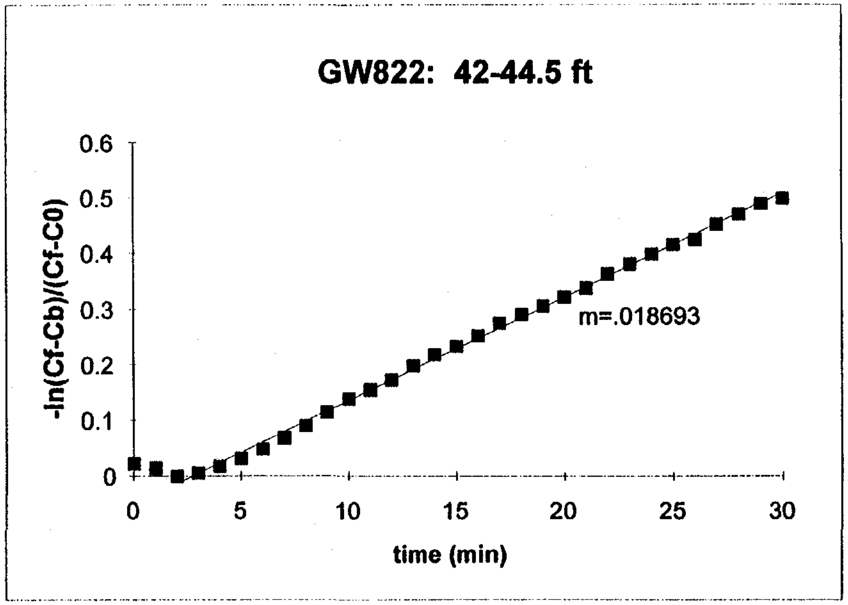
GW822: 42-44.5 ft
-ln(Cf-Cb)/(Cf-C0)
time (min)
m=.018693

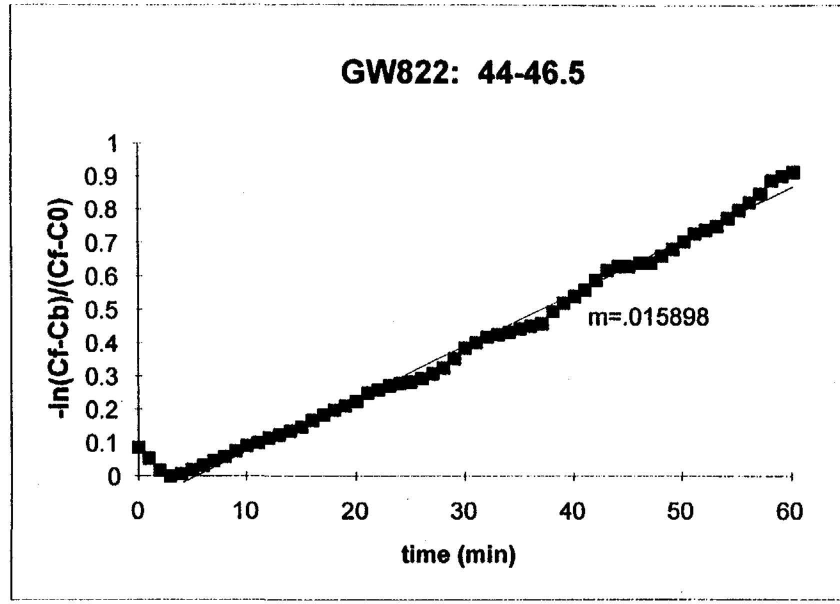
GW822: 44-46.5
-ln(Cf-Cb)/(Cf-C0)
time (min)
m=.015898

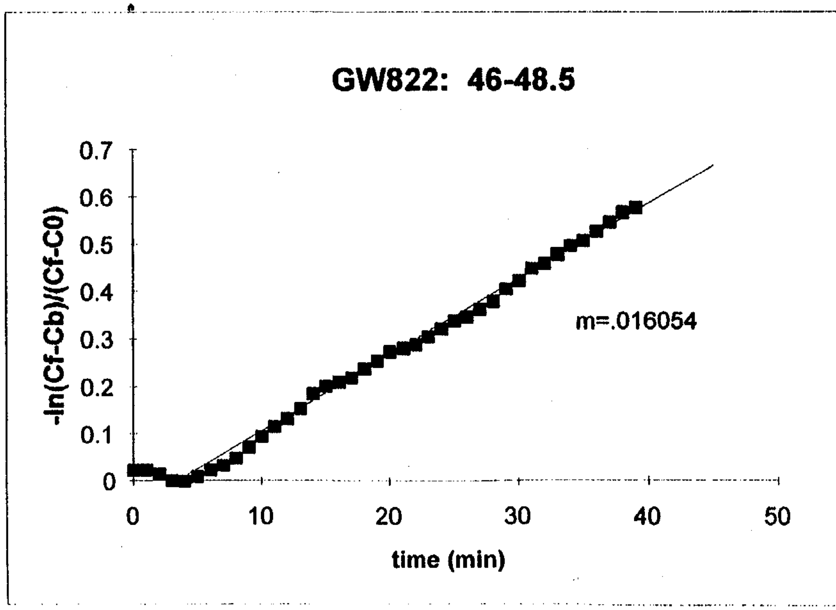
GW822: 46-48.5
-ln(Cf-Cb)/(Cf-C0)
time (min)
m=.016054

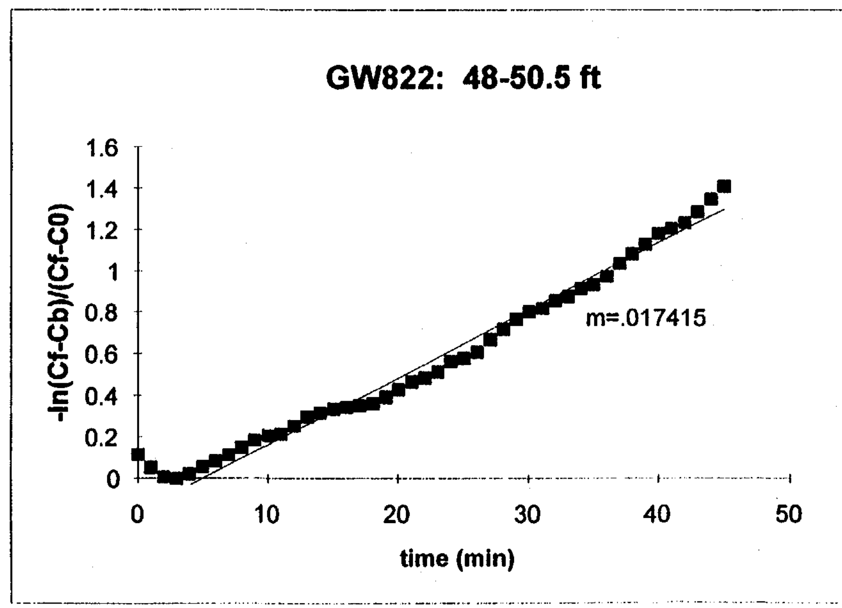
GW822: 48-50.5 ft
-ln(Cf-Cb)/(Cf-C0)
time (min)
m=.017415

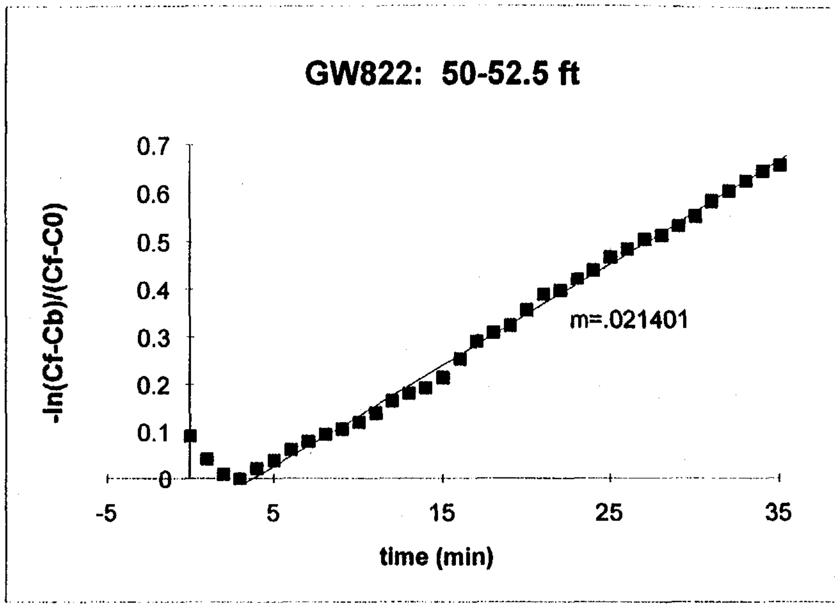
GW822: 50-52.5 ft
m=.021401
-ln(Cf-Cb)/(Cf-C0)
time (min)

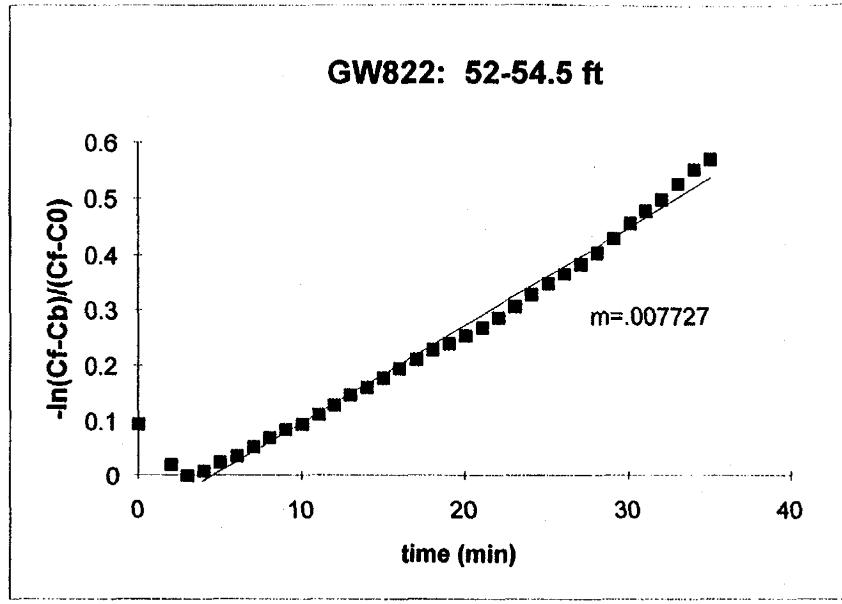
GW822: 52-54.5 ft
m=.007727
-ln(Cf-Cb)/(Cf-C0)
time (min)

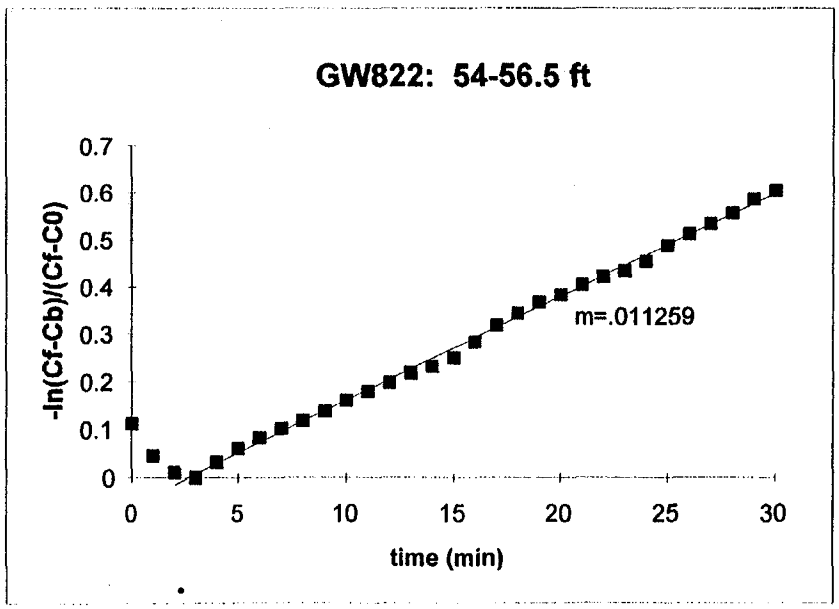
GW822: 54-56.5 ft
m=.011259
-ln(Cf-Cb)/(Cf-C0)
time (min)

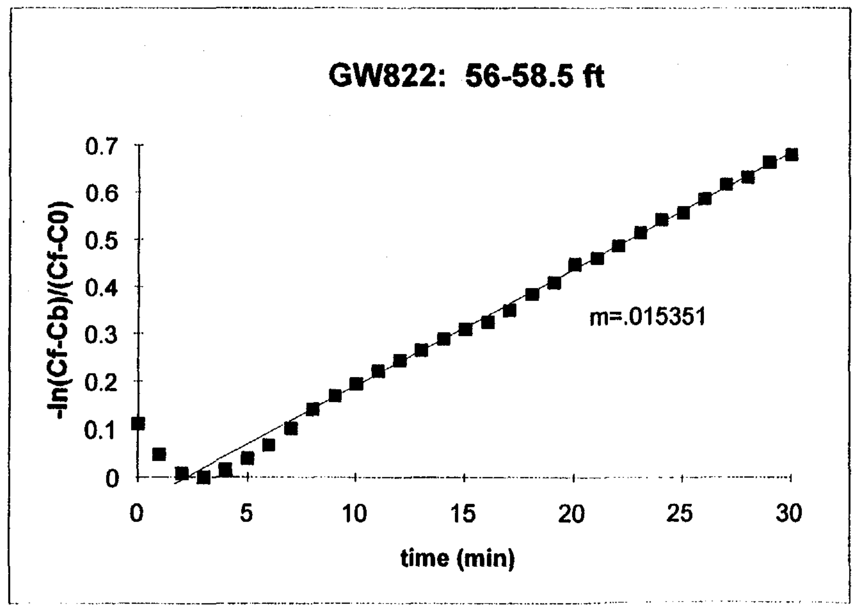
GW822: 56-58.5 ft
m=.015351
-ln(Cf-Cb)/(Cf-C0)
time (min)

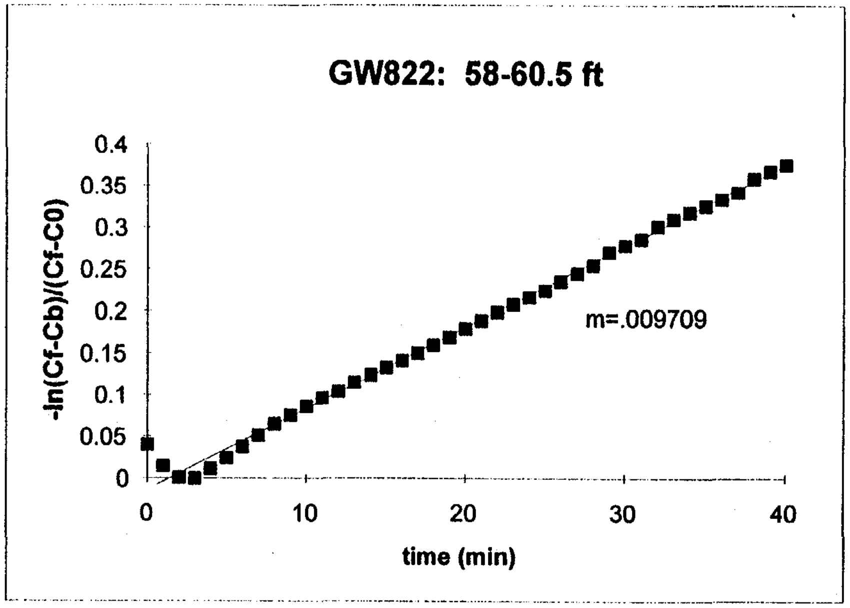
GW822: 58-60.5 ft
-ln(Cf-Cb)/(Cf-C0)
0.4
0.35
0.3
0.25
0.2
0.15
0.1
0.05
0
m=.009709
0
10
20
30
40
time (min)

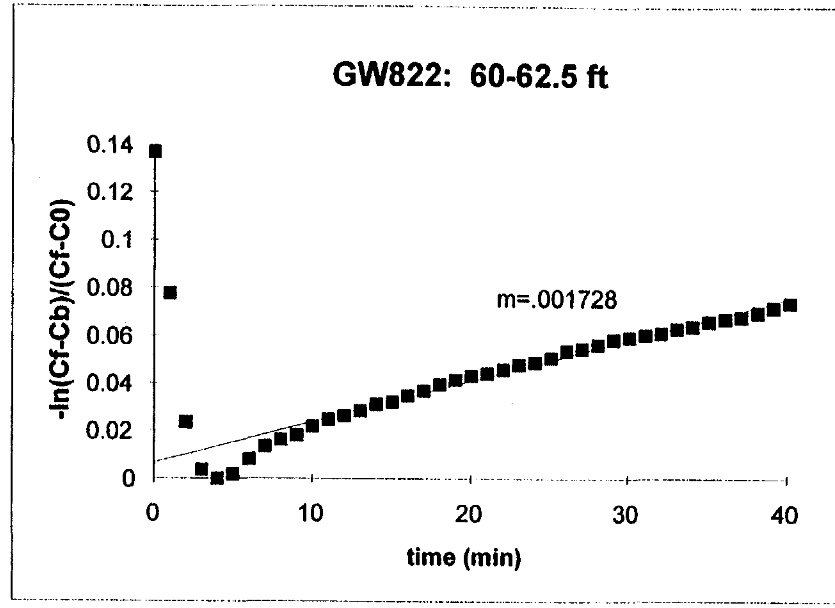
GW822: 60-62.5 ft
-ln(Cf-Cb)/(Cf-C0)
0.14
0.12
0.1
0.08
0.06
0.04
0.02
0
m=.001728
0
10
20
30
40
time (min)

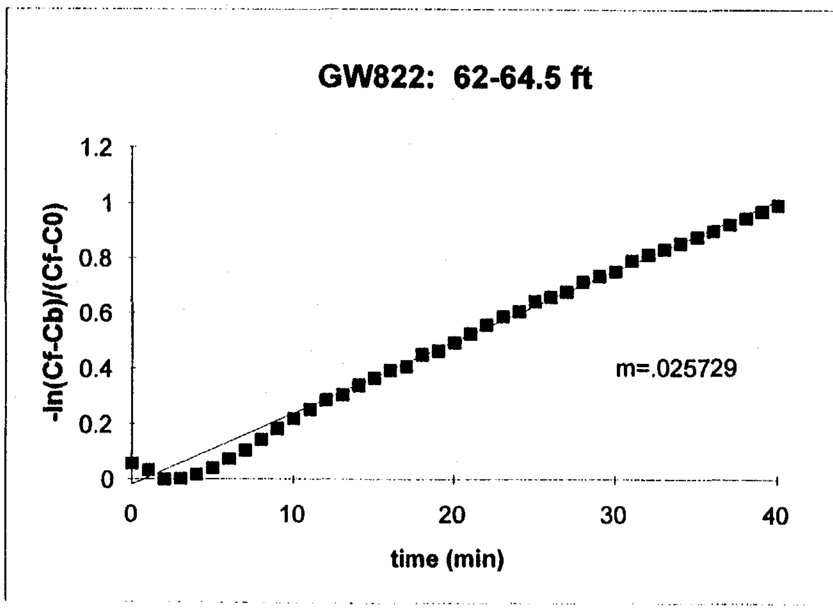
GW822: 62-64.5 ft
-ln(Cf-Cb)/(Cf-C0)
1.2
1
0.8
0.6
0.4
0.2
0
m=.025729
0
10
20
30
40
time (min)

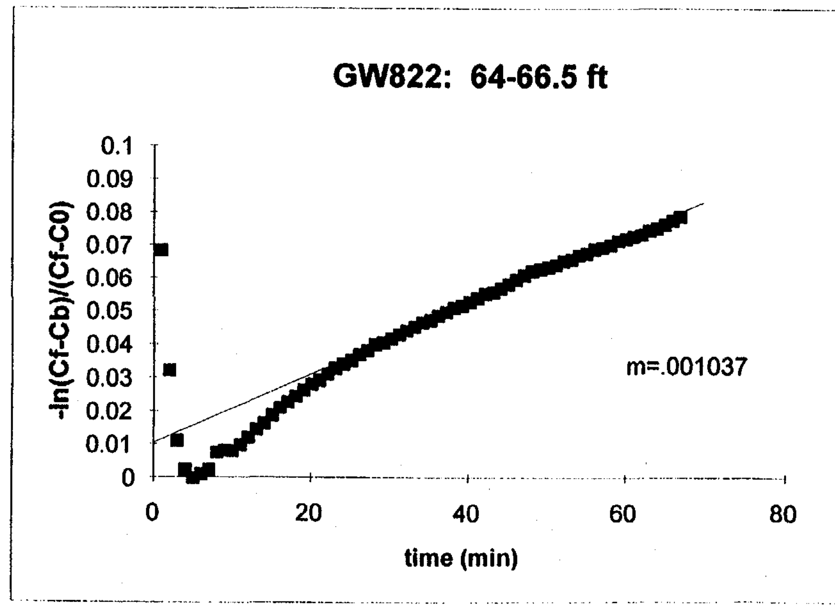
GW822: 64-66.5 ft
-ln(Cf-Cb)/(Cf-C0)
0.1
0.09
0.08
0.07
0.06
0.05
0.04
0.03
0.02
0.01
0
m=.001037
0
20
40
60
80
time (min)

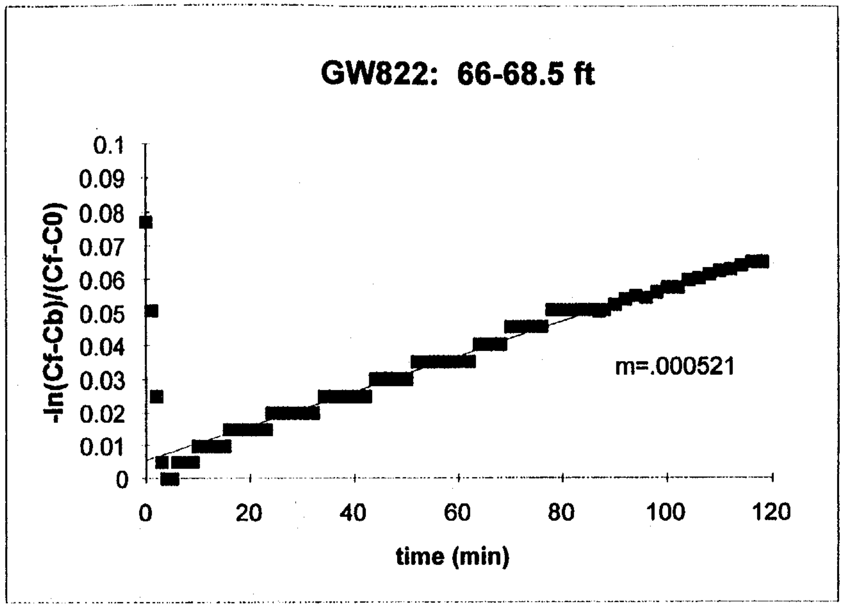
GW822: 66-68.5 ft
-ln(Cf-Cb)/(Cf-C0)
0.1
0.09
0.08
0.07
0.06
0.05
0.04
0.03
0.02
0.01
0
m=.000521
0
20
40
60
80
100
120
time (min)

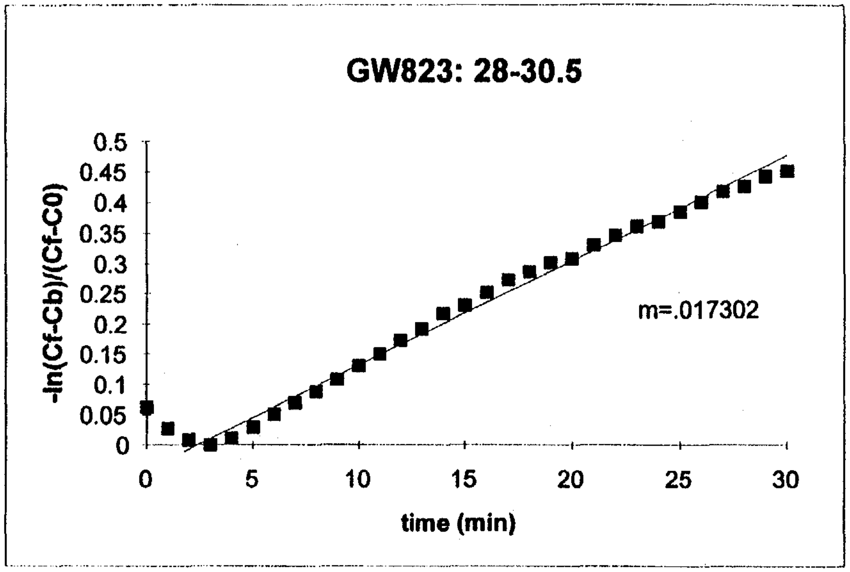

GW823: 28-30.5
-ln(Cf-Cb)/(Cf-C0)
m=.017302
time (min)

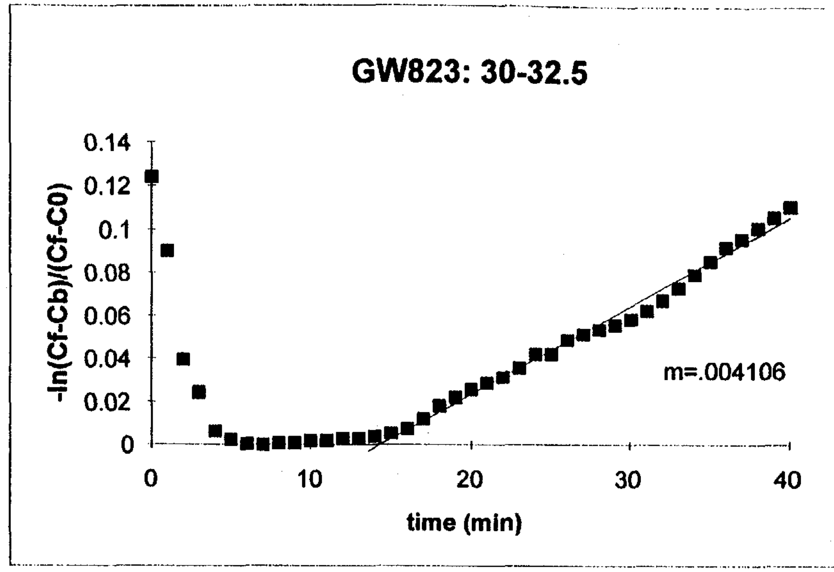

GW823: 30-32.5
-ln(Cf-Cb)/(Cf-C0)
m=.004106
time (min)

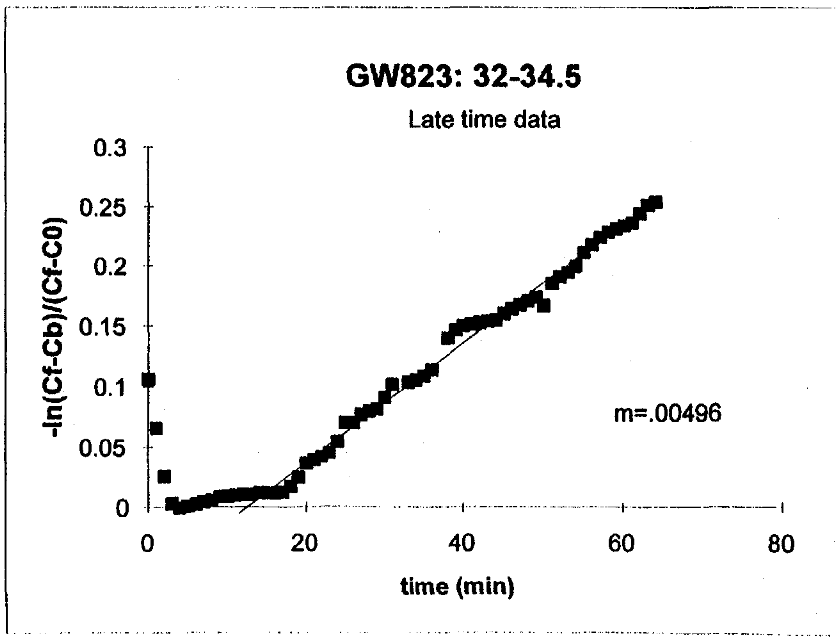

GW823: 32-34.5
Late time data
-ln(Cf-Cb)/(Cf-C0)
m=.00496
time (min)

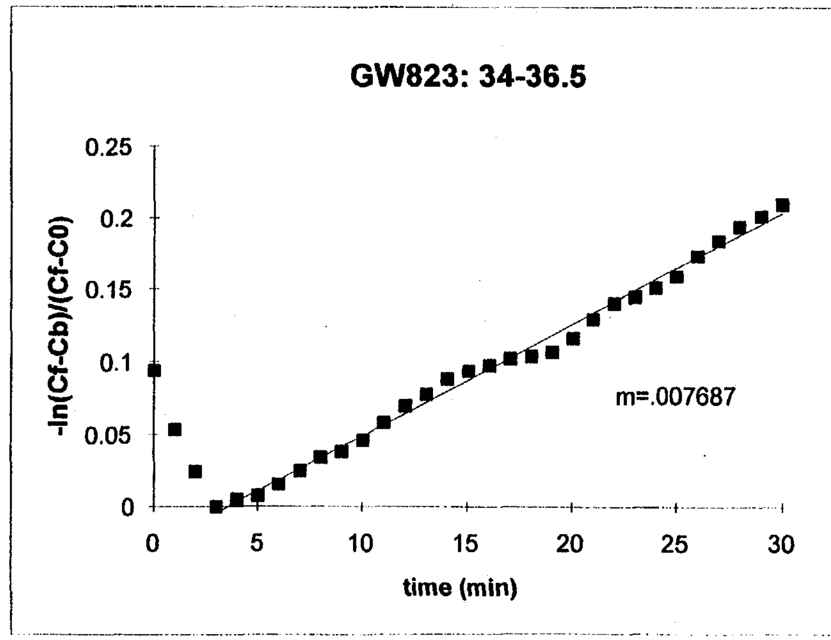

GW823: 34-36.5
-ln(Cf-Cb)/(Cf-C0)
m=.007687
time (min)

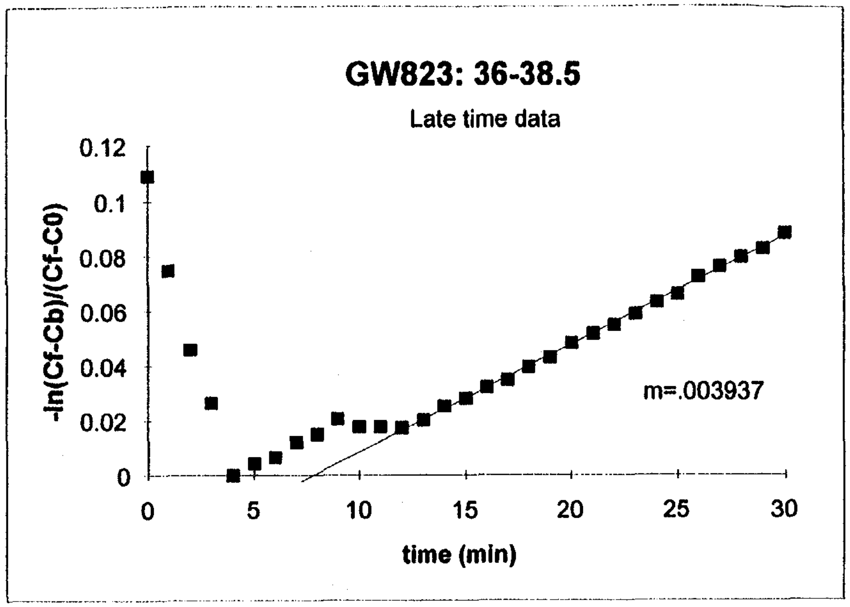
GW823: 36-38.5
Late time data
-ln(Cf-Cb)/(Cf-C0)
0.12
0.1
0.08
0.06
0.04
0.02
0
0
5
10
15
20
25
30
time (min)
m=.003937

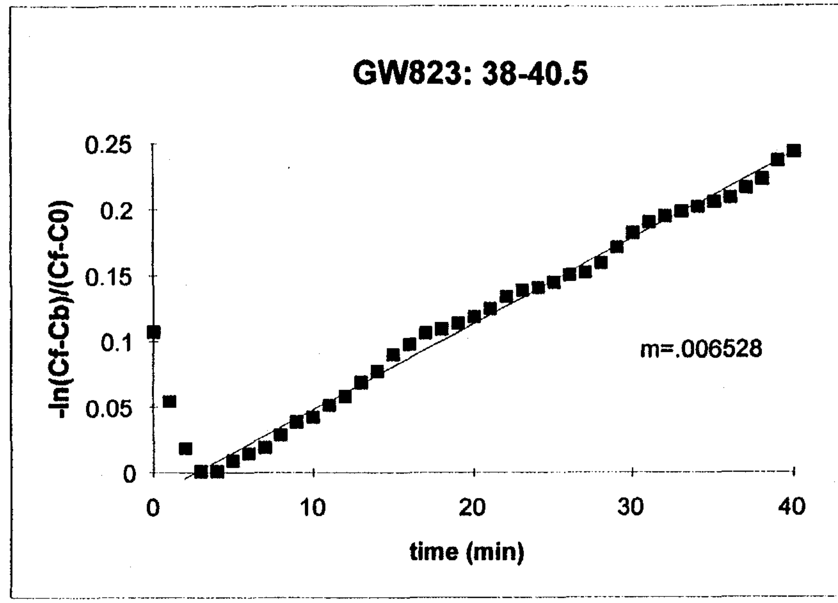
GW823: 38-40.5
-ln(Cf-Cb)/(Cf-C0)
0.25
0.2
0.15
0.1
0.05
0
0
10
20
30
40
time (min)
m=.006528

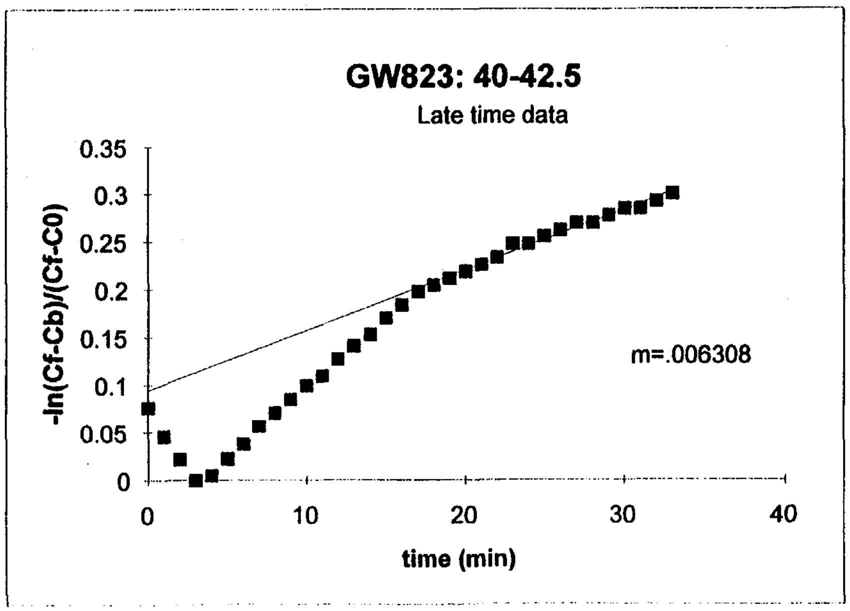
GW823: 40-42.5
Late time data
-ln(Cf-Cb)/(Cf-C0)
0.35
0.3
0.25
0.2
0.15
0.1
0.05
0
0
10
20
30
40
time (min)
m=.006308

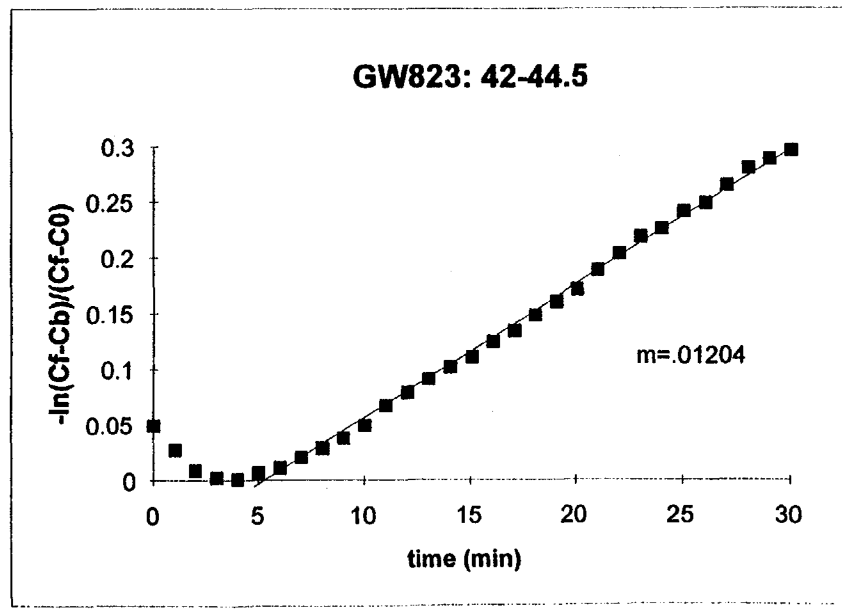
GW823: 42-44.5
-ln(Cf-Cb)/(Cf-C0)
0.3
0.25
0.2
0.15
0.1
0.05
0
0
5
10
15
20
25
30
time (min)
m=.01204

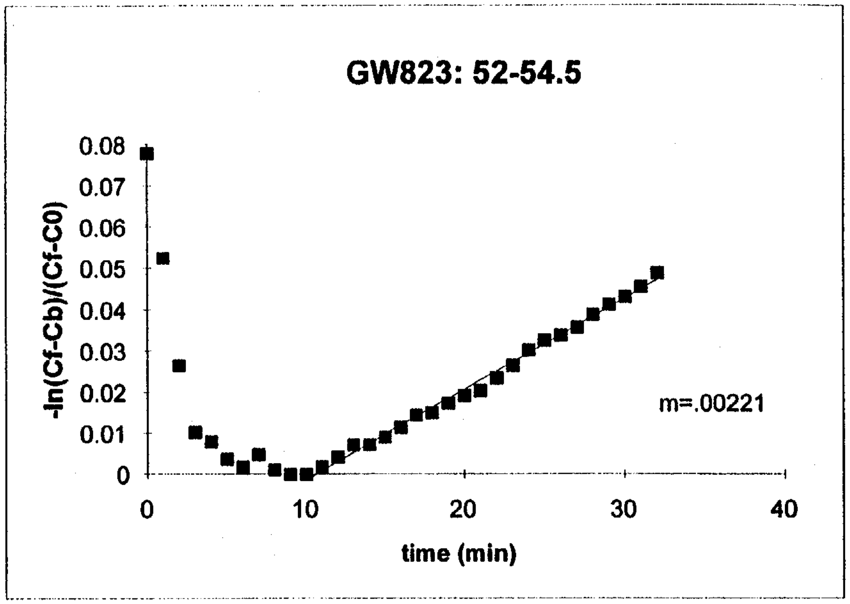
GW823: 52-54.5
-ln(Cf-Cb)/(Cf-C0)
0.08
0.07
0.06
0.05
0.04
0.03
0.02
0.01
0
0
10
20
30
40
time (min)
m=.00221

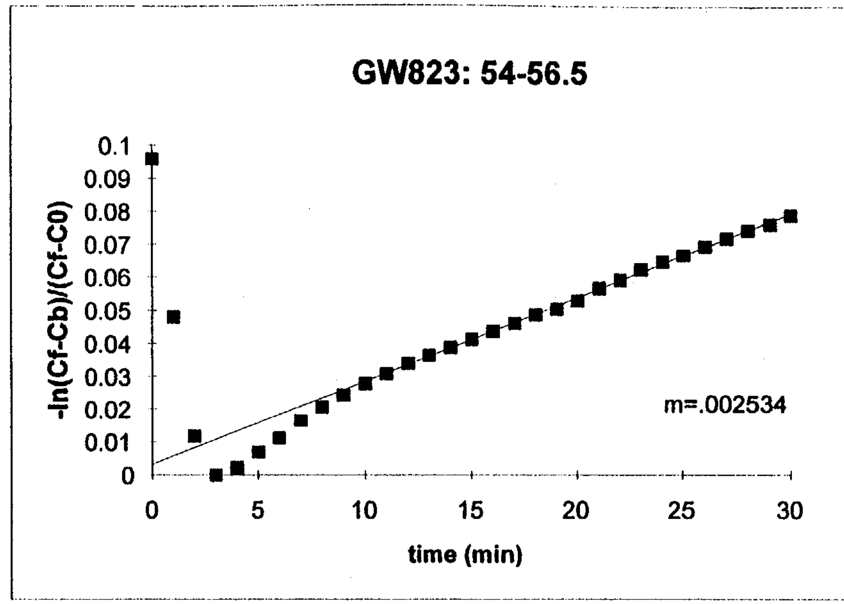
GW823: 54-56.5
-ln(Cf-Cb)/(Cf-C0)
0.1
0.09
0.08
0.07
0.06
0.05
0.04
0.03
0.02
0.01
0
0
5
10
15
20
25
30
time (min)
m=.002534

INTERNAL DISTRIBUTION

1. F. A. Anderson
2. L. V. Asplund
3. P. E. Barndt
4. R. 0. Barnett
5. L. D. Bates
6. F. P. Baxter
7. D. T. Bell
8. H. L. Boston
9. R. B. Clapp
10. K. W. Cook
11. T. K. Cothron
12. J. H. Cushman
13. F. P. Delozier
14. A. Diefendorf
15. R. B. Dreier
16. T. 0. Early
17. J. M. Forstrom
18. D. E. Fowler
19. C. W. Gehrs
20. P. A. Gourieux
21. C. S. Haase
22. S. G. Hildebrand
23. D. D. Huff
24. G. K. Jacobs
25. W. K. Jago
26. P. Kanciruk
27. R. H. Ketelle
28. H. L. King
29. A. J. Kuhaida
30. G. R. Miller
31. G. R. Moline
32. G. K. Moore
33. C. A. Motley
34. J. B. Murphy
35. M. J. Norris
36. R. S. Poling
37. D. E. Reichle
38. C. T. Rightmire
39. T. H. Row
40. W. E. Sanford
41. F. E. Sharples
42. D. S. Shriner
43. E. D. Smith
44. S. H. Stow
45. L. E. Toran
46. L. 0. Vaughan
47. D. B. Watson
48. S. H. Welch
49. R. K. White
50. S. L. Winters
51. T. F. Zondlo
52. Central Research Library

53-67. ESD Library

68. Laboratory Records Dept.
69. Laboratory Records, ORNL-RC
70. ORNL Patent Section
71. ORNL Y-12 Technical Library

EXTERNAL DISTRIBUTION

72. Benfield, Tennessee Department of Environmental Conservation, U.S. Department of Energy Oversite Office, 761 Emory Valley Road, Oak Ridge, TN 37831

73. G. W. Bodenstein, U.S. Department of Energy, Oak Ridge Operations Office, IRC Building, P.O. Box 2001, Oak Ridge, TN 37838-8541

74. P. Craig, Environmental Consulting Engineers, Inc., P.O. Box 22668, Knoxville, TN 37933

75. E. K. Evans, Jacobs Engineering, 125 Broadway Avenue, Oak Ridge, TN 37831

76. R. N. Farvolden, Professor, Department of Earth Sciences, University of Waterloo, Waterloo, Ontario N2L 3G I Canada

77. D. W. Freckman, Director, College of Natural Resources, 101 Natural Resources Building, Colorado State University, Fort Collins, CO 80523

78. R. C. Harriss, Institute for the Study of Earth, Oceans, and Space, Science and Engineering Research Building, University of New Hampshire, Durham, NH 03824

79. B. Jenks, CDM Federal, 800 Oak Ridge Turnpike, Suite 500, Oak Ridge, TN 37830

80. S. W. Jones, Tennessee Department of Environmental Conservation, U.S. Department of Energy Oversite Office, 761 Emory Valley Road, Oak Ridge, TN 37831

81. G. Y. Jordy, Director, Office of Program Analysis, Office of Energy Research, ER-30, G-266, U.S. Dpeartment of Energy, Washington, DC 20545

82. Larry D. McKay, University of Tennessee, Department of Geology, 306 G&G Building, Knoxville, TN 37996-1410

83. G. K. Moore, Route 4, Box 927, Waynesboro, TN 38485

84. D. P. Moss, SAID, 800 Oak Ridge Turnpike, P.O. Box 2502, Oak Ridge, TN 37831

85. R. H. Olsen, Professor, Microbiology and Immunology Department, University of Michigan, Medical Sciences II, #5605, 1301 East Catherine Street, Ann Arbor, MI 48109-0620

86. J. P. Ottinger, Tennessee Department of Environmental Conservation, U.S. Department of Energy Oversite Office, 761 Emory Valley Road, Oak Ridge, TN 37831

87. A. Patrinos, Director, Environmental Sciences Division, Office of Health and Environmental Research, ER-74, U.S. Department of Energy, Washington, DC 20585

88. S. P. Riddle, U.S. Department of Energy, Oak Ridge Operations Office, IRC Building, P.O. Box 2001, Oak Ridge, TN 37838-8541

89. M. E. Schreiber, Dept. Of Geology and Geophysics, University of Wisconsin Madison, 1215 W. Dayton, Madison, WI 53706

90. R. C. Sleeman, U.S. Department of Energy, Oak Ridge Operations Office, IRC Building, P.O. Box 2001, Oak Ridge, TN 37838-8541

91. D. K. Solomon, Department of Geology and Geophysics, 717 W. C. Browning Building, Salt Lake City, UT 84112-1183

92. D. A. Webster, U.S. Geological Survey, 810 Broadway, Suite 500, Nashville, TN 37203

93. F. J. Wobber, Environmental Sciences Division, Office of Health and Environmental Research, ER-74, U.S. Department of Energy, Washington, DC 20585

94-95. Office of Assistant Manager for Energy Research and Development, U.S. Department of Energy Oak Ridge Operations, P.O. Box 2001, Oak Ridge, TN 37831-8600

96-97. Office of Scientific and Technical Information, P.O. Box 62, Oak Ridge, TN 37831